



BOOK OF ABSTRACTS

Organized by:

Book of Abstracts of 11th Iberian Conference on Tribology

Edited by: Ana Paula Serro, Ana Catarina Branco, Carla Carneiro, Diana Silva,
Mafalda Guedes, Célio Figueiredo-Pina

Editor: Instituto Politécnico de Setúbal

Date: October 2022

ISBN: 978-989-53890-4-9

Participants have responsibility for the book content.

Oral Communications and Posters were peer-reviewed.

EDITORIAL

During the last decades, tribology has emerged as an important knowledge area. The significant developments that we have seen on transport and manufacturing sectors were largely due to the advances in this field. Research in tribology also extended to other topics such as: biotribology (when dealing with biological systems), green tribology (reduction of tribological losses), geotribology (glaciers and faults) and space tribology (involving extreme temperatures and vacuum conditions). In a transversal way, the investigation of the tribological phenomena at nanoscale (nanotribology), the use of modelling tools to describe such phenomena (computational tribology) or the application of artificial intelligence, machine learning and big data methods to tribological systems (triboinformatics) have assumed an increasing relevance. This raising interest results from the recognition of the high costs associated to the performance of the tribological systems. In fact, it is estimated that almost one quarter of the energy consumption at global level is due to tribological issues. New advances in materials, lubricants and contact design shall allow to reduce friction and wear, leading to significant savings at short (about 18% in 8 years) and long term ($\approx 40\%$ in 15 years). This is critical to ensure the competitiveness of industry, to minimize the environmental impact and, in last instance, contribute to the progress of humanity.

IBERTRIB 2022 brought together researchers from Portugal and Spain, but also from other points of the globe (e.g., Mexico, Austria, Brazil, United Kingdom, Netherlands, USA), that work in tribology, to discuss the most recent developments, advances, and challenges in different tribology topics. The participants had the opportunity to share and discuss their work with other researchers and stakeholders from academy and industry. It was a privileged forum to promote the collaboration between research groups and integrate young researchers. The conference counted with 36 oral communications and 16 posters distributed by 8 main topics:

- Friction and wear
- Characterization techniques and testing methods
- Biotribology
- Modelling and simulation in tribology
- Surface engineering, surface treatment and coatings
- Lubricants and additives
- Micro and nanotribology
- Tribocorrosion

in 6 sessions that extended for almost two days. Four plenary sessions were given by renown specialists, which share their experience and knowledge with an audience of researchers of different

generations. Finally, an attractive social program, which included the visit to an industrial unit, allowed to learn in the field while promoting an informal interaction among researchers.



Célio Figueiredo-Pina and Ana Paula Serro

(Chairs of the IBERTRIB 2022)

ORGANIZING COMMITTEE

Célio Figueiredo-Pina	Instituto Politécnico de Setúbal, Setúbal, Portugal
Ana Paula Serro	Instituto Superior Técnico, Lisbon, Portugal
Mafalda Guedes	Instituto Politécnico de Setúbal, Setúbal, Portugal
Carla Carneiro	Instituto Politécnico de Setúbal, Setúbal, Portugal
Ana Catarina Branco	Instituto Superior Técnico, Lisbon, Portugal
Diana Silva	Instituto Superior Técnico, Lisbon, Portugal

SCIENTIFIC COMMITTEE

Albano Cavaleiro	University of Coimbra, Portugal
Alessandro Ruggiero	University of Salerno, Italy
Amaya Igartua	Fundación TEKNIKER, Spain
Amélia Almeida	Instituto Superior Técnico, Lisbon, Portugal
Ana Paula Serro	Instituto Superior Técnico, Lisbon, Portugal
Antólin Battez	University of Oviedo, Spain
Célio Figueiredo-Pina	Instituto Politécnico de Setúbal, Setúbal, Portugal
Elena Gordo	University of Carlos III de Madrid, Spain
Ian Hutchings	Institute for Manufacturing, United Kingdom
Iñaki Garcia Diego	CENIM-CSIC, Spain
Jesús Rodríguez	University of Rey Juan Carlos, Spain
Jorge Seabra	University of Porto, Portugal
José Gomes	University of Minho, Portugal
José Viesca	University of Oviedo, Spain
José Sanes Molina	Polytechnic University of Cartagena, Spain
Josefa Fernández	University of Santiago de Compostela, Spain
Juan Carlos Sánchez-Lopéz	Instituto de Ciencia de Materiales de Sevilla – ICMSE, Spain
Maria Dolores Bermúdez	Polytechnic University of Cartagena, Spain
Markus Wimmer	Rush University Medical Center, Chicago, USA
Manuel Belmonte	Instituto de Cerámica y Vidrio – CSIC, Spain
Mathew Mathew	University of Illinois, Chicago, USA
Paulo Davim	University of Aveiro, Portugal
Peter Dearnley	Boride Services Ltd, United Kingdom
Rafael Rodríguez	University of Navarra, Spain
Rogério Colaço	Instituto Superior Técnico, Lisbon, Portugal
Rubén Rodríguez	University of Oviedo, Spain

INDEX

EDITORIAL	3
ORGANIZING COMMITTEE	5
SCIENTIFIC COMMITTEE	5
PROGRAMME	9
ORAL COMUNICATIONS	12
KEYNOTE 1 – Prof. Ian Hutchings - <i>Tribology in Leonardo da Vinci's Codex Madrid</i>	14
Session A1: FRICTION AND WEAR	15
O1 <u>Fátima Mariño Fernandes</u> – <i>Tribology behavior of nanolubricants containing oleic acid coated ZnO nanoadditives</i>	16
O2 <u>Josefa Fernandez</u> – <i>Reviewing Stability over Time and Tribological Performance of Non-Aqueous Lubricants containing Chemical Modified Nanoadditives</i>	18
O3 <u>José Del Rio</u> – <i>Tribological behavior enhancement using coated TiO₂ nanoparticles as PAO₈ additives</i>	20
O4 <u>Luis Vilhena</u> – <i>Strain hardening behavior of CoCrMo</i>	22
O5 <u>Luiz Sanchez</u> – <i>Cutting tool with micro-grooves filled with carbon nanotubes</i>	24
O6 <u>Mariano Torres</u> – <i>Tribological behavior of cutting tool on Ti6Al4V sample with different grades of self-emulsifying esters with and without anti-corrosion additives</i>	26
Session A2: FRICTION AND WEAR	28
O7 <u>José Lopes</u> - <i>Evaluation of grinding with two different CBN grains applied to austempered ductile iron (ADI)</i>	29
O8 <u>Eduardo Bianchi</u> - <i>Effect of grinding hardened steel by applying MQL diluted with wheel cleaning jet</i>	31
O9 <u>Miguel Angel</u> - <i>Effect of the spraying temperature on the erosion behavior of 316L coatings deposited by Cold-Spray</i>	33
O10 <u>Lais Lopes</u> - <i>The challenge of measuring friction and wear of industrial components on the lab scale</i>	35
O11 <u>Ulises García-Ramírez</u> - <i>Erosive behavior of AISI 310 stainless steel under impact of cryogenic jets</i>	37
O12 <u>Todor Vuchkov</u> - <i>Tribological studies of sputtered WSC coatings with conventional and graded composition</i>	39

	KEYNOTE 2 – Prof. Markus Wimmer - Cartilage Lubrication and Wear: Knowns and Unknowns	42
	SESSION B: CHARACTERIZATION TECHNIQUES AND TESTING METHODS	43
O13	<u>Fernando Lopez-Uruñuela</u> - Study of the early stages of WEA formation in pre-cracked and hydrogen charged 100Cr6 bearing steel	44
O14	<u>Sharjeel Ahmed Khan</u> - A Crossed Cylinder Tribological Test against New Multi-material (CFRP-Ti) Stacks Configuration	46
O15	<u>Amilcar Ramalho</u> - Friction of soft contact lenses	48
O16	<u>Paul Staudinger</u> - A Tribological Test Method for PVA Hydrogels and Articular Cartilage	50
O17	<u>Álvaro Rico</u> - Using Contact Mechanics to describe the time dependent behavior of Polyacrylamide based hydrogels	52
O18	<u>Amaya Igartua</u> - Ceramic tribocoatings for die protection in Low Pressure Die Casting process	54
	SESSION C: BIOTRIBOLOGY/ MODELLING AND SIMULATION IN TRIBOLOGY	56
O19	<u>Diana Silva</u> - Effects of non-conventional sterilization methods on PBO-reinforced PVA hydrogels for cartilage replacement	57
O20	<u>Ana Branco</u> - 3D printing of leucite-based materials reinforced with zirconia for dentistry	59
O21	<u>Juan Sánchez-López</u> - Low friction/wear properties of snake skins: a case study for mimicking nature tribological behavior	61
O22	<u>Jorge Seabra</u> - Torque loss model for axially pre-loaded tandem rolling element bearings	63
O23	<u>Lais Lopes</u> - How can we simulate bio-medical tribological contacts on the lab scale?	65
O24	<u>Deepak Veeregowda</u> - Traction, Stribeck and scuffing characteristics of lubricants in rolling-sliding contacts using twin disc	67
	KEYNOTE 3 – Prof. Peter Dearnley - Corrosion-wear (tribocorrosion) mechanisms of hard coated stainless steels	69
	SESSION D1: SURFACE ENGINEERING, SURFACE TREATMENT AND COATINGS	70
O25	<u>Albano Cavaleiro</u> - Tribological performance of laser-treated WSC sputtered coatings sliding against NBR rubber	71
O26	<u>María García Guimarey</u> - Study of 2D Nano-coated Steel Surfaces for Wear Reduction	73
O27	<u>Raquel Bayón</u> - Plasma Electrolytic Oxidation coatings on a secondary cast Al-Si alloy for brake applications	75
O28	<u>Juan Vazquez Martinez</u> - Enhancing the lubrication effect on tribological response of laser textured PH stainless steel surfaces	77
O29	<u>Irene Del Sol</u> - Study on the effect of LST atmosphere on the tribological wear behavior of Ti6Al4V	79
O30	<u>Ivan Rodrigues</u> - Dry sliding wear of a laser-clad NiCrBSi-WC composite coating	81

	KEYNOTE 4 – Prof. Mathew Mathew - Tribocorrosion Aspects of Biomedical Implants: Where are we now?	84
	SESSION D2: SURFACE ENGINEERING, SURFACE TREATMENT AND COATINGS/ LUBRICANTS AND ADDITIVES/ MICRO AND NANOTRIBOLOGY/ TRIBOCORROSION	85
O31	<u>Bernardo Diniz</u> - Wear resistance of laser clad 25NiCr – 75CrC coatings	86
O32	<u>Bernardo Tormos</u> - Performance assessment of different base oils for e-thermal fluids applications in BEVs	88
O33	<u>Rúben Gonzalez</u> - Oxidation influence on the electrical conductivity of transmission fluids in electric vehicles	90
O34	<u>Jesús Rodriguez</u> - A molecular dynamics study of adhesion in metallic contacts	92
O35	<u>Daniel Ramírez-Arreola</u> - Influence of swirl number and incidence angle on erosion-corrosion behavior of API steel pipe under swirling jets	94
	POSTER PRESENTATIONS	96
P1	<u>M. V. Biezma-Moraleda</u> - Characterization of cavitation corrosion behavior of different copper systems in artificial seawater.	97
P2	<u>María J.G. Guimarey</u> - Electrochemically exfoliated 2D materials as lubricant additives	99
P3	<u>J.R. Gomes</u> - Effect of grooves and their geometry on the wear behavior of structured grinding wheels	101
P4	<u>Fátima Mariño</u> - Effect of SiO₂ and coated SiO₂-SA nanoparticles on the lubricant properties of a paraffinic base oil	103
P5	<u>Mónica Antunes</u> - Protic Ionic Liquids for Lubrication in Nanotechnology	105
P6	<u>Josefa Fernández</u> - Tribological enhancement using Mn₃O₄-Graphene nanocomposites as additives for potential transmission fluids of electric vehicles	107
P7	<u>José M. Liñeira del Río</u> - Transmission fluids based on a low-viscosity polyalphaolefin and ZrO₂ and CeO₂-ZrO₂ nanoparticles as additives	109
P8	<u>R. Bayón</u> - Multifunctional TiO₂ coatings by Plasma Electrolytic Oxidation on TiNbZrTa alloy for dental applications	111
P9	<u>L. Sánchez-López</u> - Functionalization of CoCr surfaces with graphene oxide	113
P10	<u>C.S Abreu</u> - Dynamic aspects of oral processing of curcumin-loaded solid lipid nanoparticles yoghurts by rheology and soft tribology assessment	115
P11	<u>B. Chico</u> - Effect of Normal Load and Rotational Rate on the Coefficient of Friction of CoCr Alloy in Hyaluronic Acid as Lubricant	117
P12	<u>C.G. Figueiredo-Pina</u> - Wear performance of 3D printed PLA, PC and PEI	119
P13	<u>A.C. Branco</u> - The influence of glaze on the tribological properties of zirconia dental pieces obtained by subtractive and additive manufacturing	121
P14	<u>Carolina Marto Costa</u> - Alginate-based hydrogels loaded with ibuprofen for articular cartilage substitution	123
P15	<u>Francisco Santos</u> - Tribomechanical behavior of gamma-irradiated Nomex® reinforced poly(vinyl alcohol)-based hydrogels for articular cartilage replacement	125
P16	<u>J. Perdigoto</u> - Tool condition monitoring of self-lubricating coatings to improve the lifetime of cutting tools	127
P17	<u>J. Costa</u> - Optimized surface engineering solutions for glass mould industry	129
	ATTENDEES	131
	SPONSORS	133

PROGRAMME

PROGRAMME - 6th OCTOBER 2022

- 08:30-09:00 AM REGISTRATION
- 09:00-09:15 AM OPENING SESSION
- 09:15-09:45 AM **KEYNOTE 1** – Prof. Ian Hutchings - *Tribology in Leonardo da Vinci's Codex Madrid*
- 09:45-11:15 AM **SESSION A1: FRICTION AND WEAR**
CHAIRS: Dr. Ian Hutchings and Dr. Rogério Colaço
- 09:45-10:00 AM Fátima Mariño Fernandes – *Tribology behavior of nanolubricants containing oleic acid coated ZnO nanoadditives*
- 10:00-10:15 AM Josefa Fernandez – *Reviewing Stability over Time and Tribological Performance of Non-Aqueous Lubricants containing Chemical Modified Nanoadditives*
- 10:15-10:30 AM José Del Rio – *Tribological behavior enhancement using coated TiO₂ nanoparticles as PAO₈ additives*
- 10:30-10:45 AM Luis Vilhena – *Strain hardening behaviour of CoCrMo*
- 10:45-11:00 AM Luiz Sanchez – *Cutting tool with micro-grooves filled with carbon nanotubes*
- 11:00-11:15 AM Mariano Torres – *Tribological behavior of cutting tool on Ti6Al4V sample with different grades of self-emulsifying esters with and without anti-corrosion additives*
- 11:15-11:30 AM COFFEE BREAK / POSTERS SESSION / TECHNICAL EXHIBITIONS
- 11:30-01:00 PM **SESSION A2: FRICTION AND WEAR**
CHAIRS: Dr. Albano Cavaleiro and Dr. Ruben Rodrigues
- 11.30-11.45 AM José Lopes - *Evaluation of grinding with two different CBN grains applied to austempered ductile iron (ADI)*
- 11:45-12:00 PM Eduardo Bianchi - *Effect of grinding hardened steel by applying MQL diluted with wheel cleaning jet*
- 12:00-12:15 PM Miguel Angel - *Effect of the spraying temperature on the erosion behavior of 316L coatings deposited by Cold-Spray*
- 12:15-12:30 PM Lais Lopes - *The challenge of measuring friction and wear of industrial components on the lab scale*
- 12:30-12:45 PM Ulises García-Ramírez - *Erosive behavior of AISI 310 stainless steel under impact of cryogenic jets*
- 12:45-01:00 PM Todor Vuchkov - *Tribological studies of sputtered WSC coatings with conventional and graded composition*
- 01:00-02:00 PM LUNCH
- 02:00-02:30 PM **KEYNOTE 2** – Prof. Markus Wimmer - *Cartilage Lubrication and Wear: Knowns and Unknowns*
- 02:30-04:00 PM **SESSION B: CHARACTERIZATION TECHNIQUES AND TESTING METHODS**
CHAIRS: Dr. Jorge Seabra and Dr. Amaya Iguarta

- 02:30-02:45 PM** Fernando Lopez-Uruñuela - *Study of the early stages of WEA formation in pre-cracked and hydrogen charged 100Cr6 bearing steel*
- 02:45-03:00 PM** Sharjeel Ahmed Khan - *A Crossed Cylinder Tribological Test against New Multi-material (CFRP-Ti) Stacks Configuration*
- 03:00-03:15 PM** Amilcar Ramalho - *Friction of soft contact lenses*
- 03:15-03:30 PM** Paul Staudinger - *A Tribological Test Method for PVA Hydrogels and Articular Cartilage*
- 03:30-03:45 PM** Álvaro Rico - *Using Contact Mechanics to describe the time dependent behavior of Polyacrylamide based hydrogels*
- 03:45-04:00 PM** Amaya Igartua - *Ceramic tribocoatings for die protection in Low Pressure Die Casting process*
- 04:00-04:15 PM** **COFFEE BREAK / POSTERS SESSION / TECHNICAL EXHIBITIONS**
- 04:15-05:45 PM** **SESSION C: BIOTRIBOLOGY/ MODELLING AND SIMULATION IN TRIBOLOGY**
CHAIRS: Dr. Amilcar Ramalho and Dr. Markus Weimer
- 04:15-04:30 PM** Diana Silva - *Effects of non-conventional sterilisation methods on PBO-reinforced PVA hydrogels for cartilage replacement*
- 04:30-04:45 PM** Ana Branco - *3D printing of leucite-based materials reinforced with zirconia for dentistry*
- 04:45-05:00 PM** Juan Sánchez-López - *Low friction/wear properties of snake skins: a case study for mimicking nature tribological behavior*
- 05:00-05:15 PM** Jorge Seabra - *Torque loss model for axially pre-loaded tandem rolling element bearings*
- 05:15-05:30 PM** Lais Lopes - *How can we simulate bio-medical tribological contacts on the lab scale?*
- 05:30-05:45 PM** Deepak Veeregowda - *Traction, Stribeck and scuffing characteristics of lubricants in rolling-sliding contacts using twin disc*
- 05:45-06:15 PM** **SCIENTIFIC COMMITTEE MEETING**
- 07:30-10:30 PM** **CONFERENCE DINNER**

PROGRAMME – 7th OCTOBER 2022

- 09:00- 09:30 AM** **KEYNOTE 3** – Prof. Peter Dearnley - *Corrosion-wear (tribocorrosion) mechanisms of hard coated stainless steels*
- 09:30- 11:00 AM** **SESSION D1: SURFACE ENGINEERING, SURFACE TREATMENT AND COATINGS**
CHAIRS: Dr. Josefa Fernandez and Dr. Jesus Rodrigues
- 09:30-09:45 AM** Albano Cavaleiro - *Tribological performance of laser-treated WSC sputtered coatings sliding against NBR rubber*
- 09:45-10:00 AM** María García Guimarey - *Study of 2D Nano-coated Steel Surfaces for Wear Reduction*
- 10:00-10:15 AM** Raquel Bayón - *Plasma Electrolytic Oxidation coatings on a secondary cast Al-Si alloy for brake applications*
- 10:15-10:30 AM** Juan Vazquez Martinez - *Enhancing the lubrication effect on tribological response of laser textured PH stainless steel surfaces*
- 10:30-10:45 AM** Irene Del Sol - *Study on the effect of LST atmosphere on the tribological wear behavior of Ti6Al4V*
- 10:45-11:00 AM** Ivan Rodrigues - *Dry sliding wear of a laser-clad NiCrBSi-WC composite coating*
- 11:00-11:15 PM** **COFFEE BREAK / POSTERS SESSION / TECHNICAL EXHIBITIONS**
- 11:15-11:45 AM** **KEYNOTE 4** – Prof. Mathew Mathew - *Tribocorrosion Aspects of Biomedical Implants: Where are we now?*
- 11:45-01:15 PM** **SESSION D2: SURFACE ENGINEERING, SURFACE TREATMENT AND COATINGS/ LUBRICANTS AND ADDITIVES/ MICRO AND NANOTRIBOLOGY/ TRIBOCORROSION**
CHAIRS: Dr. Mathew Mathew and Dr. José Gomes
- 11:45-12:00 PM** Bernardo Diniz - *Wear resistance of laser clad 25NiCr – 75CrC coatings*
- 12:00-12:15 PM** Bernardo Tormos - *Performance assessment of different base oils for e-thermal fluids applications in BEVs*
- 12:15-12:30 PM** Rúben Gonzalez - *Oxidation influence on the electrical conductivity of transmission fluids in electric vehicles*
- 12:30-12:45 PM** Daniel Soares - *Measuring the Behaviour of Brake Materials More Efficiently*
- 12:45-01:00 PM** Jesús Rodriguez - *A molecular dynamics study of adhesion in metallic contacts*
- 01:00-01:15 PM** Daniel Ramírez-Arreola - *Influence of swirl number and incidence angle on erosion-corrosion behavior of API steel pipe under swirling jets*
- 01:15 – 01:30 PM** **CLOSING SESSION**
- 01:30 – 02:30 PM** **LUNCH**
- 02:30 – 07:00 PM** **SOCIAL PROGRAMME**

ORAL COMMUNICATIONS

KEYNOTE 1

Tribology in Leonardo da Vinci's Codex Madrid

Ian Hutchings*

St John's College, Cambridge CB2 1TP, UK

*imh2@cam.ac.uk

Leonardo da Vinci (1452-1519) was not only a great artist, but also a scientist and an engineer with enormously broad interests. More than 6000 pages of his notes and sketches still exist, dispersed among different collections. For tribologists, one of the most important sources is the Codex Madrid I, now in the Biblioteca Nacional in Madrid. This volume of 191 double-sided pages is the closest that Leonardo ever came to writing a coherent account of the science and practice of mechanics.

Leonardo used empirical observations coupled with deep physical insight to investigate tribological phenomena. Driven by an intense curiosity, he recorded his thoughts in a mixture of words and images which is sometimes challenging to understand. Leonardo had a deep and nuanced understanding of the factors that affected friction, and applied that understanding, within the limits of his grasp of mechanics, to several mechanical systems, returning to the subject repeatedly over more than 20 years. His work pre-dated that of Amontons by 200 years. His notes on wear and lubrication show that he correctly understood many of the concepts that we still use today. He studied bearings in practical use, and by describing new designs of bearing, showed great ingenuity in extending contemporary engineering practice,

Although Leonardo's work on tribology did not become widely known until well into the 20th century, he stands in a unique position as a remarkable and inspirational pioneer of the subject.

SESSION A1: FRICTION AND WEAR

Tribology behavior of nanolubricants containing oleic acid coated ZnO nanoadditives

Fátima Mariño ^{a,*}, Enriqueta R. López ^a, Ángela Arnosa ^b, Manuel A. González Gómez ^b, Yolanda Piñeiro ^b, José Rivas ^b, Carmen Alvarez-Lorenzo ^c, Josefa Fernández ^a

^a Laboratory of Thermophysical and Tribological Properties, Nafomat Group, Department of Applied Physics, Faculty of Physics and Institute of Materials (iMATUS), Universidade de Santiago de Compostela, Santiago de Compostela, Spain;

^b NANOMAG Laboratory, Department of Applied Physics, Faculty of Physics and iMATUS, Universidade de Santiago de Compostela, Santiago de Compostela, Spain;

^c Departamento de Farmacología, Farmacia y Tecnología Farmacéutica, I+D Farma Group (GI-1645), Facultad de Farmacia, iMATUS and Health Research Institute of Santiago de Compostela (IDIS), Universidade de Santiago de Compostela, Santiago de Compostela, Spain

*fatima.marino.fernandez@usc.es

Synopsis

In this work synthesized ZnO nanoparticles (NPs) coated with oleic acid (OA) were used [1]. Polyalphaolefin 40 (PAO40) oil dispersions of ZnO-OA at different concentrations were thermophysically and tribologically characterized. Both density and viscosity increased with the concentration of NPs. Tribological tests were performed at 353.15 K. Regarding the tribological behavior, the optimal concentration was 0.25 wt% of ZnO-OA (25% of reduction in friction coefficient and 82% reduction in wear cross sectional area, respect to PAO40). Due to the spherical shape of the NPs, sliding friction changed into rolling friction. This effect together with the mending effect proved by confocal Raman microscopy, explain the better tribological performance of these nanolubricants compared to that of neat PAO40.

Introduction

About 23% of the world's total energy consumption is spent in overcoming friction, and to remanufacture worn parts and spare equipment due wear-related damage [2]. Nanolubricants have shown great potential as antifriction and antiwear additives [3]. However, dispersions of nanoparticles in base oils with long time stabilities are scarce. Surface modification consists in the functionalization of NPs with dispersants or organic molecules with functional groups that can react with the nanoparticles. ZnO NPs as additives, improve the lubricating properties of different oils [4, 5]. In addition to their good tribological properties, ZnO NPs have other interesting properties such as high diffusion, strong adsorption in metals, and large surface area-to-weight ratio [6].

Results and Discussion

1. Nanolubricant preparation and stability

Shamhari et al. [7] method was used to prepare ZnO NPs and then coated with OA using an esterification reaction [1]. 65wt% of the NPs content is OA and is coated with around 91 ± 3 OA molecules per NP surface area unit, in nm^2 , as obtained by TGA. The experimental diffraction pattern of ZnO-OA was obtained with XRD. The effective surface functionalization of these NPs was also analyzed by FTIR and Raman spectroscopies. TEM micrograph of the OA coated ZnO NPs showed spherical cores with a mean size of 10 nm.

Nanodispersions with different concentrations of ZnO-OA were prepared (0.1, 0.25, 0.5, 0.75 and 1.0 wt%). The 0.25 wt% nanodispersion stability was analyzed both visually and through refractive index measurements attaining 29-day stability. By contrast, ZnO NPs without the OA coating are not dispersible in chloroform or PAO40.

2. Thermophysical and tribological characterization

Density of the nanodispersions showed a slight increment with the mass concentration of NPs. Dynamic viscosity also increased with the concentration of ZnO-OA NPs due to the intensification of the internal shear stress of the nanolubricants. Meanwhile the viscosity indices (VI) of the nanodispersions slightly decreased compared to PAO40 and remained approximately constant regardless of the composition.

The studied dispersions reduced the coefficient of friction between 14% and 25% compared to PAO40 in a steel-steel contact. The lowest friction and wear values were achieved when 0.25 wt% ZnO-OA was added to PAO40. The greatest reductions for the wear parameters, obtained also for the nanodispersion with 0.25 wt% ZnO-OA, were 38%, 68% and 82%, in wear track width, depth and cross-sectional area, respectively. Roughness (Ra) of wear tracks was another parameter measured, the 0.25 wt% dispersion have the best polishing performance. The Raman map of the worn surface tested with PAO40 + 0.25 wt% ZnO-OA shows the presence of PAO40, oleic acid, i.e., ZnO-OA nanoparticles, and iron oxides. In addition, the presence in this tribofilm of ZnO-OA NPs was also confirmed by ICP-MS analysis of the tested nanolubricant, which contains a 16 % ZnO-OA NPs less than untested nanolubricant.

Conclusions

In the studied conditions, all the nanolubricants show better tribological behavior than that of PAO40, being the optimal concentration 0.25 wt% of ZnO-OA (25% friction reduction and 82% cross sectional area reduction). The improvement of the tribological performance of the nanolubricants respect to PAO40 could be due to the occurrence of rolling and mending mechanisms owing to the spherical shape and the adsorption of the additives on the rubbed steel surfaces.

Acknowledgments

The authors thank Repsol for providing the PAO40 sample. This work was supported by the Ministry of Science, Innovation and Universities - State Research Agency (AEI) of Spain and the European Regional Development Fund (ERDF, FEDER in Spanish) through the ENE2017-86425-C2-2-R project, and by the Xunta de Galicia through ED431C 2020/10.

References

- [1] F. Mariño, et al., ZnO nanoparticles coated with oleic acid as additives for a polyalphaolefin lubricant, *Journal of Molecular Liquids*, 348 (2022) 118401.
- [2] K. Holmberg, A. Erdemir, Influence of tribology on global energy consumption, costs and emissions, *Friction*, 5 (2017) 263-284.
- [3] W. Dai, et al., Roles of nanoparticles in oil lubrication, *Tribology International*, 102 (2016) 88-98.
- [4] J. Zhao, et al., Nanolubricant additives: A review, *Friction*, 9 (2021) 891-917.
- [5] S.B. Mousavi, et al., Viscosity, tribological and physicochemical features of ZnO and MoS₂ diesel oil-based nanofluids: An experimental study, *Fuel*, 293 (2021) 120481.
- [6] L. Wu, et al., Tribological properties of oleic acid-modified zinc oxide nanoparticles as the lubricant additive in poly-alpha olefin and diisooctyl sebacate base oils, *Royal Soc. Chem. Adv.*, 6 (2016) 69836-69844.
- [7] N.M. Shamhari, et al., Synthesis and characterization of zinc oxide nanoparticles with small particle size distribution, *Acta Chim. Slov.*, 65 (2018) 578-585.

Reviewing Stability over Time and Tribological Performance of Non-Aqueous Lubricants containing Chemical Modified Nanoadditives

Fátima Mariño, José M. Liñeira del Río, Enriqueta R. López, Josefa Fernández*

Laboratory of Thermophysical and Tribological Properties, Nafomat Group, Department of Applied Physics, Faculty of Physics and Institute of Materials (iMATUS), Universidade de Santiago de Compostela, Santiago de Compostela, Spain

*josefa.fernandez@usc.es

Synopsis

Currently, nanotechnology is being used to improve the performance of lubricants because, in general, nanoadditives have better tribological properties compared to traditional additives. This work reports an overview of the advances in this field, reviewing the preparation methods and the results of tribological behavior for lubricants containing modified nanomaterials as additives, which are called nanolubricants.

Introduction

Nanotechnology is considered to play a leading role in the development of the 21st century. Different studies have already shown that nanoadditives can reduce friction and/or wear in mechanical systems. Nevertheless, the use of nanoadditives in lubrication implies a challenge that must be considered: achieving homogeneous dispersions of nanoadditives and base oils and guaranteeing their temporal stability. In most publications on tribology of nanolubricants, their stability is not thoroughly studied. In recent years, there has been a growing interest in the surface modification of nanoparticles, that is, in their functionalization [1]. The particles obtained in this way are called coated nanoparticles, functionalized nanoadditives or hybrid nanomaterials. Homogeneous and long-term stable nanolubricants can be designed by combining physical and chemical treatments (use of surfactant or surface modification) [2].

In this work a review on the stability over time as well as the tribological performance of non-aqueous lubricants containing chemical modified nanoadditives is presented. Firstly, the results on the temporal stability of the nanodispersions are shown, followed by a review of the articles with the tribological behavior of nanolubricants with temporal stabilities greater than four weeks.

Results and Discussion

The study of nanolubricants is a topic of growing interest as can be observed in Figure 1, where are presented the number of the articles published since 1998 containing the topics “lubricant” “nano” “additive” and excluding water-based lubricants determined using Web of Science. The same search but also restricted to chemically modified nanoparticles leads to almost half of published articles.

1. Time stabilities

The main results of the literature on the stability of lubricants containing chemical modified nanomaterials (carbon-based nanomaterials, metals, metal oxides, metal sulfides and nanocomposites among others) were reviewed. Base oils were mainly mineral oils followed by polyalphaolefins (PAOs). Among the more stable nanodispersions are those containing modified metal oxide nanoparticles; finding the best stabilities over time, greater than 11 months for dispersions of superparamagnetic nanoparticles in trimethylolpropane trioleate, probably due to the mutual affinity since the base oil contains three oleate groups and being the functionalizing agent oleic acid and the use a rotary evaporator. In addition, it was found that the stability over time depends strongly on the viscosity of the base oil.

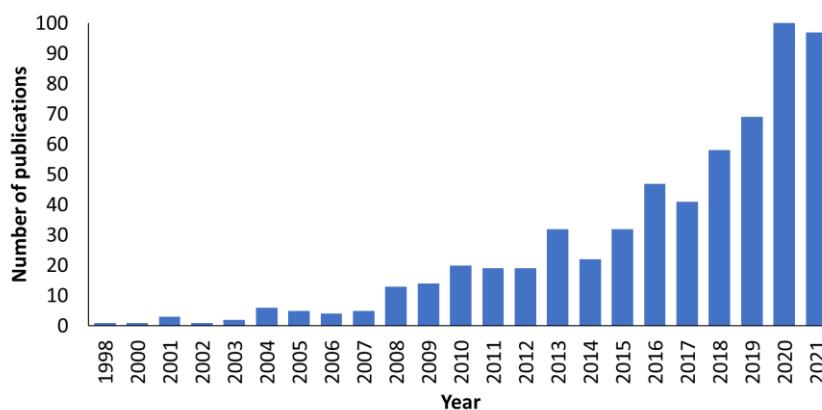


Figure 1. Number of published articles for the search “lubricant” “nano” “additive” excluding water based lubricants using WOS

2. Tribological Behavior

The tribological results from those articles reviewed in the previous section, involving nanolubricants with stabilities of at least 28 days, were analyzed. Articles comparing the performance of the nanolubricant containing the bare nanomaterial and the corresponding containing the modified nanomaterial are scarce. Although mineral base oils are the most used in tribological studies, in general, the best tribological reductions due to the modified nanoparticles were obtained with PAO base oils. In most cases, regardless of base oil, modified nanoparticle dispersions improve wear by a greater percentage than friction. Reductions in friction of up to 85 % and in wear of up to 97 %, (in terms of wear volume, which appears to be the most sensitive wear parameter) were found. Regarding the tribological mechanisms involving nanoadditives, regardless of the nature of the nanoadditive, and independently of what other mechanisms may be present, the formation of both adsorbed films and tribochemical reaction films on worn surfaces are those reported most often.

Conclusions

Unfortunately, in most of the literature, information on stability over time of nanolubricants is unclear or even non-existent. Time stability of more than 11 months was reported for some dispersions. Regarding tribological behavior, the lack of uniformity in the conditions and the materials of the experiments, makes it very difficult to compare several results with others. Standard measurement conditions should be defined in a near future to improve the reliability of the comparisons of the tribological results, among them those obtained using nanoparticles as additives.

Acknowledgments

The authors wish to express their thanks for the financial support of the State Research Agency (AEI) of Spain and the European Regional Development Fund (ERDF, FEDER in Spanish) through the ENE2017-86425-C2-2-R and PID2020-112846RB-C22 projects, and of Xunta de Galicia through ED431C 2020/10.

References

- [1] Y. Chen, P. Renner and H. Liang, Dispersion of Nanoparticles in Lubricating Oil: A Critical Review, *Lubricants* 7 (2019) 7.
- [2] N.F. Azman and S Samion, Dispersion Stability and Lubrication Mechanism of Nanolubricants: A Review, *International Journal of Precision Engineering and Manufacturing-Green Technology* 6 (2019) 393.

Tribological behavior enhancement using coated TiO₂ nanoparticles as PAO8 additives

José M. Liñeira del Río ^{a,b,*}, Fatima Mariño ^a, David E. P. Gonçalves ^b, Jorge H. O. Seabra ^c, Enriqueta R. López, Josefa Fernández ^a

^a Laboratory of Thermophysical and Tribological Properties, Nafomat Group, Department of Applied Physics, Faculty of Physics and Institute of Materials (iMATUS), Universidade de Santiago de Compostela, Santiago de Compostela, Spain

^b Unidade de tribologia, vibrações e manutenção industrial, INEGI, Universidade do Porto, Porto, Portugal

^c FEUP, Faculdade de Engenharia da Universidade do Porto, Porto, Portugal

*josemanuel.lineira@usc.es

Synopsis

This work presents the antifriction and antiwear properties of TiO₂ nanoparticles coated with oleic acid, TiO₂-OA, as additives of a low viscosity polyalphaolefin base oil, PAO8. For this aim, four PAO8 based nanodispersions were formulated: PAO8 + 0.10 wt% TiO₂-OA, PAO8 + 0.25 wt% TiO₂-OA, PAO8 + 0.35 wt% TiO₂-OA and PAO8 + 0.50 wt% TiO₂-OA, to find the optimal mass concentration of nanoadditive. Tribological tests were carried out at pure sliding conditions and rolling-sliding conditions at 393.15 K, with the aforementioned formulated nanolubricants and with PAO8 base oil. The wear generated during the tribological tests was characterized by means of a 3D profilometer, whereas the possible tribological mechanisms were analyzed using Raman mapping and the roughness values.

Introduction

Nowadays, the industry demands improved lubricants to enhance energy efficiency and sustainability [1]. This requirement is critical for electric vehicles (EVs) as around 60% of the energy provided to an EV is used to overcome friction: 40% to rolling resistance and 20% to inertia at acceleration and braking [2]. To meet the lubricant requirements for upcoming EVs, it is essential to add new additives to base oils [3]. Hence, the study of nanomaterials as additives can help the development of a new generation of transmission fluid (low-viscosity lubricants) specially adapted to the needs and detailed driving structures of EVs. Besides, many nanoparticles are environmentally friendly in contrast to other conventional additives [4].

Results and Discussion

All the studied TiO₂-OA nanolubricants showed friction coefficients lower than those obtained with PAO8 base oil (Figure 1), reaching a maximum reduction for the 0.35 wt% TiO₂-OA nanolubricant, for both test conditions (pure sliding and rolling-sliding). Regarding the rolling-sliding tests, it should be noted that the TiO₂-OA nanoparticles play a crucial role in reducing friction, especially at low speeds. Tribological specimens studied under pure sliding conditions with designed TiO₂-OA nanolubricants evidenced lower wear than that tested with PAO8 base oil, obtaining the lowest wear values with the PAO8 + 0.35 wt% TiO₂-OA nanolubricant. Thus, the obtained reductions were of 26%, 65% and 73 %, for wear scar diameter, maximum depth and transversal area, respectively. Furthermore, through confocal Raman microscopy and roughness evaluation of worn tribological samples, it can be suggested that polishing and tribofilm formation mechanisms occur.

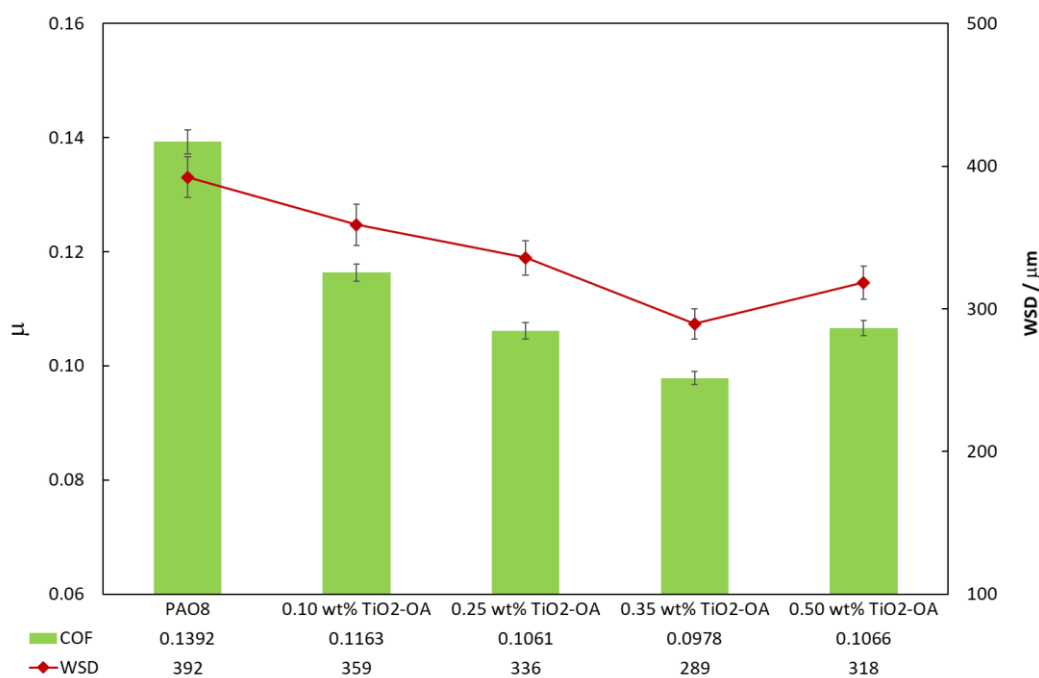


Figure 1. Friction coefficient, μ , and wear scar diameter (WSD), obtained with PAO8 and its dispersions containing TiO₂ coated with oleic acid nanoparticles.

Conclusions

Oleic acid coated TiO₂ nanoparticles were successfully synthesized. The friction coefficients obtained with TiO₂-OA nanolubricants are lower than those observed for neat PAO8 oil. For rolling-sliding tests, the antifriction capacity of TiO₂-OA nanoparticles is greater at low speeds. For all the TiO₂-OA nanolubricants the wear generated in pins is much lower than for the PAO8 base oil being the best reductions of 26%, 65% and 73 % in width, depth, and area respectively (PAO8 + 0.35 wt% TiO₂-OA nanolubricant). Through roughness and Raman investigation of worn pins, it is suggested that the lubrication mechanism can be explained by the adsorbed tribofilm as well as the polishing effect.

Acknowledgments

The authors wish to express their thanks for the financial support of the State Research Agency (AEI) of Spain and the European Regional Development Fund (ERDF, FEDER in Spanish) through the PID2020-112846RB-C22 project, and of Xunta de Galicia through ED431C 2020/10.

References

- [1] G.B. Calderon Salmeron, Enabling More Efficient E-Mobility: Grease Development by a Novel Bearing-Grease Test Machine, (2019): 569 MSc Thesis TRITA-ITM-EX 2019:569, KTH Industrial Engineering and Management Machine Design.
- [2] K. Holmberg and A. Erdemir, The impact of tribology on energy use and CO₂ emission globally and in combustion engine and electric cars, *Tribology International*, 135 (2019) 389-396.
- [3] S.C. Tung, M. Woydt, R. Shah, Global Insights on Future Trends of Hybrid/EV Driveline Lubrication and Thermal Management, *Frontiers in Mechanical Engineering*, 6 (2020).
- [4] W. Dai, B. Kheireddin, H. Gao, H. Liang, Roles of nanoparticles in oil lubrication, *Tribology International*, 102 (2016) 88-98.

Strain hardening behavior of CoCrMo

Luís Vilhena ^a, Gonçalo Coutinho ^a, Amílcar Ramalho ^a

^a CEMMPRE – Centre for Mechanical Engineering, Materials and Processes, University of Coimbra, Coimbra, Portugal

* luis.vilhena@uc.pt

Synopsis

The Co28Cr6Mo alloy is used in several biomedical applications subject to high wear caused by continuous mechanical stresses (knee, shoulder, hip joint prostheses, etc.). Since there is a big difference between the yield strength and the ultimate strength, the potential for work hardening of Co28Cr6Mo alloy is higher. The aim of the present research work is to identify and optimized conditions for the mechanical surface treatment of Co28Cr6Mo alloy, using a lathe in order to improve its mechanical characteristics, namely its wear behavior.

Introduction

To understand whether a material is prone to hardening and to quantify this proneness, it is necessary to consider the definition of toughness. Toughness is the ability of a material to absorb energy and deform plastically without fracturing. A material with a high toughness allows favorable conditions for its hardening. There is a large difference between the yield strength (503 MPa) and the ultimate tensile strength (952 MPa) of CoCrMo alloy [1]. The area of the graph between these two values represents the extent associated with the strain hardening. The greater this difference, the greater its ability to harden. Thus, this Co28Cr6Mo alloy proves to be favorable for mechanical treatment as it has a very high toughness. The hardening of this Co28Cr6Mo alloy is particularly important for the purpose of this research work as it promotes increased wear resistance (it allows a lower wear rate) which is the ultimate objective since this alloy is used in biomedical applications and its longevity on human body is essential for the patient's life quality.

Materials and Methods

In the mechanical lathe, a cylinder of Co28Cr6Mo was positioned crossed against a cylinder of a much higher Young's modulus material, WC-Co in order to simulate a rigid body. 10 passages were taken into account in every test as exemplified in Fig. 1.



Figure 1. Top view of the contact between the Co28Cr6Mo and the WC cylinders.

Results and Discussion

Fig. 2 shows the grain deformation using SEM (Scanning Electron Microscope) while the Fig. 3 shows the Radial hardness analysis after the Hardening of the alloy samples on the lathe.

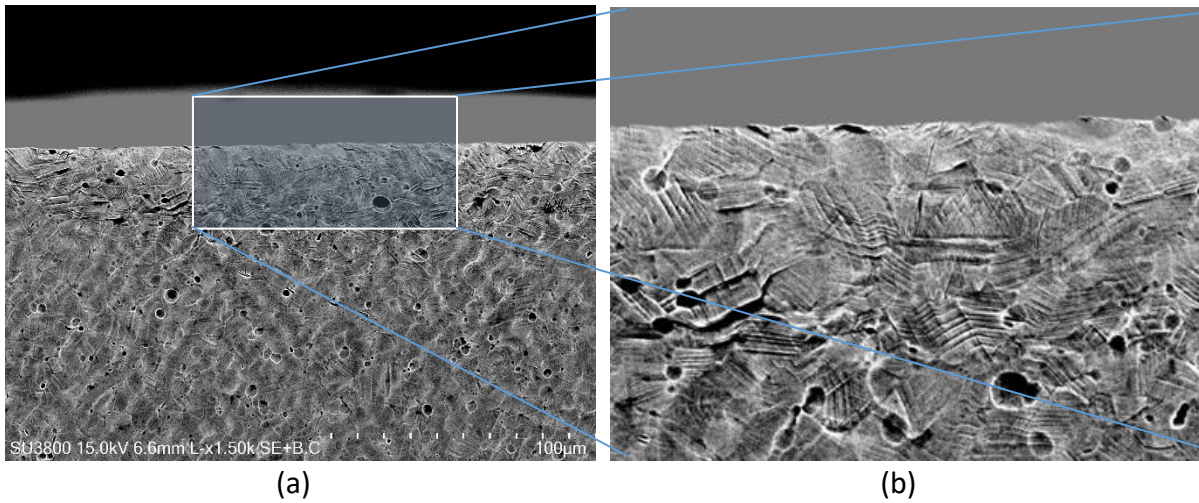


Figure 2. SEM micrographs showing grain deformation of the cross-section: (a) lower magnification (b) higher magnification.

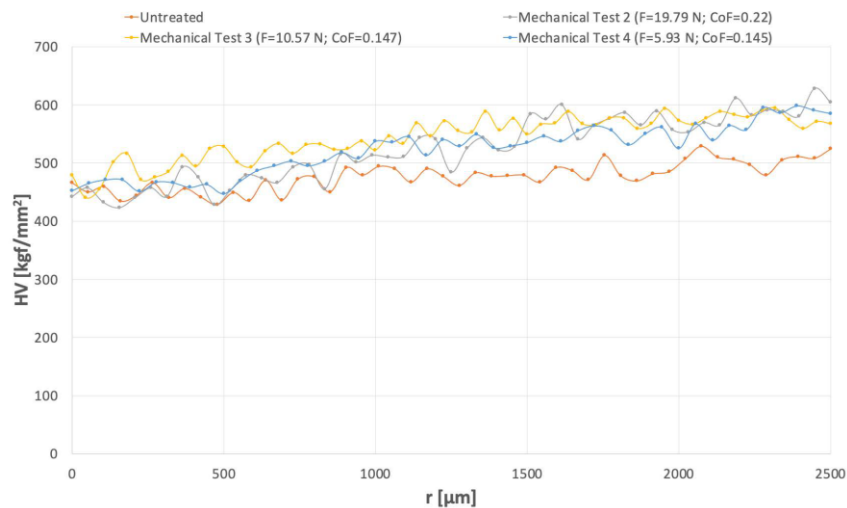


Figure 3. Evolution of the Hardness with the radial distance for specimens subject to different hardenings (untreated, 5.93 N, 10.57 N and 19.79 N).

Conclusions

It was clear from the experimental results presented in this research work that is possible to induce the hardening of the Co28Cr6Mo specimens, with consequent gains in wear resistance.

References

- [1] Balagna, C., S. Spriano, and M.G. Faga (2012), 'Characterization of Co–Cr–Mo alloys after a thermal treatment for high wear resistance', *Materials Science and Engineering: C*, 32 (7), 1868-1877.

Cutting tool with micro-grooves filled with carbon nanotubes

Fernando S. F. Ribeiro ^a, Luiz E. A. Sanchez ^{a*}, Gilberto M. B. Gonçalves ^a, Eduardo C. Bianchi^a

^a Department of Mechanical Engineering - Sao Paulo State University – Unesp, Bauru - SP

*luiz.sanchez@unesp.br

Synopsis

In this study, micro-grooves on the rake surface of turning cutting tool were made, parallel to the cutting edge, filling them with carbon nanotubes (CNTs), which thermal conductivity is about 80 times higher than the cutting tool material (cemented carbide). In addition to the thermal effect of heat dissipation, the improvement of tribological conditions promoted by the micro-grooves and the progressive spreading of the nanotubes at the chip/tool interface was aimed. The study evaluated the performance of the following cutting tools: micro-grooved filled with carbon nanotubes compared to conventional cutting tools; micro-grooves without carbon nanotubes; and textured (i.e., small micro-grooves) with the most common geometries found in the literature. The micro-grooves filled with CNTs showed the most promising results among all the textures tested.



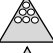

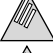



Introduction

Textured cutting tools can increase the life of cutting tools due to the improvement of tribological conditions at the chip/tool interface by minimizing friction, reducing the chip-tool contact area, and increasing convection heat exchange. [1,2]. Filling textures with a material of high thermal conductivity can help transport heat from higher temperature regions to beyond them, modifying the temperature gradient of the cutting tool. At the same time the beneficial characteristics of the textures remain, and the formation of a friction-reducing film can occur. At the same time, the beneficial characteristics of the textures remain, and the formation of a friction reduction film can occur. In the search for a material with these characteristics, the carbon nanotube (CNT) is highlighted since its thermal conductivity is between 2000 and 6000 W/m.K. This work proposes the compaction of carbon nanotubes inside the textures with the main objective of maximizing the heat dissipation from the chip-tool contact zone and additionally introducing a third body capable of minimizing friction at this interface. To evaluate the work, cutting tools with different texture depths (0.25, 0.50, and 0.75 mm with a length of 0.3 mm) were filled with CNTs. Their performance in terms of tool life and machining force were compared with a conventional cutting tool, micro-grooved with depth 0.1 and 0.25 mm besides texture with micro-holes (depth of 0.005 and diameter of 0.05 mm) and small micro-grooves (depth of 0.005 and length of 0.02 mm), these two latter found in the literature [3]. The cutting conditions used in the tests were: cutting speed 150m/min; depth of cut 1.0 mm; and feed 0.1 mm/rev.

Results and Discussion

Table I shows the types of cutting tools used in the tests, while Figure 1 presents the tool life, which it is possible to observe that the three highest lives were obtained with the filling of CNTs. Compared to the other textures, the superior performance of micro-grooves filled with CNTs is due to both the thermal effect and the presence of CNT that works as a third body at the chip-tool interface, leading to a decrease in machining forces, as can be seen in Figure 2. Among the texture without CNTs, the micro-groove of depth 0.25 mm presented the best performance since its capability to accumulate debris is larger. Although not shown, the behavior of the temperature followed the machining force, proving the beneficial thermal influence of CNTs.

Table I – Types of cutting tools used in the work.

Conventional		Micro grooves of 250 µm	 0.25
Micro holes from literature		Micro grooves of 250 µm with CNTs	 0.25
Micro grooves from literature		Micro grooves of 500 µm com CNTs	 0.75
Micro grooves of 100 µm	 0.10	Micro grooves de 750 µm com CNTs	 0.50

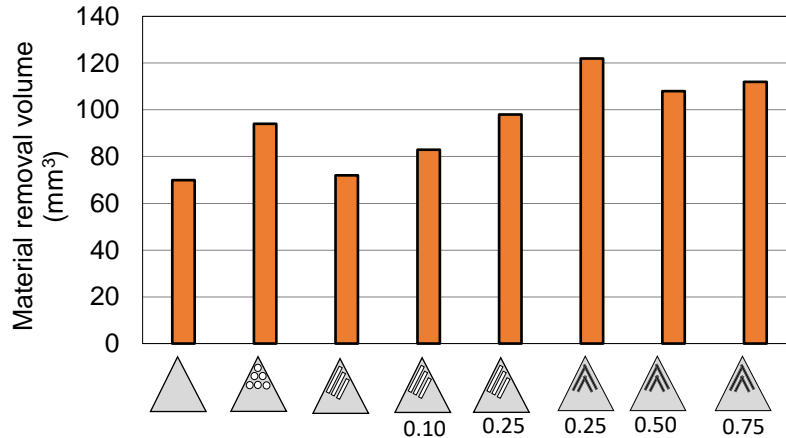


Figure 1. Tool life in material removal volume for the test conditions.

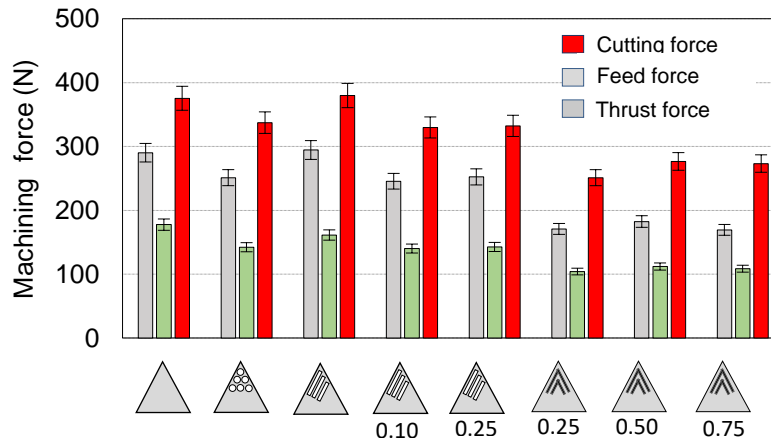


Figure 2. Machining force components for the test conditions.

Conclusions

The confection of micro-grooves larger than textures from literature presented better performance since they allow for storing debris formed on the chip-tool contact inside them. On the other hand, the micro-grooves filled with CNTs reached the best results of all tests once allied the thermal and tribological effect from the third body to the textures.

References

- [1] F.S.F. Ribeiro, J.C. Lopes, E.C.Bianchi, L.E.A. Sanchez, Applications of Texturization Techniques on Cutting Tools-a survey. *Int. J. Manuf. Technol.*, 109 (2020), 1117-1135.
- [2] T.Özel, D. Bierman, T. Enomoto, P. Mativenga, Structured and Textured Cutting Tool Surfaces for Machining Applications. *CIRP Annals*, 70, (2021) 495-518.
- [3] T. Sugihara, R. Kobayashi, T. Enomoto, Direct Observations of Tribological Behavior in Cutting with Textured Cutting Tools. *Int. J. of Mach. & Tools Manuf.*, 168 (2021), 103726.

Tribological behavior of cutting tool on Ti6Al4V sample with different grades of self-emulsifying esters with and without anti-corrosion additives

Mariano Planells ^{a*}, Giselle Ramírez ^a, Núria Cuadrado ^a, Montserrat Vilaseca ^a, Gerard Cañellas ^b, Ariadna Emeric ^b, Angel Navarro ^b, Mar Combarros ^b, Lluís Beltran ^b

^aFundació EURECAT, Manresa, Spain;

^bIndustrial Química Lasem, S.A.U., Castellgalí, Spain

* mariano.planells@eurecat.org

Synopsis

Improved machining processes for titanium alloys remain unresolved, due to excessive wear and catastrophic failure of cutting tools. This phenomenon generates low productivity with any available machining system. To avoid this problem, different grades of self-emulsifying esters and water-based anticorrosive additives has been developed for titanium alloy machining processes. In this study, the tribological behavior of the different self-emulsifying ester has been evaluated using a modified “tool-on-disc” configuration test, where Ti6Al4V alloy was selected as disc material. It was observed that the flank wear of tools tends to decrease in the presence of anti-corrosion inhibitors, but in return the COF tends to increase compared to esters without inhibitor.

Introduction

Most of the problems related to the conventional machining of titanium alloys are determined by its high hardness at high temperatures, opposing the plastic deformation necessary for the formation of chips. The low thermal conductivity and high specific heat hinder heat dissipation and a low modulus of elasticity causing the piece to move away due to the action of the shear force. The high consumption of the cutting tools, due to excessive wear, because of the generation of high temperatures in the cutting zone, is the main problem in the conventional machining of titanium alloys [1].

Water is a low-cost lubricant with a high cooling capacity, but its low viscosity and corrosive properties make it unacceptable for most tribological applications. To adjust the performance and improve the properties of water-based lubricants, high quality additives are used to improve wear, prevent corrosion and adhesion between the tool and the workpiece. For this purpose, the anti-corrosion additive reduce corrosion by either forming a protective coating on the metal surface or by neutralizing corrosive contaminants in the fluid by maintaining the pH in a suitable range [2].

In this study, different grades of self-emulsifying esters and anticorrosive additives have been developed to improve titanium machining processes. The main objective of this study is the design of a test to evaluate the coefficient of friction and wear in a cutting tool on Ti6Al4V samples.

Experimental procedure

Tribological tests were carried out using a modified “cutting tool-on-disc” configuration by means of UMT Tribolab equipment. The selected cutting tool was a commercial insert from Ceratizit Group (XDLX 09T308ER-F40 CTC5240), while the disc used is made of a titanium alloy, more precisely, Ti6Al4V. During the test, the specimens were immersed in a small container with lubricant. To simulate machining conditions, the inside edge of the cutting tool was placed in contact with the outer edge of the disc. The linear cutting speed applied for lab test was 60 m/min, this is a conventional value used in industrial machining processes. All tests were performed at 5N of load during with a total distance of 208 m.

For this study, 6 self-emulsifying esters were used with (3% ester, 1.5% anti-corrosion additive and 95.5% water) and without anti-corrosion additive (3% ester and 97% water), obtaining a total of 12 different lubricants. In each lubrication condition, the friction coefficient was obtained and recorded on-line during the test, while a 3D optical profilometer was used to compute the cutting edge of the used tool. Then, comparing the cutting edge profiles at the initial condition and after the test, it has been possible to quantify the wear on the cutting edge of the tool for the different lubrications test conditions.

Results and Discussion

Figure 1 shows the friction coefficient results for the 6 different self-emulsifying esters analyzed and the length of the flank wear of the cutting tools at the end of the test. It is observed that Ester 6 and Ester 5 without anti-corrosion additive show the best results in coefficient of friction, while with anti-corrosion additives they show the best results in wear on the length of the flank. On the other hand, it is observed that the tests performed with lubricant and anticorrosion additives show less wear compared with the tests without additives.

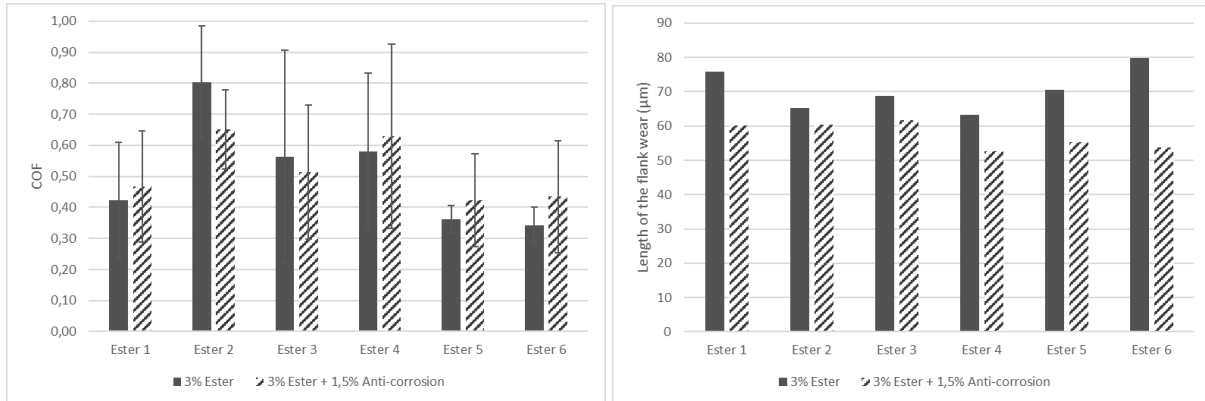


Figure 1. Left: Coefficient of Friction of tool on Ti6Al4V disk test. Right: Length of the flank of tool on Ti6Al4V disk test

Conclusions

Cutting edge wear tends to decrease in presence of anti-corrosion inhibitors, but in return the COF tends to increase compared to esters without inhibitor. Likewise, the inhibitor in some cases increases the dispersion of the friction values during the test.

References

- [1] C. F. Wyen, K. Wegener, Influence of cutting edge radius on cutting forces in machining titanium, CIRP Annals - Manufacturing Technology, vol. 59, n° 1, pp.93-96, 2019.
- [2] A. Tomala, A. K, Tribological properties of additives for water-based lubricants. Wear, 804-810, 2010.

SESSION A2: FRICTION AND WEAR

Evaluation of grinding with two different CBN grains applied to austempered ductile iron (ADI)

José Claudio Lopes^{a,*}, Luiz Eduardo De Angelo Sanchez^a, Eduardo Carlos Bianchi^a

^a Department of Mechanical Engineering, São Paulo State University “Júlio de Mesquita Filho”, São Paulo, Brazil

*claudio.lobes@unesp.br

Synopsis

The grinding process is a vital part of manufacturing that is justified by its capacity to produce precise dimensions and a high-quality surface finish. The austempered ductile iron grinding process was performed using two grinding wheels with cubic boron nitride (CBN) abrasive grains with a variation of friability (GL and GS), which can be studied in tribological aspects related to lubrication conditions because the friability is wide influenced by friction resulted of the process. The performance of each wheel was compared in this study, being CBN low friability (GL) and high friability (GS). Furthermore, the flood lubri-refrigeration process was employed with three different feed rates (0.5, 1.0, and 1.5 mm/min). The test showed that the CBN GL produced the best results in all output metrics due to its better performance caused by the homogenization of the abrasive grain surface that trend to minimized dimensional variations effects in the workpiece surface.

Introduction

The tribological aspects and chemical affinity between the abrasive grains and the workpiece material are factors critical to be considered by industry in the grinding process. As a result, the correct choose abrasive grain is essential to there is a balance between friction and lubrication, improving material removal during the workpiece's shear. Other factors influencing this decision include grain size, bond type, structure, and hardness [1]. The abrasive grains are applied in wheels used for hard steels and nickel-based alloy grinding, and they're becoming common in the manufacturing industry. Thus, the ADI grinding process has been much promise because it has a great combination of mechanical qualities, making it a significant material in the mechanical industry. However, few studies on ADI grinding are performed, being needed more research about the theme. The abrasive grains are applied in wheels used for hard steels and nickel-based alloy grinding, becoming common in the manufacturing industry. Therefore, the ADI grinding process has much promise because it has a great combination of mechanical properties and significant material in the industry. Beyond that, this material is widely used in applications that require resistance to abrasive wear and high hardness, for example, crankshafts, pistons, and other automotive and aeronautic elements.

Results and Discussion

Surface roughness (Ra) and roundness error

Surface roughness is essential to consider while researching and designing elements for other manufacturing processes to be grinding. It determines the workpiece's degree of finishing and dimensional control [2]. As shown in Fig. 1a, the GL wheel (which is less friable) had a lower Ra in all feed rate adjustments, and thereby increasing the feed rate increased the workpiece's Ra. As the feed rate rises, the pressure is exerted between the wheel and the workpiece and the chip's equivalent thickness [3]. This increase is due to the grains' requirement to remove a significant quantity of material in less time to compensate for the higher feed rate. In addition, to compensate for the wheel's higher penetration rate in the workpiece, the forces become more considerable, resulting in more abrupt breakage in the grains and the generation of uneven cutting edges, contributing to the form of an irregular wheel cutting surface. This irregular cutting surface occurs due to the friable aspect of the abrasive grain generates several tribological problems in the accuracy workpiece. Still, it can be solved by improving lubrication and decreasing the friction between the abrasive grain and the workpiece

surface. As a result, it was discovered that a more intensive material removal contributes to an increase in the plowing phenomena resulting in a workpiece with more significant surface irregularity.

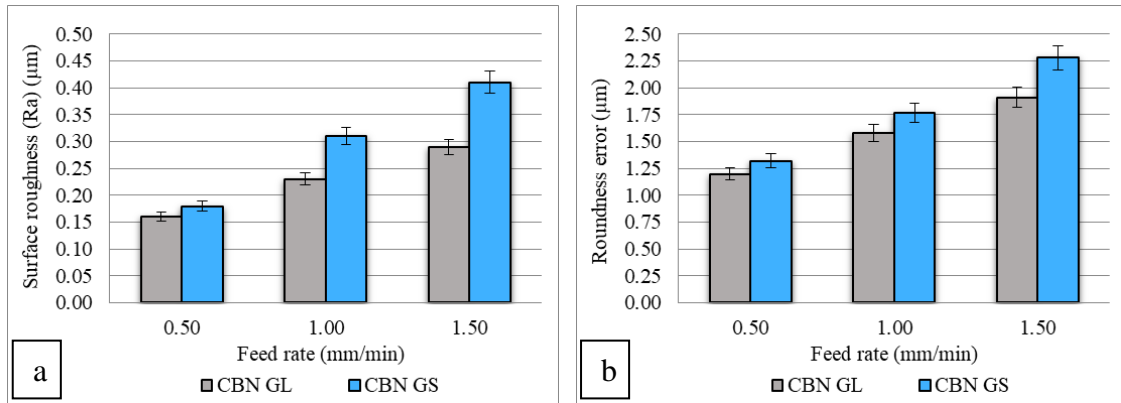


Figure 1. Surface roughness (a) and Roundness error (b) for each setup condition.

The roundness error analysis is critical for determining any mechanical stresses or thermal expansion and complements the roughness analyses. As demonstrated in Fig. 1b, the GL grinding wheel resulted in lower roundness error values than the GS wheel compared to the more friable wheel. Furthermore, the workpiece experiences fewer deformations due to the decreased friability of abrasive grains, preserving their integrity for more extended periods. As a result, the GL wheel demonstrates micro-fracture wear, and its cutting edges are generally more straightforward than other abrasive grains [2]. This uniformity results in a ground surface with minor deformation and roundness error, beyond improved machined material finishing and surface roughness. However, as the feed rate rises, the frequency of friction between the grinding wheel and the workpiece increases, generating much heat in the cutting region and, as a result, causing expansions and deformations on the workpiece's surface. This heat generation can be decreased using other alternatives techniques to lubri-refrigeration, creating a balance between abrasive grain friability and the lubricant method applied. Consequently, the adoption of the GL wheel produced the best roundness error values in all input variables about the flood lubri-refrigerate used in this test.

Conclusions

In the surface roughness parameter, the usage of the CBN GL grinding wheel produced improved results at all analyzed feed rates. Furthermore, using a less friable grinding wheel increased surface stability during the operation, resulting in micro-fractures. As a result, the CBN GL causes minor damage to the workpiece surface than the CBN GS. In the roundness evaluation, this homogeneity characteristic of the abrasive grains also exhibited encouraging results, with the GL wheel presenting the best results.

References

- [1] Sato BK, Lopes JC, Diniz AE, et al (2020) Toward sustainable grinding using minimum quantity lubrication technique with diluted oil and simultaneous wheel cleaning. *Tribology International* 147:106276.
- [2] de Martini Fernandes L, Lopes JC, Volpato RS, et al (2018) Comparative analysis of two CBN grinding wheels performance in nodular cast iron plunge grinding. *The International Journal of Advanced Manufacturing Technology* 98:237–249.

Effect of grinding hardened steel by applying MQL diluted with wheel cleaning jet

Eduardo Carlos Bianchi ^{a,*}, Luiz Eduardo De Angelo Sanchez ^a, Gilberto M. Bento Gonçalves ^a

^a Department of Mechanical Engineering, São Paulo State University “Júlio de Mesquita Filho”, São Paulo, Brazil

*eduardo.bianchi@unesp.br

Synopsis

Cutting fluids have an important role in grinding because they are responsible for the lubri-refrigeration of the cutting zone. Nonetheless, they may harm the environment and the operators' health. Cutting fluids reduce thermal damage, geometric errors, and deterioration of the workpiece's surface integrity. While the typical approach uses a significant amount of oil or an emulsion of oil with water, the minimal quantity lubrication (MQL) technique uses a small amount of oil delivered by a jet of compressed air, yielding results that are equivalent to the conventional method in many circumstances. However, MQL's low cooling capacity and the heat chips clogging the wheel pores are challenges that must be overcome. Therefore, the addition of water to the MQL method in the external cylindrical plunge grinding of AISI 52100 steel is evaluated in this study. Surface roughness (Ra) and roundness error for the conventional method, MQL with pure oil (1:0) and MQL with water (1:1, 1:3, and 1:5 oil-water proportions) with and without grinding wheel cleaning jet (WCJ) were investigated in this study. Furthermore, the diluted MQL 1:5 associated with WCJ was the alternative approach close to the conventional technique, showing potential for the industry.

Introduction

World manufacturing is currently seeking economically viable techniques that maintain the environment and the health of employees. The international society is now mobilizing to regulate and support change in industry's present tactics. Consequently, the development of sustainable manufacturing practices has received attention. Grinding is the most widely utilized abrasive machining technology in applications requiring dimensional precision and minimal surface roughness. Material removal in the form of chips results from several contact points between the workpiece and the abrasive grains in the cutting zone. A considerable amount of energy in this process is dissipated as heat, resulting in high temperatures [1]. Furthermore, heated chips can induce severe wear and clogging of the grinding wheel's pores, increasing surface roughness and roundness error [2]. Cutting fluids are used to reduce the temperature in the wheel-workpiece contact zone, but colonies of bacteria and fungus can develop mostly in the fluid reservoirs of emulsions, degrading them and causing phase separation. Some innovative solutions, such as the minimal quantity lubrication (MQL) technique, are emerging due to the challenges highlighted. Besides, the MQL does not require reuse of the fluid, which reduces the cost of storage, recirculation and maintenance [3]. Nonetheless, Rodriguez et al. (2020) observed that the MQL method's pressurized air did not efficiently remove chips from the cutting zone. Given the difficulties of the environment, human health, and technological deficiency, this work analyzed a new technique that compares the performance of the MQL with and without WCJ and the MQL with pure and diluted oil to the conventional method in the grinding AISI 52100 steel to improve and expand its use.

Results and Discussion

Surface roughness (Ra) and roundness error

According to Fig. 1a, the conventional procedure produced the lowest surface roughness value among all methods evaluated. However, the addition of a 1:5 oil-water diluted with a wheel cleaning jet produced results that were significantly better than the others when compared to the conventional method, demonstrating the positive potential of incorporating water and WCJ into the grinding process. Therefore, the higher chip removal ability and greater cooling capacity of the conventional method are the reasons for this technique's superior performance compared to the MQL 1:5 with WCJ. Still, the results obtained for MQL diluted in water were more satisfactory than those obtained for traditional MQL.

Additionally, the WCJ technique preserved the tendency at lower surface roughness values. Thus, adding water in combination with the WCJ improves the MQL technique significantly.

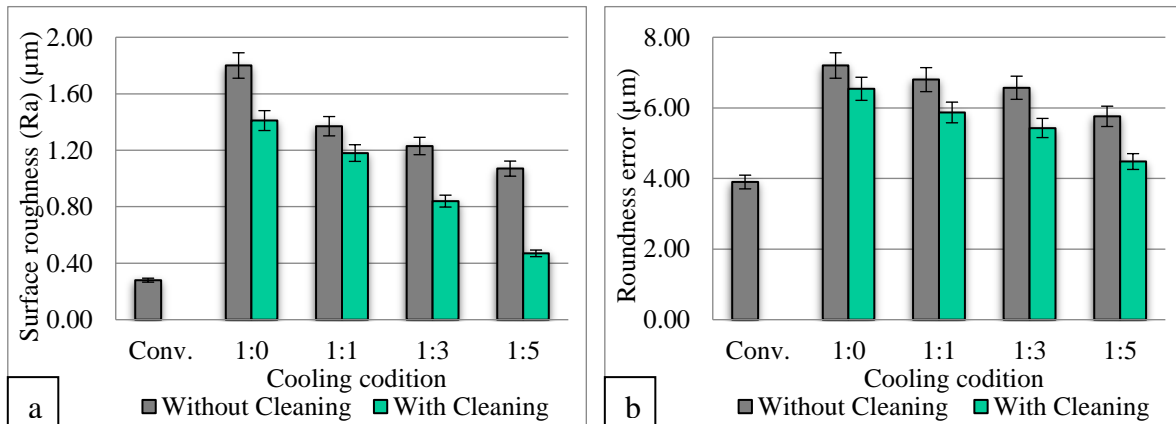


Figure 1. Surface roughness (a) and Roundness error (b) for each setup condition.

The roundness error data for each lubri-refrigeration technique are shown in Fig. 1b. The increase in temperature in the cutting zone causes thermal dilations in the workpiece, which directly affects the geometrical deviation parameters of the workpiece, including roundness error. Compared to the conventional method, the MQL with pure oil has low cooling performance [2]. Therefore, thermal expansion significantly impacts roundness errors in conventional MQL. This fact justifies the technique's low performance compared to the other techniques tested. Thus, the increase in the quantity of water in an emulsion with oil under MQL improves roundness errors. This can be explained by the water boiling in contact with the cutting surface, removing heat from the area, and attenuating the workpiece's thermal expansion.

Conclusions

The addition of water and WCJ to MQL reduces surface roughness and roundness errors compared to the conventional MQL. Aside from that, it produces somewhat lower outcomes than the conventional methods. However, the results and increased durability of the diluted MQL + WCJ make its deployment feasible. Compared to the conventional technique, MQL's reduced coolant capacity with pure oil and lower MQL lubricating capacity with water results in increased grinding wheel wear.

References

- [1] Malkin S, Guo C (2008) Grinding Technology: Theory and Applications of Machining with Abrasives, 2aed. Industrial Press Inc, New York.
- [2] Rodriguez RL, Lopes JC, Garcia MV, et al (2020) Application of hybrid eco-friendly MQL+WCJ technique in AISI 4340 steel grinding for cleaner and greener production. Journal of Cleaner Production 124670.
- [3] Shokrani A, Dhokia V, Newman ST (2012) Environmentally conscious machining of difficult-to-machine materials with regard to cutting fluids. International Journal of Machine Tools and Manufacture 57:83–101.

Effect of the spraying temperature on the erosion behavior of 316L coatings deposited by Cold-Spray

R. Cortés ^a, M.A. Garrido ^{a,*}, P. Poza ^a

^a DIMME – Durability and Mechanical Integrity of Structural Materials, Escuela Superior de Ciencias Experimentales y Tecnología, Universidad Rey Juan Carlos, Madrid, Spain

*miguellangel.garrido@urjc.es

Synopsis

Metallic infrastructures suffer deterioration during their service life, compromising their performance. When a metallic component reaches a damage threshold value, it is commonly replaced by a new one. The coatings' deposition has been revealed as a suitable alternative to repair damaged components, reducing the maintenance costs and residues, and increasing their service life. Recently, the cold-spray deposition process (CS) is being widely used as an effective coating technology to make dense and thick metallic coatings without high temperature oxidation and phase transformation. In this work, the effect of the spraying temperature on the tribological behavior of 316L stainless steel coatings deposited on S355J2 carbon steel by the cold-spray technique has been analyzed. Spraying gas temperatures of 800°C, 900°C, 1000°C and 1100°C combined with a gas pressure of 60 bars were selected. Erosion tests were conducted using angular alumina powder of 50µm as erosive material with an impingement angle of 90°. The results showed a significant effect of the spraying temperature on the erosion resistance of the coatings deposited by CS.

Introduction

Metallic structures undergo damage by erosion due to the continuous impacts of the fine particles carried by air. Carbon steel is widely used in civil metallic infrastructures where the corrosion acts as an additional mechanism of damage [1]. Both mechanisms produce continuous deterioration of these steel components. Once a damage threshold value is reached, the component is replaced by a new one. However, an alternative to reduce residues and maintenance costs consists of repairing the component by spraying a coating onto the damaged area. Thermal spray techniques are widely used for this purpose. High temperature spraying methods, where the particles are projected at temperatures above their melting point, generate coatings characterized by a microstructure different from that of the particles and high residual stresses. These problems may be avoided by the cold-spray technique (CS), where fine solid particles are accelerated by high pressure gas flow up to supersonic velocities and subsequently impinge and deposit on a substrate material. Because the working gas temperature is below the melting point of particle materials, particle deformation and bonding are performed in a solid-state during impact process [2], avoiding oxide formation during deposition. The aim of the present work is to analyze the influence of the carrier gas temperature on the erosion resistance of 316L coatings deposited onto structural carbon steel by CS. A comparative study of the erosion rates of the CS coatings sprayed at 800°C, 900°C, 1000°C and 1100°C of gas temperatures with a constant pressure of 60 bars, was carried out. Erosion tests were conducted by impacting angular alumina particles with an average size of 50 microns and at a speed of 80 m/s. The impingement angle was 90°. The wear rates were estimated by the relation between the difference in mass of the sample before and after the erosion test (in grams) and the mass of the total impingement particles (in grams).

Results and Discussion

Table 1 shows the values of the thickness, porosity, and Vickers microhardness values of the coatings. Figure 1 shows the erosion rates of the coatings. Among the CS coatings, the one deposited at 1100°C showed the lower erosion resistance. Similar wear rates were exhibited by the coatings sprayed at 800°C, 900°C and 1000°C. The coatings revealed higher erosion resistance than substrate and 316L bulk material. Additionally, the coatings sprayed at 1000°C and 1100°C exhibited the lower porosity with relatively high thickness.

Table I. Values of the thickness, porosity, and Vickers microhardness of the coatings. The Vickers microhardness values of the substrate and 316L bulk are also included. The parentheses represent the standard deviations

Material	Thickness (μm)	Porosity (%)	Vickers hardness (GPa)
CS 800°C and 60 bars	689 (± 25)	3.73 (± 0.74)	3.52 (± 0.28)
CS 900°C and 60 bars	467 (± 21)	4.03 (± 0.42)	3.51 (± 0.34)
CS 1000°C and 60 bars	512 (± 22)	2.24 (± 0.22)	3.51 (± 0.21)
CS 1100°C and 60 bars	537 (± 35)	0.49 (± 0.09)	3.38 (± 0.26)
S355J2 substrate	-	-	1.15 (± 0.05)
316L bulk	-	-	2.12 (± 0.09)

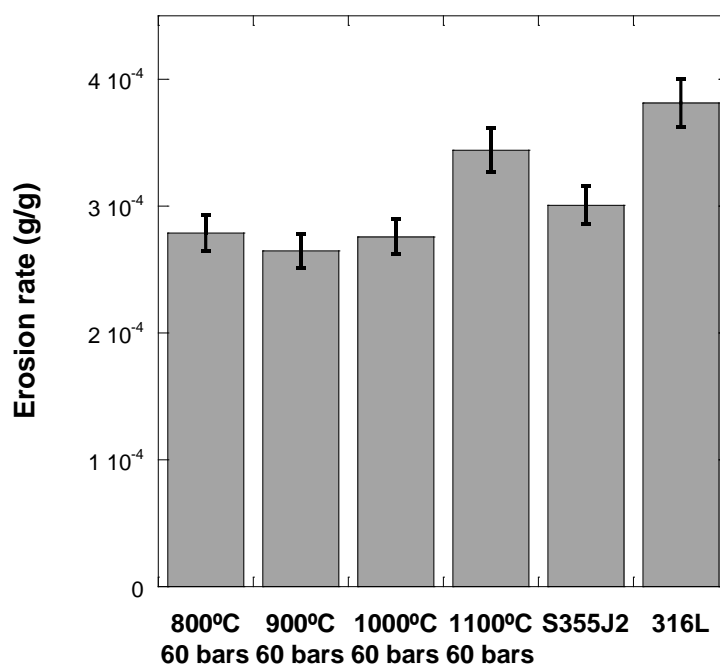


Figure 1. Erosion rates of the coatings, substrate and 316L bulk.

Conclusions

The results revealed that the optimal spraying temperature to deposit 316L CS coatings for repairing purpose was 1100°C. These spraying conditions also provided coatings with reduced porosity and high thickness.

References

- [1] R. Cortés, M.A. Garrido-Maneiro, A. Rico, C.J. Múnez, P. Poza, A.M. Martos, S. Dosta, I. García, Effect of processing conditions on the mechanical performance of stainless steel cold sprayed coatings, *Surface and Coatings Technology*, 394 (2020), 125874.
- [2] P. Poza, M.A. Garrido-Maneiro, Cold-sprayed coatings: Microstructure, mechanical properties, and wear behavior, *Progress in Materials Science*, 123 (2022) 100839.

The challenge of measuring friction and wear of industrial components on the lab scale

D. Drees^{a,*}, L.M. Lopes^a, M.D. Bilde^a, E.P. Georgiou^a

^aFalex Tribology NV, Rotselaar, Belgium

*ddrees@falex.eu

Synopsis

This work focuses on the challenge of measuring tribological properties of industrial components with relevant tests on the lab scale. In most lab tests, industrial components are downscaled, the tribo-contact is (over)simplified, and the contact conditions are altered to accelerate testing. However, by doing so the wear mechanisms/phenomena can be different from reality and subsequently the lab test results do not correlate well to the actual application. In this work, we present how we modified existing equipment to directly test on industrial components, under relevant application conditions. In particular, examples for testing on shock absorbers, USB connectors and oxygen regulators are presented.

Introduction

One of the most difficult industrial issues related to tribology, is the prediction of long-term functionality, be it wear or friction. Indeed, many industrial components and products are required to operate for thousands of hours with minimum wear damage. However, the majority of tribological tests that are performed on lab scale are accelerated and use high contact pressures and simplified contacts. Such tests have a high risk of generating wear mechanisms that do not simulate the in-field application. The safest approach to perform relevant measurements is to perform the tests on the actual components and fine tune the test conditions to accelerate the duration of the test without changing the wear mechanisms. Finding the optimum balance between test time, cost and correlation to the application is one of the main challenges in the tribology world. In this work, we present how we adapt existing methods and equipment to test on actual industrial components and simulate the same contact and motion as in reality. After doing so, the conditions had to be finetuned to accelerate the tests without losing the correlation to the application. This approach is illustrated with three different industrial examples, namely shock absorbers, USB connectors and oxygen regulators. A detailed description of the tested approach, obtained results and added value will be given.

Results and Discussion

Shock absorber tests: To get a match between in-field conditions and the lab-scale testing, a modification of a reciprocating TE-77 tester was performed, enabling the use of actual components: shock absorber rods and rod guides (seals). In these tests two aspects are evaluated: (a) the friction of the system, expressed by the coefficient of friction and (b) the wear on the coated rod, which indicates material loss. One of the main advantages of this method in comparison to component tests is that it allows to monitor the evolution of the coefficient of friction of the rod in the rod guide during sliding. The evolution of the coefficient of friction can be used for relative ranking of the frictional performance of various materials, Figure 1a. Post testing 3D confocal analysis provides a relative ranking of the materials durability, Figure 1b.

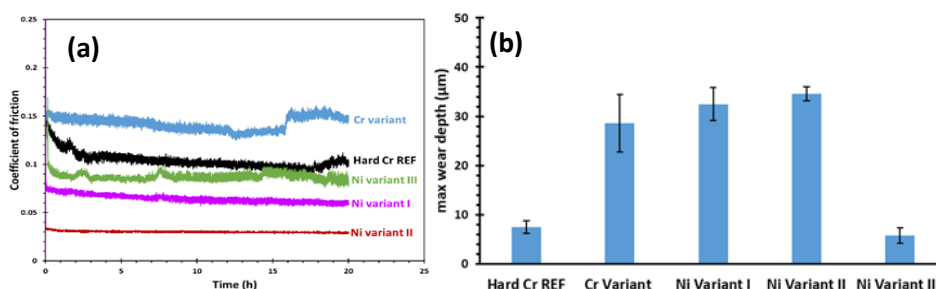


Figure 1. Relative ranking of (a) friction and (b) wear of different coated shock absorber rods.

USB connector tests: The main tribological issue in an automotive application with a USB-connector, is the loss of conductivity due to wear of connecting pins by sliding, caused by automotive vibrations. To avoid this, specialized greases are used to minimize these wear phenomena. However, until now there was no method to measure the failure-time and performance of such a lubricated system. By modifying a TE-77 tester, the complete USB connector can be fixed onto the machine. By adjusting stroke and frequency, the vibrating motion can be recreated. With this method, the friction due to vibrations can be easily measured, as well as the failure time by conductivity measurement, Figure 2.

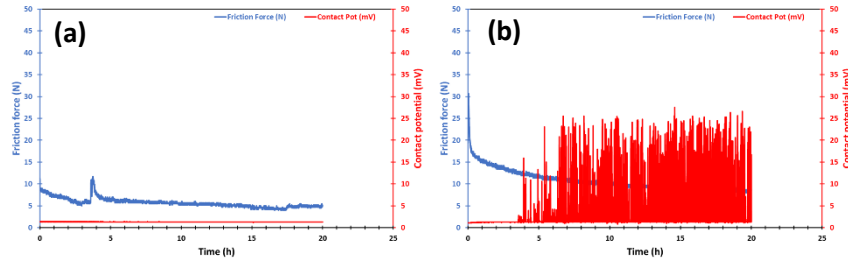


Figure 2. Evolution of the coefficient of friction and contact potential during vibrations of USB connectors. Example (a) without and (b) with failure, indicated by the fluctuation of the contact potential.

Oxygen regulator tests: Failure can occur in flow regulators, due to sticking or wear particles in a rotary contact. This is caused by the generation of wear particles during sliding of an electroformed Nickel disk and rubber o-rings. In this test method, an MCTT tester was used to directly mount the components (Figure 3a) and recreate the rotary reciprocating sliding motion that occurs in the actual application. The performance of the system can be evaluated by the friction evolution, whereas the lifetime is identified by the in-situ monitoring of the wear depth (Figure 3b).

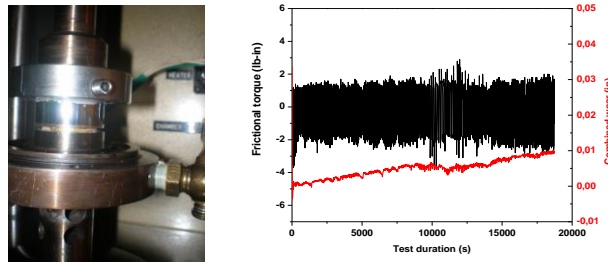


Figure 3. Assembly for evaluating flow-meter components. (b) Evolution of friction and wear during component test.

Conclusions

- Different/modified tribological approaches are needed to simulate different applications and contacts for industrial applications.
- Testing on industrial components is essential to recreate the same contact conditions and failure/wear mechanisms.

Erosive behavior of AISI 310 stainless steel under impact of cryogenic jets

Ulises Alberto García-Ramírez ^a, César Sedano-de la Rosa ^a, Martín Flores-Martínez ^b, Karlos Espinoza ^b, Ezequiel A. Gallardo-Hernández ^c

^a Universidad de Guadalajara, Centro Universitario de la Costa Sur (CUCSUR), Jalisco, México

^b Universidad de Guadalajara, Centro Universitario de Ciencias Exactas e Ingenierías (CUCEI), Jalisco, México

^c Instituto Politécnico Nacional, ESIME U Zac. CdMX, México

*cesar.sedano@academicos.udg.mx

Synopsis

The erosive effect of jets on 310 austenitic stainless steel at low temperatures was analyzed. Four incidence angles were used under impact of Al₂O₃ particles with an average size of 50 μm and 20 ms⁻¹. The total exposure time for the tests was 480 s using a novel cryotribometer designed and constructed by CUCSUR-Tribology group. The test apparatus has an indirect heat exchanger filled with liquid nitrogen. SEM microscopy technique was used to evaluate the wear mechanisms, also superficial hardness was monitored along the experiments. According to the erosion test results the maximum mass loss was observed at high angles of incidence, which showed a brittle tendency of the material.

Introduction

Solid particle erosion (SPE) is a phenomenon that affects several mechanical components, such as turbines, walls of gas turbines, pipes, among others, causing progressive loss of material by the repeated action of solid abrasive particles impacting a surface. In many applications, SPE is a useful phenomenon such as sandblasting, abrasive deburring, dry ice blasting and high-speed abrasive water jet cutting [1]. Moreover, austenitic stainless steels are extensively used for service at sub-zero temperatures. This work was realized due to the limited information on jet flows at cryogenic temperatures [2]. Furthermore, to gain knowledge about the ductile-brittle behavior in SPE tests on stainless-steel samples at low temperatures [3].

Results and Discussion

Figure 1(a) shows a micrograph where plastic deformation can be seen as the main wear mechanism in the wear scar under an impact angle of 45°. Figure 1 (b) displays the mass loss as a function of incidence angle at -100 °C monitored during the experiments. The maximum value was observed at 60° accompanied by a shorter incubation period (up to 300 s of exposure time). The minimum mass loss was observed at 30°, similar mass loss trends were observed for angles of 30° and 45° both with longer incubation periods. Tendencies with higher mass losses were observed at angles close to normal (60° and 90°). Figure 1 (c) displays profilometry traces exhibiting the distribution of erosive wear along the surface due to the impact of particles at 90°. Finally, operating conditions for SPE tests are given in Table I.

Table I. Operating conditions for SPE tests on stainless steel AISI 310

Nozzle diameter	6.35 mm
Standoff distance	6.35 mm
Test gas	Dry compressed air, cooled whit liquid nitrogen
Test duration	120 s, 240 s, 480s
Test temperature	-100 +/-10 °C
Incidence angles	30°, 45°, 60°, 90°
Abrasive particles	Al ₂ O ₃ whit average size of 50 μm
Particle velocity	20 ms ⁻¹

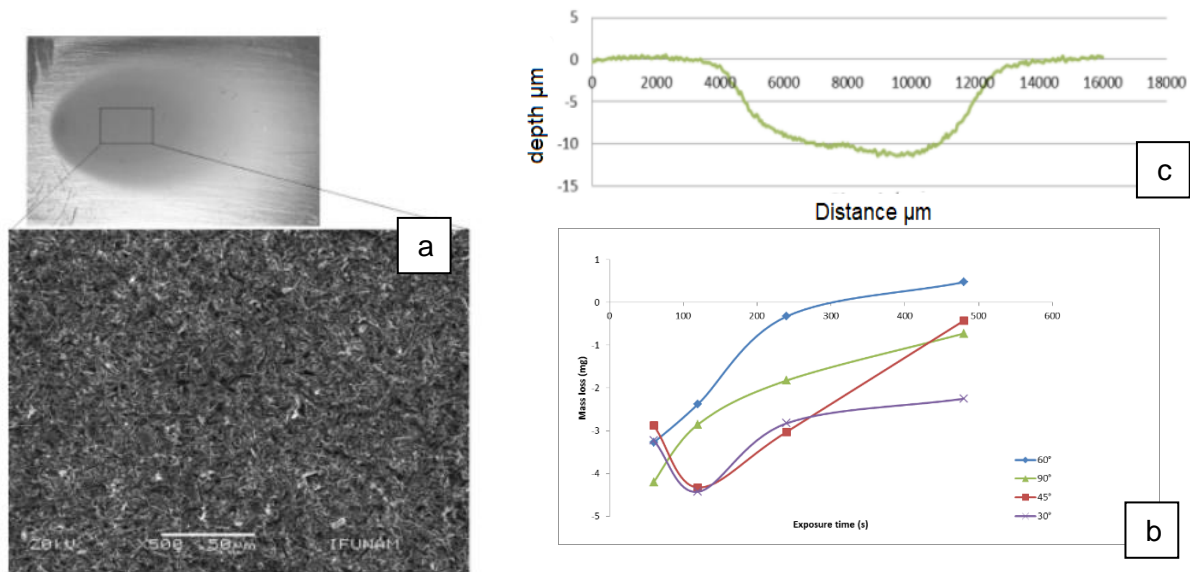


Figure 1. a) Micrograph of wear scar of a test sample, b) Mass loss as a function of incidence angle at $-100\text{ }^{\circ}\text{C}$, c) Profilometry of the cross section of the wear scar.

Conclusions

According to the cryogenic erosion test results the maximum mass loss was observed at 60° of incidence. The cryogenic jet flows enhance an additional aspect which can modify the behavior of the target material. This is due to the fact that the SPE behavior against the surface can be classified as ductile or brittle depending on the angle where the maximum erosion occurs; that is, when the highest erosion occurs at low angles the material has a ductile behavior, if it occurs at angles close to the normal, the material has a brittle behavior. High erosive incubation periods were observed at low incidence angles (30° and 45°). The main wear mechanism observed was plastic deformation.

References

- [1] J. Zaragoza-Granados, E. A. Gallardo-Hernández, M. Vite-Torres, and C. Sedano-de la Rosa, "Erosion behaviour of AISI 310 stainless steel at $450\text{ }^{\circ}\text{C}$ under turbulent swirling impinging jets," *Wear*, vol. 426–427, pp. 637–642, Apr. 2019.
- [2] A. G. Gradeen, J. K. Spelt, and M. Papini, "Cryogenic abrasive jet machining of polydimethylsiloxane at different temperatures," *Wear*, vol. 274–275, pp. 335–344, Jan. 2012.
- [3] J. Ibarra, E. Rodríguez, M. A. González, S. L. Cuenca, A. Medina, and G. I. Vásquez, "Erosion behavior of 440C stainless steel cryogenically treated," *Revista Mexicana de Ingeniería Química*, vol. 19, no. 3, pp. 1255–1264, Sep. 2020.

Tribological studies of sputtered WSC coatings with conventional and graded composition

Todor Vuchkov ^{a,b,*}, Albano Cavaleiro ^{a,b}

^a University of Coimbra, Department of Mechanical Engineering, SEG-CEMMPRE, Coimbra, Portugal

^b IPN - LED & MAT - Instituto Pedro Nunes, Laboratory for Wear, Testing and Materials, Coimbra, Portugal

* todor.vuchkov@ipn.pt

Synopsis

Self-lubricating tungsten-sulfur-coatings (W-S-C) coatings with a graded composition ranging from carbon rich to pure WS_x were deposited and compared to ones with constant composition of 30 and 50 % at. of carbon. The results revealed that every coating had an advantageous operating environment. Carbon-rich coatings performed better in ambient air conditions while the coatings with low carbon performed better in inert environments.

Introduction

W-S-C coatings are sputtered coatings consisting of an amorphous carbon matrix with WS_2 platelets embedded in it. WS_2 is a transition metal dichalcogenide (TMD) compound which has a layered structured with low shear strength. Due to their crystal structure with low shear strength, these compounds are often used for friction reduction. These sputtered coatings have a unique ability to provide friction and wear reduction in various operating conditions, ranging from ambient air to dry N_2 , vacuum environments and elevated temperatures up to 400°C. This is due to the fact that during sliding the TMD crystals can orient with their basal planes in the direction of sliding [1]. The chemical composition of these coatings was often aimed at ~40-50 % at. of carbon [2]. Recent studies showed that even lower carbon content ~30% at. of carbon can provide good tribological performance. One potential issue with these coatings is the formation of the tribolayer as reorientation of the TMD crystals is needed. A potential solution for improvement of the formation of the TMD-rich tribolayers can be the deposition of coating with graded composition.

Materials and Methods

We used magnetron sputtering to deposit a WSC coating with graded composition, starting with carbon-rich (~50 % at. C) bottom layers and a gradual decrease of the C content towards the top layers. Finally, a pure WS_2 layer (~100 nm) was deposited. For comparison we deposited WSC coatings with a constant ~30 and ~50 at. % of C. The morphological and structural assessment was performed using scanning electron microscopy, X-ray diffraction and Raman spectroscopy. The mechanical properties were studied using nanoindentation and scratch testing. Tribological testing was performed using a reciprocating ball-on-disk in three different environments: ambient air, dry N_2 and at an elevated temperature of 200°C.

Results and Discussion

All of the coatings deposited showed compact featureless morphologies. In terms of crystallinity only the coating with graded composition showed distinct diffraction peaks during X-ray analysis. These peaks were WS_2 ones and can be present due to WS_2 rich top-layers of the coating.

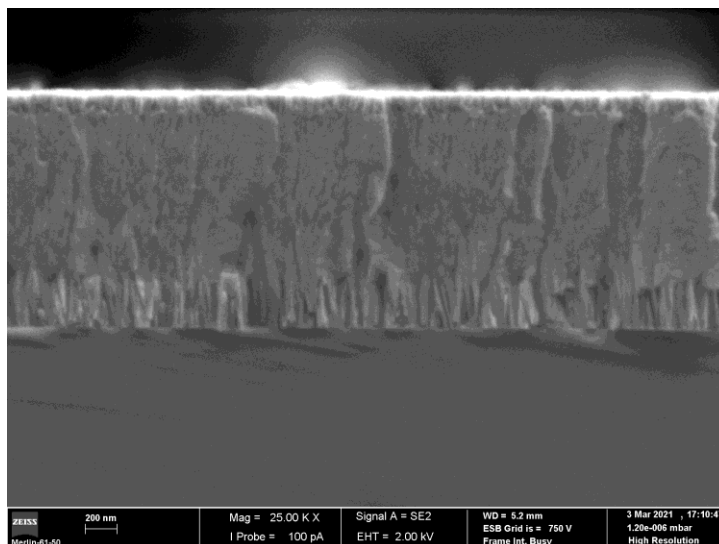


Figure 1. A cross-sectional micrograph of the coating with graded composition

In terms of hardness, it had a value of 5-6 GPa, with the highest value for the coating with ~50 % at. C and a lowest value for the coating with graded composition. This is expected as the a-C phase is inherently harder than the WS₂ phase. In relation to the adhesion, the scratch testing revealed Lc₂ loads in the range of ~20 N and Lc₃ loads of ~30 N for the coatings with conventional structure. The coating with graded composition had a Lc₂ load of 28 N with no large area delamination/chipping (no Lc₃ load observed). In terms of tribological performance all coatings showed good friction and wear performance. In ambient air the coatings with constant composition showed better wear resistance compared to the coating with graded composition. In dry N₂ environment the coatings showed similar wear resistance ($1-1.5 \times 10^{-7} \text{ mm}^3/\text{Nm}$) with a slightly better frictional response for the coating with graded composition.

Conclusions

WSC coatings with a composition of 30-50 % at. C can provide good friction and wear reduction during dry sliding against steel counterparts in different environments. Nevertheless, if the operating conditions are well known, the coating composition can be adapted. For example, if operation in ambient condition dominates higher carbon contents can be used. For operation in inert environments the carbon content can be reduced towards 20-30 % at. C and the usage of a soft top layer of WS₂ should be considered.

References

- [1] Yaqub T Bin, Vuchkov T, Bruyère S, Pierson J-F, Cavaleiro A. A revised interpretation of the mechanisms governing low friction tribolayer formation in alloyed-TMD self-lubricating coatings. *Appl Surf Sci* 2022;571:151302.
- [2] Polcar T, Cavaleiro A. Review on self-lubricant transition metal dichalcogenide nanocomposite coatings alloyed with carbon. *Surf Coatings Technol* 2011;206:686–95.

KEYNOTE 2

Cartilage Lubrication and Wear: Knowns and Unknowns

Markus A. Wimmer

Rush University Medical Center, Chicago, USA

* markus_a_wimmer@rush.edu

One focus of this presentation will be on the lubrication mechanisms of cartilage as related to the friction coefficient, as the primary function of articular cartilage is to provide a near-frictionless interface between joints. To allow for smooth movement during daily activity, articular cartilage is an “optimal natural biological bearing”, that in healthy conditions, is capable of undergoing millions of cycles within a lifetime. In the past several years progress has been made in the understanding of lubrication mechanisms that often act simultaneously to provide a low-friction bearing.

Much less is known about cartilage tribology in the context of osteoarthritis (OA). In fact, historically, OA has been considered a disease of ‘cartilage wear’, as a hallmark of this disease includes the loss of integrity of the surface layer. While it is now well-established that OA is not simply a disease of tissue wear, but a multifactorial condition involving biological and mechanical mechanisms, understanding of how OA leads to loss of tribological properties may be an additional perspective in disease progression. Future work to better understand how tissue pathology may affect tribological properties is therefore necessary.

**SESSION B:
CHARACTERIZATION
TECHNIQUES AND
TESTING METHODS**

Study of the early stages of WEA formation in pre-cracked and hydrogen charged 100Cr6 bearing steel

Fernando José López-Uruñuela^{1,2*}, Beatriz Fernandez-Diaz¹, Bihotz Pinedo¹,
Josu Aguirrebeitia²

¹ Tekniker, Tribology Unit, Eibar, Spain.

² Department of Mechanical Engineering, University of the Basque Country (UPV/EHU), Bilbao, Spain.

*fernando.lopez@tekniker.es; +34 603754458

Synopsis

In this work, results from several studies were collected with the aim of giving a broad insight about this premature failure. Indeed, the initial stages of research focused on developing a test method to accelerate the generation of WEC and subsurface cracks in bearing steels are presented. To this end, artificially preloaded hydrogen is used. This method would allow the study of non-destructive analysis techniques, the testing of coatings that prevent the hydrogen diffusion in steels, as well as the study of the initial stages of subsurface crack formation.

Introduction

Rolling element bearings undergo unfavorable work conditions in wind turbine gearboxes. Thus, they suffer a premature failure mode, which is driven by subsurface early cracks and it entails a reduction of a 1-20 % of the bearing's life, hence the wind turbine lifetime is reduced from the estimated 20 years to less than 2 years [1]. WEC morphologies appear to be connected to this failure mode, however, a clear understanding has not been reached yet among the scientific community. WEC failure consists of networks of microcracks connected with microstructural alterations, called "White Etching Area" (WEA). Several factors such as non-metallic inclusions, hydrogen, overloads, sliding kinematics, inefficient lubrication or passage of residual electrical currents have been proposed as WEC drivers.

The premature reproduction of WEC morphologies similar to those found in failed field bearings could help to understand how quickly these crack networks form and propagate under specific accelerators.

Several trials in Disc-on-Disc tribometer under transient conditions were conducted in order to reproduce WEC in hydrogen precharged discs. After testing a full metallographic analysis was carried out. For hydrogen uptake, discs were immersed in sulfuric acid (H_2SO_4) (0.1 mol/l) solution and potassium thiocyanate (KSCN) (1g/l) under a -1.2 V potential for 4 h [2].

Results and Discussion

Non-hydrogen pre-charged test

Despite transient conditions were in line with those used in literature, neither WEC or superficial failure was detected in test without hydrogen uptake. Authors consider the number of cycles was not enough to reproduce this failure mode, as the premature failure found in literature was up to 28.5 million of cycles [3] and the test presented herein only last 1.01 million of cycles.

Hydrogen pre-charging tests

Hydrogen pre-charging tests resulted in surface and subsurface damage. At subsurface level, several WECs and cracks were identified. It shall be noted that there is a great similarity between WEC from the field bearings [4] and those generated under laboratory conditions in the tests presented herein. Moreover, few cycles were needed to reproduce WEC by this methodology. This test methodology allows to study the early stage of surface and subsurface crack formation and propagation, as well as the study of new nondestructive analysis techniques or the influence of hydrogen in steel and coatings against this phenomenon. It is of interest to note that in one of the tests conducted WEC was reproduced without superficial damage and only 0.6 million of cycles were needed.

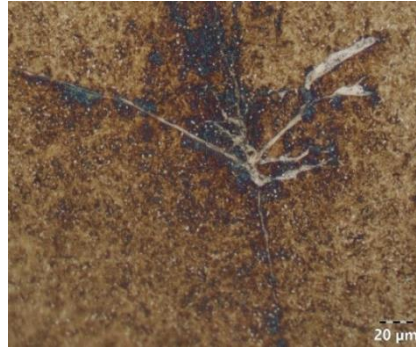


Figure 1. WEC triaxial branching formation in a circumferential section from tested disc.

References

- [1] Greco A et al., "Material wear and fatigue in wind turbine Systems", *Wear* 2013;302:1583–91.
- [2] Ruellan A et al., "Tribological analysis of White Etching Crack (WEC) failures in rolling element bearings", *NREL Wind Turbine Tribol Semin* 2014 2014.
- [3] Broeckmann C et al., "Reproduction of white etching cracks under rolling contact loading on thrust bearing and two-disc test rigs", *Wear* 2017;390–391:23–32.
- [4] Bruce T et al., "Characterisation of white etching crack damage in wind turbine gearbox bearings", *Wear* 2015;338–339:164–77.

A Crossed Cylinder Tribological Test against New Multi-material (CFRP-Ti) Stacks Configuration

Sharjeel Ahmed Khan ^{a,b,*}, Nazanin Emami ^a, Amilcar Ramalho ^b

^a Department of Engineering Sciences and Mathematics, Luleå University of Technology, Sweden

^b Department of Mechanical Engineering, CEMMPRE, University of Coimbra, Portugal

*sharjeel.ahmed.khan@ltu.se

Synopsis

Machining of Carbon Fiber Reinforced Plastic - titanium (CFRP-Ti) stacks undergo complex tribomechanical interaction of tool due to the involvement of dissimilar workpiece constituents. The common tribotest like reciprocating and pin-on-disc are not capable of simulating the contact state of the mating surface experienced by the tool during the machining process. Cross-cylinder tribotest could effectively present the contact situation and provide fresh workpiece surface during sliding. However, a cross-cylinder tribological test with new multi-material arrangement of disparate materials rings of CFRP and Ti stacked in alternative fashion is proposed to simulate CFRP-Ti drilling. The benefit of this test over machining is high degree of control to analyze the tribological interaction of tool wear while avoiding edge deterioration affect caused by plastic deformation or chipping in cutting tools.

Introduction

With the increased demands for improved fuel efficiency and environmentally friendly alternatives the use of light weight composite structural parts for the aerospace and aeronautic industry is growing at a rapid pace. Specifically, the use of CFRP coupled with titanium are gaining popularity due to high strength to weight ratio, good galvanic corrosion resistance and excellent load bearing capabilities making it desirable material for new range of modern aircrafts. In Airbus A350 and Boeing 787, CFRP-Ti stacks have been used in primary aircraft structural components like fuselage, aircraft wing spar and ribs to benefit from properties of both materials [1]. The demand of CFRP-Ti stacks is expected to sore in the coming future due to increasing trend toward sustainability.

However, with exceptional material characteristic of CFRP-Ti stacks the major problem lies in drilling and machining of such material combination, as it is well known that both CFRP and Ti were categorized as difficult-to-machine materials. Thus, the tool experience higher degree of wear with shorter tool service-life and at the same time yields poor surface roughness and hole quality of the machined holes. Researchers have tried to study the effect of different coatings to improve the tool life and understand the tribomechanical interaction of the tool with the CFRP-Ti stacks. However, there is no simple evaluation method available to analyze the wear mechanism of the uncoated/coated tools caused due to the interaction of the tool with disparate materials.

Cross-cylinder tribotest is a simple yet effective way to reproduce the contact during the machining operation by generating freshly available surface for interaction. Recently, the effectiveness of this tribotest-configuration has been demonstrated for study of tool wear mechanism during machining of titanium alloy [2]. Although this testing configuration is not new and was proposed in 1989 by Hedenqvist [3]. But was recently been used in studies to simulate tribological contacts scenarios for forming and machining operation [4], [5]. However, to the best of our knowledge, cross-cylinder tribological test against new multi-material configuration with the alternating arrangement of disparate material i.e., CFRP-Ti rings has not been investigated earlier and would be considered in this study.

Materials and Test equipment

Carbon fiber reinforced plastic (CFRP) plates of 300x300x7.3mm were procured from INEGI which were prepared by using Hexply 8552 prepreg unidirectional laminate with epoxy matrix in $[0,90]_{10s}$ orientation using 5bar curing pressure in an autoclave. Whereas, for titanium (Ti6Al4V) tubes of OD=40mm and ID=30mm were procured from TSM Technology China.

In order to manufacture shaft with multi-materials configuration, firstly CFRP and Ti rings were prepared. Abrasive water jet machining was used for machining of CFRP plate using water pressure of 5400 bar

and garnet as abrasive at feed rate of 385 g/min to make rings with OD=40mm and ID=30mm (Figure 1a). Moreover, the titanium tubes were machined with 7.3mm thickness to obtain the rings (Figure 1b). The rings of CFRP and Ti were arranged in alternative fashion on a shaft with tight dimensional tolerances and further secured by mechanical fastener as shown in Figure 1c, d.

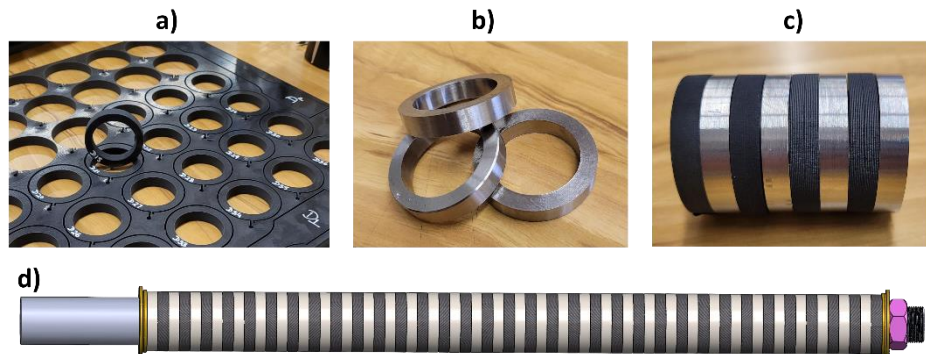


Figure 1. a) CFRP rings machined by abrasive waterjet machining of CFRP plates. b) Ti6Al4V rings c) stacks of CFRP and Ti rings d) Schematic of workpiece rod with alternative arrangement of CFRP (black) and Ti (silver) rings assembled and secured with nut on the shaft.

Conclusions

The new multi-material stack configuration for cross-cylinder tribological testing has been proposed for CFRP-Ti stacks, however, the testing technique could easily be extended for other multi-material stacks combinations like CFRP-Al and CFRP-Al-GFRP etc.

References

- [1] J. Xu, C. Li, M. Chen, and F. Ren, "A comparison between vibration assisted and conventional drilling of CFRP/Ti6Al4V stacks," *Mater. Manuf. Process.*, vol. 34, no. 10, pp. 1182–1193, 2019.
- [2] P. Olander and J. Heinrichs, "Initiation and propagation of tool wear in turning of titanium alloys – Evaluated in successive sliding wear test," *Wear*, vol. 426–427, no. January, pp. 1658–1666, Apr. 2019.
- [3] K. H. Park, A. Beal, D. D. W. Kim, P. Kwon, and J. Lantrip, "Tool wear in drilling of composite/titanium stacks using carbide and polycrystalline diamond tools," *Wear*, vol. 271, no. 11–12, pp. 2826–2835, 2011.
- [4] B. Zhu, J. Mardel, and G. L. Kelly, "An investigation of tribological properties of CN and TiCN coatings," *J. Mater. Eng. Perform.*, vol. 13, no. 4, pp. 481–487, 2004.
- [5] J. Gerth, J. Heinrichs, H. Nyberg, M. Larsson, and U. Wiklund, "Evaluation of an intermittent sliding test for reproducing work material transfer in milling operations," *Tribol. Int.*, vol. 52, pp. 153–160, 2012.

Friction of soft contact lenses

Amilcar Ramalho^{a, *}, Luís Vilhena^a

^aDepartment of Mechanical Engineering, CEMMPRE, University of Coimbra, Coimbra, Portugal.

* amilcar.ramalho@dem.uc.pt

Synopsis

The aim of the present research work is to investigate the tribological behavior of different soft contact lenses under different contact conditions. A tribometer has been developed for this purpose, which operates with vibration horizontal movement. The friction assessment method is based on the evaluation of the free damping vibration movement, of the mass - spring system. This technique proved to have adequate sensitivity for the biologically relevant conditions, light normal load, high speed and hydrodynamic lubrication.

Introduction

Soft contact lenses (SCLs) are widely used today by over 140 million people worldwide to correct vision problems. Although the high development in recent years of SCLs there is still a high dropout rate in their use due to the discomfort caused. This discomfort has been associated with several factors, namely the friction that occurs between the upper eyelid and the anterior surface of the contact lens during blinking process. In this process eye movements occur under mainly hydrodynamic lubrication regime. Typical value of the eyelid pressure on the cornea at rest being around 1 kPa and during muscle contractions of a blink is in the range of 3 to 8 kPa. Regarding the eyelid's sliding speed, it is estimated that the speed can reach values as high as 100 to 200 mm/s. Thus, tribological SCLs studies should focused on lubricated contact, pressures up to 10 kPa, sliding speeds higher than 100 mm/s and several millimeters of stroke. These conditions are completely out of the limits of the test conditions of current conventional tribometers.

The aim of the present research work is to investigate the tribological behavior of SCLs using a new technique, as an alternative to conventional tribometers. A special test machine was developed in order to be used as a tribometer, which operates as an oscillator with vibration horizontal movement and that can be modeled as a vibratory mass - spring – damper mechanical system. The friction assessment method is based on the evaluation of the free damping vibration movement, of the mass - spring system, induced by an initial non-equilibrium condition. The contact of the SCLs against the counterbody acts as a supplementary dissipation of energy and the friction is determined by inverse analysis optimized by comparison to the analytical equation of motion.

Experimental work

A dynamic tribometer has been design and built during the present research work. The tribometer operates as a pendulum with vibration horizontal movement. In order to simulate the conditions of the human eye, the contact geometry used was plane-sphere. As shown in Figure 1, the contact lens was assembled over a hemispheric silicone rubber and a glass lamella was used as counter material. Different weights of controlled mass were used in order to apply a normal force between the lens and the glass lamella.

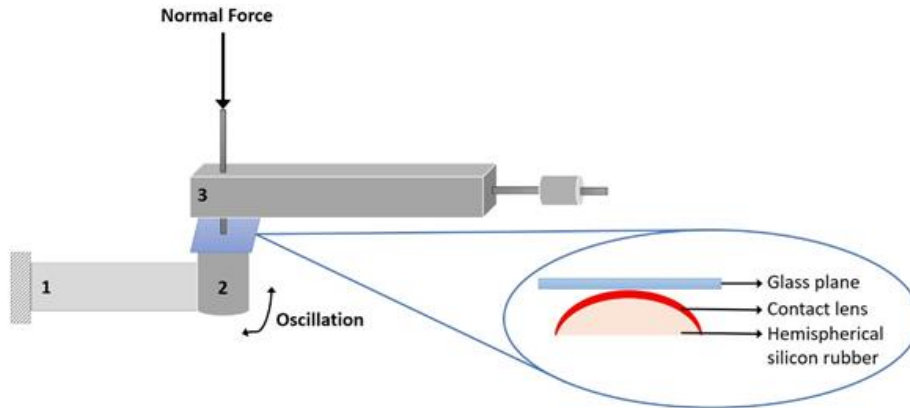


Figure 1. Schematic view of the vibration tribometer

Three different commercial lens, made of different materials, namely Silicon hydrogel, hypergel and hydrogel, were tested.

The friction assessment method is based on the evaluation of the free damping vibration movement, of mass-spring system, induced by a mechanical impulse. The contact with the contact lenses acts as a supplementary dissipation of energy and the friction is determined by inverse analysis. The numerical integration of the second-order differential equation of the motion will allow the calculation of the friction, minimizing the error between the experimental motion and the numerical solution, figure 2.

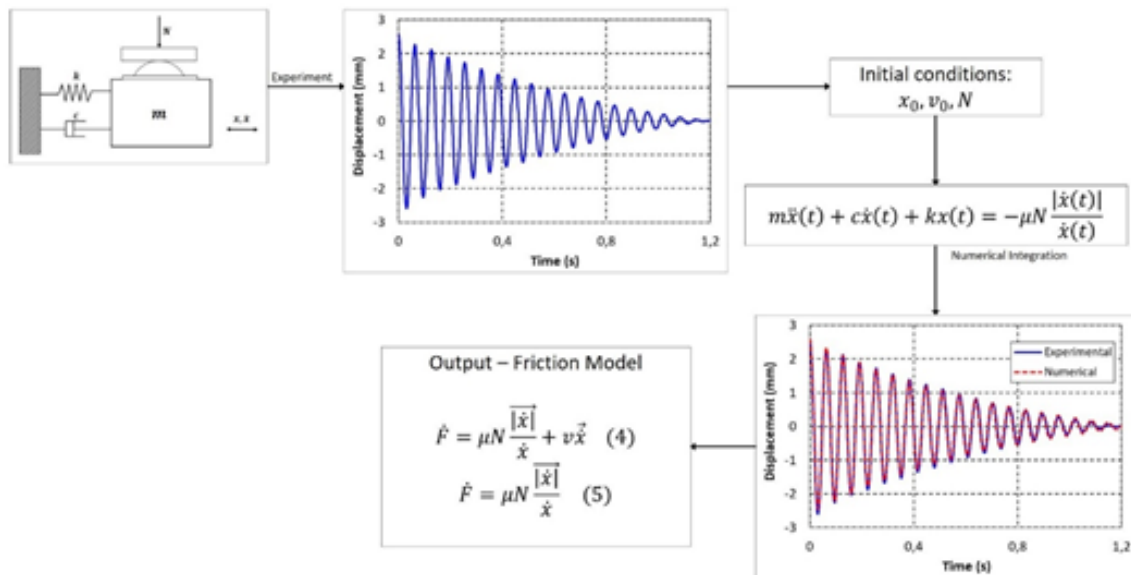


Figure 2. Flowchart of the experimental protocol.

Conclusions

- The experimental device based on the energy dissipated by friction during free vibration, proved to have adequate sensitivity for the biologically relevant contact conditions.
- Applying this technique to the friction study of contact lenses shows that the friction model, that best describes the friction of contact lenses, includes a Coulomb part plus a viscous component.

A Tribological Test Method for PVA Hydrogels and Articular Cartilage

Paul Staudinger ^{a,*}, Florian Rummel ^b, Jiri Nohava ^c, Renate Kohl ^a, Kartik S. Pondicherry ^d

^a Anton Paar GmbH, Graz, Austria

^b Anton Paar Germany GmbH, Ostfildern, Germany

^c Anton Paar TriTec, Corcelles, Switzerland

^d Anton Paar India, Hyderabad, India

* paul.staudinger@anton-paar.com

Synopsis

Hydrogels are considered promising replacement materials for articular cartilage. Friction conditions in biological systems such as joints are complex and their simulation requires tribological tests that closely model the real life conditions. The current work presents a methodology for manufacturing and tribological characterization of polyvinyl alcohol (PVA) hydrogels and porcine articular cartilage using a special setup of a commercial rheometer. Measurements of elastic modulus and zeta potential of the PVA hydrogel allowed for a deeper understanding of the tribosystem's behavior. The results showed that the presented setup can be used for evaluation of the tribological performance of a PVA hydrogel compared to real cartilage.

Introduction

In a total knee or hip arthroplasty the whole joint is replaced by an artificial implant. Choosing the right material is a challenge since two or more parts of the joint are in relative motion in the daily life and, hence, may experience different frictional behavior and even wear [1, 2]. In order to recover the full functionality of the joint and to relieve the patient's pain, the implants should have the same frictional properties as the joint. Understanding the tribology of a joint replacement is therefore crucial for development of new implant materials. Polyvinyl alcohol (PVA) hydrogels are considered as one of the most suitable candidates for joint cartilage replacement because they are biocompatible and have mechanical properties similar to the joint cartilage [3]

Methods

The PVA hydrogels (61,000 g/mol.) were prepared from freeze-thaw technique through 5 temperature cycles from -20 °C to 8 °C directly in the tribological cell of a MCR rheometer. The tribological measurements were performed using the same MCR Tribometer with pin-on-disc setup (see Figure 1) and with special clamping adapters to accommodate the in-situ produced PVA hydrogel specimen. Oscillatory tests along with sliding velocity ramps were carried out over several orders of sliding speed and results are shown in the form of extended Stribeck curves [4].

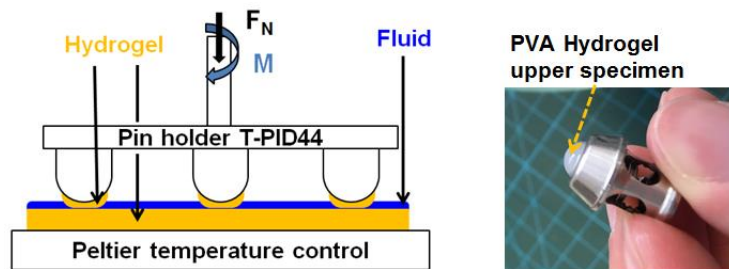


Figure 1. Schematic of the pin-on-disc setup (left) and adapter for soft specimen (right).

Zeta potential was measured with an electrokinetic analyzer for solid surfaces with one of its proprietary measuring cells. The elastic modulus was measured using instrumented indentation technique by applying a 100 μ N load on a spherical indenter.

Results and Discussion

The work demonstrates how a combination of complementary measurement techniques can be used for characterization of tribological, chemical and mechanical properties of PVA hydrogel. The tribological measurements with PVA on PVA configuration as well as PVA on porcine knee cartilage configuration provided information about the friction coefficient at various sliding speeds occurring during daily motion. The friction factor trend observed on the PVA gel with different artificial synovial fluids was similar to that observed on porcine cartilage specimen. This indicates that the PVA gel corresponds well to the real friction behavior in the joint. The surface charge measurements corroborated the tribological result while the indentation results confirmed that the elastic modulus of the PVA hydrogel is similar to that of the outer surface of the joint cartilage. The methodology and analysis used in this study will further be expanded to understand the long-term friction and wear behavior of these materials.

References

- [1] K. Knahr, European Federation of National Associations of Orthopaedics and Traumatology, eds., "Tribology in total hip and knee arthroplasty: potential drawbacks and benefits of commonly used materials," Springer, Heidelberg, 2014.
- [2] M. A. Hamilton et al., "Quantifying Multidirectional Sliding Motions in Total Knee Replacements," *J. Tribol.* 127 (2005) 280–286.
- [3] M. Kobayashi, "Development and Evaluation of Polyvinyl Alcohol-Hydrogels as an Artificial Articular Cartilage for Orthopedic Implants," (2010) 19.
- [4] K. S. Pondicherry et al., "Extended Stribeck curves for food samples, *Biosurface and Biotribology*," Vol. 4, Iss. 1, 2018, 34 – 37.

Using contact mechanics to describe the time dependent behavior of Polyacrylamide based hydrogels

Carlos Reinhardts – Hervás^a, Álvaro Rico^{a,*}, Jesús Rodríguez^a

^a Durability and Integrity of Structural Materials. Universidad Rey Juan Carlos, Madrid, Spain

* alvaro.rico@urjc.es

Synopsis

Polyacrylamide hydrogels are widely used in several fields. Due to their ability to be swollen by water they are highly biocompatible. Additionally, they show a very similar mechanical behavior than natural tissues [1]. All these characteristics make them suitable to be used as “in vitro” models to develop experimental techniques to advance in the knowledge about the very complex mechanical behavior of natural materials. They are very flexible and soft solids, but the main feature governing the mechanical performance is their very marked time – dependent behavior. This time - dependent response lay on two mechanisms. On one side, the polymeric nature of the matrix lead to a viscoelastic deformation when a load is applied on the hydrogel. Conversely, flux of water can be also produced inside the material under stress, driving to a secondary relaxation phenomenon, the so called poroelasticity. Global mechanical response can be built by considering both contributions. Poroelasticity is size dependent while viscoelasticity is not. In this work, we developed an experimental and constrained fitting technique using indentation at different scales from macro to nano, explaining experimental relaxation curves using a contact mechanical model [2]. The constrained fitting method can be used to enlighten how the composition of the hydrogel can be tuned to obtain different time dependent responses.

Introduction

Alginate/Polyacrylamide (Alg/PAAm) hydrogels are hybrid materials formed by a double cross-linked network. These hydrogels are formed by a three-dimensional polymeric network forming a porous structure, providing a permeable character. This permeability, together with the high-water absorption capacity of these materials, give hydrogels their compositional and microstructural uniqueness and their interesting mechanical behavior. For example, due to their permeability, hydrogels can be used for drug delivery, tissue scaffolds or tissue engineering, among others. These materials tend to have a time-dependent behavior and an important dependence on deformation rates. They show a viscoelastic behavior due to the conformational chain changes inside the polymeric structure. Additionally, poroelasticity is also observed due to the migration of the water through the pores of the polymeric mesh under mechanical stress. Both behaviors present temporal dependence but poroelasticity also presents size dependence. In several studies, fracture tests, fatigue, unconfined uniaxial compression and biocompatibility tests have been carried out on these materials [1], but until now time dependent behavior of these types of materials has received low attention. Additionally, relation between initial composition of the hydrogel and global mechanical behavior remains under study.

Results and Discussion

Alg/PAAm hydrogel samples were synthesized following a two-step procedure. The covalent cross-linking of the acrylamide polymer chains, and the ionic cross-linking of the alginate chains was carried out in two different steps. Samples with different amount of alginate were obtained. Indentation tests were carried out using a microindenter Agilent G200 with a Keysight XP indentation head coupled with a 500 mN load. A spherical ruby tip of 800 μm radius was used. Tests were carried out in milli-Q water immersion. The spherical tip penetrates the sample to a target depth of 25 μm , 20 μm and 15 μm for each material. Once the target depth was reached, it remained constant for a time of 1200 s. A constrained fitting method was developed by the authors and it is used to describe relaxation behavior of the samples by considering viscoelastic and poroelastic contributions. Details of the model can be consulted in [2].

In figure 1, relaxation curves measured at three penetration depths for samples with different Alginate composition are presented (black lines). Each experimental curve was fitted to the analytical indentation model (red lines). Once the fitting is performed, viscoelastic and poroelastic contribution on the global

response can be obtained (green and blue curves, respectively). Alginate composition strongly affects the time - dependent behavior of the hydrogels. The highest the Alginate concentration, the more important is the poroelastic contribution on the global mechanical response. For the lowest alginate concentrated hydrogel, viscoelastic contribution explains by itself the global relaxation curve.

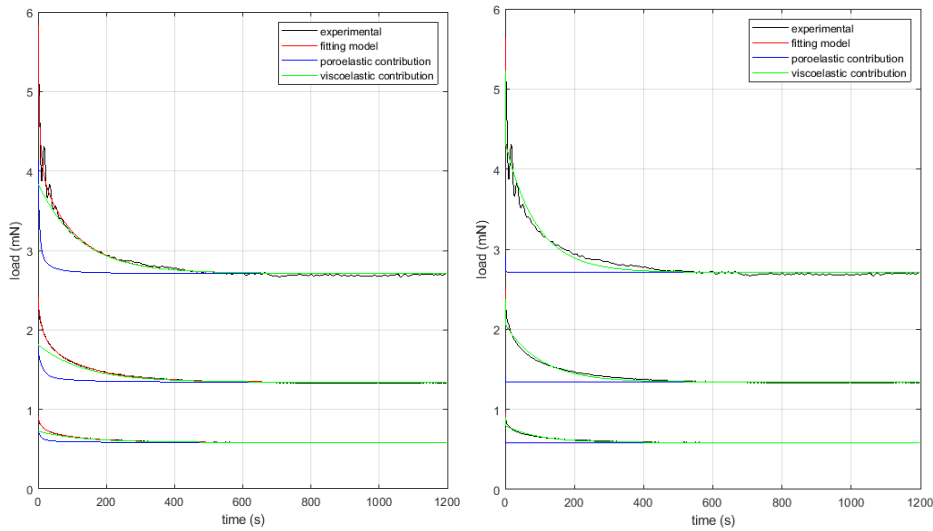


Figure 1. Relaxation curves measured at different penetration depth. Left) Alginate/Polyacrylamide sample with the highest alginate concentration. Right) Alginate/Polyacrylamide sample with the lowest alginate concentration.

Conclusions

Relaxation tests using spherical indentation were performed at different penetration depths on Polyacrylamide based hydrogels with different Alginate concentration. Time – dependent behavior was assessed by means of an analytical contact mechanical model that consider both, the viscoelastic and poroelastic contributions. The model was fitted to experimental curves. From results, it can be concluded that Alginate concentration has a key role on the mechanical behavior of the material. As the Alginate concentration increased, the poroelastic contribution became more important on the global response. Interestingly, the time – dependent behavior of the hydrogel can be tuned by controlling the amount of Alginate during the manufacturing of the sample.

References

- [1] D. Caccavo, G. Lamberti, A. A. Barba, Mechanics and Drugs release from poroviscoelastic Hydrogels: Experiments and modelling, *European Journal of Pharmaceutics and Biopharmaceutics* 152 (2020) 299 – 306.
- [2] C. Reinhardt – Hervás, A. Rico, J. Rodríguez, Crosslinker concentration effect on the poroviscoelastic relaxation of polyacrylamide hydrogels using depth-sensing indentation, *Polymer Testing*, 100 (2021) 107265.

Ceramic tribocoatings for die protection in Low Pressure Die Casting process

B. Zabala^a, O. Areitioaurtena^a, A. López-Ortega^a, E. Fuentes^a, A. Igartua^{a,*}, L. Merchán^b, E. Pardo^b, J.Montero^c, R. Granados^d, I. Mtz de la Pera^e, J.Mendizabal^f

^aTekniker, Basque Research and Technology Alliance (BRTA), Eibar, Spain

^bFoseco Española S.A., Izurtza, Spain

^cBefesa Aluminio S.L., Erandio, Spain

^dAalberts, Atxondo, Spain

^eAurrenak S. Coop. L., Gazteiz, Spain

^fEdertek S. Coop, Arrasate, Spain

*amaya.igartua@tekniker.es; +34 943206744

Introduction

Aluminum and its alloys are nowadays the most commonly used non-ferrous metals, due to their versatility and unique relation of properties [1]. Aluminum alloys can be cast by several processes, where LPDC has arisen as a preferred method for castings high quality components such as car wheels or cylinder heads [2]. One of the most important factors in the LPDC process, is the heat transfer during the solidification of the molten alloys, which is the responsible of the resulting microstructure, on which the quality of the cast piece is based. The use of foundry coatings has been lately suggested as a proper strategy to control the heat transfer, while protecting bonded molds from aluminum adhesion by providing a barrier between the surface and the liquid metal. LPDC die coatings failure usually comes from the loss of adherence or excessive wear originated in the successive filling processes, which requires stopping production for the reapplication of the coating. In the present work, coatings with different insulation capabilities have been evaluated, in terms of adherence and wear tests, in order to select the most promising alternative for LPDC die coating. As a result of this study some recommendations of the application method of the coating have been highlighted as well.

Materials and Methods

The substrate material employed in the work was an AISI H11 (1.2343) steel at 37-38HRC, as representative for the typical die steel used in LPDC processes. The size of the samples manufactured for this work was of 100x100x5mm³. Three different surface finishing pre-treatments were evaluated: grinding, polishing, and shot blasting.

All the coatings were applied above a 50µm primer layer. In some samples, the coatings were applied without primer layer, to evaluate the influence of this layer on the adhesion and performance of the coatings in the tests. The target thickness of the coatings was of 150µm.

The coatings selected in this work were new experimental developments of Foseco, conceived in the frame of the industrial ETORGAI project "ALEPRE", with different thermal conductivity and insulation capacities. The seven coatings selected were: a reference coating with very high insulation (A1) and a new development with similar insulation capacity (A2); a coating with medium insulation capacity (D1); a coating as reference of average insulation capacity (B1), a variant of B1 with extra binder (B2) and a new development based on B1 (B3); and a conductive coating containing graphite for improved release of the casted samples (C1). The composition of the coatings is confidential, but, in general terms, the high insulation coatings are manufactured with filler materials such as talc, mica, TiO₂, limestone or quartz, sodium silicate as a binder, and water as a thinner. In the case of the conductive coatings, half-colloidal graphite was employed as filler.

The adhesion was assessed by pull-off tests (ISO 4624), which has been considered the most appropriate to simulate the failure of coatings when it is extracted from the die due to sticking of the aluminium. The wear of the coatings was evaluated by falling abrasive and taber abrasion tests, to simulate erosion and abrasion taking place in the filling process, respectively. Furthermore, basic characterization of the thickness and roughness have been performed.

Results and Discussion

The criteria for best coating selection have been built through a comparison table, where a value for each test has been calculated.

The calculation method for these values and the selection criteria are the following:

- **Roughness:** ratio between each coating mean roughness value and the coating with maximum roughness (A1 - 46,3µm).
- **Adherence:** ratio between each coating adhesion force mean value and the highest value registered for all the coatings (B3 - 16MPa).
- **Falling:** ratio between each coating abrasion resistance and the highest value registered for all the coatings (B3 – 100,72 gr/µm)
- **Taber:** ratio between each coating abrasion resistance and the highest value registered for all the coatings (B3 – 70,7 cycles/µm)
- **Conductivity:** ratio between each coating conductivity and the highest value registered for all the coatings (C1-1760 Wm⁻²K⁻¹)

	<55% Low >55% High	<40% <50%	<10% <30%	<3% <5%	>70% >50% <50%
% from max	ROUGHNESS	ADHERENCE	FALLING	TABER	CONDUCTIVITY
A1	100,00	81,06	3,02	0,21	41,88
A2	57,01	40,31	18,50	4,48	39,20
D1	67,21	57,25	16,62	3,67	56,82
B1	40,36	37,38	21,57	1,84	83,52
B2	38,52	62,88	25,30	3,43	83,52
B3	28,97	100,00	100,00	100,00	82,39
C1	39,14	45,19	15,23	1,70	100,00

Table 1. Summary table used to compare the different coating alternatives

Conclusions

- The **surface preparation** of the molds is vital to achieve an adequate adhesion of the coatings. In this regard, the cleanliness of the surface was found to be a critical aspect.
- **The high roughness and the low conductivity** (or high insulation) are directly related with the refractory particle size of the coating's formulation. On the one hand, the higher particle size will lead to a worst surface finishing of the aluminum casted part, which could affect the surface topography of the casted part. But, on the other hand, higher particle size could improve the fluidity through a slower solidification of the aluminum due to the higher insulation and the breakage of the oxide surface layer of the fluid melted aluminum.
- When **average insulation** coatings with good surface finishing are required, **B3 coating is clearly the very best solution**. The performance of the classical formulation of average insulation coating was notably improved in terms of adherence and wear resistance, as well as lower roughness while maintaining similar conductivity values. The extra binder employed with B2 compared to B1 did not show any considerable improvement on the performance.
- For the selection of a **coating with high insulating capacity**, A2 has demonstrated a considerable improvement on the wear resistance compared to A1, keeping the insulation degree for a much lower surface roughness. However, A2 presented a much lower adherence than A1. D1, which has a lower insulation capacity, presented similar results to those obtained for A1 and A2 coatings. All in all, the wear resistance of all these insulation coatings with coarser grain size was lower than that of B3 coating.
- The results obtained for **C1 conductive coating** were similar to those of B2 and B1.
- Finally, the use of the **primer layer was found to be highly recommendable to improve the adherence and wear resistance of the coatings**.

References

- [1] D. Brough, H. Jouhara, The aluminium industry: A review on state-of-the-art technologies, environmental impacts and possibilities for waste heat recovery, Int. J. Thermofluids. 1–2 (2020) 100007.
- [2] I. J.R. Brown. Foseco Non-ferrous foundryman's Handbook. Butterworth-Heinemann 1999. ISBN: 978-0-7506-4286-6.

SESSION C: BIOTRIBOLOGY/ MODELLING AND SIMULATION IN TRIBOLOGY

Effects of non-conventional sterilization methods on PBO-reinforced PVA hydrogels for cartilage replacement

Tomás Pires ^a, Andreia Sofia Oliveira ^{a,b}, Célio G. Figueiredo-Pina ^{c,d,e}, Madalena Salema-Oom^e,
Diana Silva ^{a,*} and Ana Paula Serro ^{a,e}

^a Centro de Química Estrutural (CQE), Institute of Molecular Sciences, Departamento de Engenharia Química, Instituto Superior Técnico, Universidade de Lisboa, Portugal

^b Instituto de Engenharia Mecânica, Instituto Superior Técnico, Universidade de Lisboa

^c CDP2T, Escola Superior de Tecnologia de Setúbal, Instituto Politécnico de Setúbal

^d CeFEMA, Instituto Superior Técnico, Universidade de Lisboa

^e Centro de Investigação Interdisciplinar Egas Moniz (CiiEM), Instituto Universitário Egas Moniz

* E-mail: dianacristinasilva@tecnico.ulisboa.pt

Synopsis

Cartilage substitution by biomaterials is often needed when the natural tissue is extensively damaged. PVA (poly-vinyl alcohol) hydrogels are promising candidates for this purpose due to their biocompatibility and similarities with the biological tissues regarding physical properties. However, their mechanical resistance is generally low and reinforcement is needed to better mimic cartilage. PBO (poly(p-phenylene-2,6-benzobisoxazole) nanofibers were used in this work with this purpose. Since cartilage replacement materials are intended to be implanted in the human body, their sterilization is mandatory to ensure the biological. Hydrogels are often sensitive to conventional sterilization methods. Therefore, alternative processes that do not impair the materials' properties have been pursued. The main objective of this work to evaluate the effect three non-conventional sterilization methods: microwave (MW), high hydrostatic pressure (HHP) and argon plasma (PM), on the properties of a PVA hydrogel reinforced with PBO.

Introduction

Articular cartilage degradation affects millions of people worldwide. Being an avascular tissue, cartilage has limited healing capacity, and current therapeutic strategies based on physiotherapy, use of anti-inflammatories or viscosupplementation show several limitations [1]. Hydrogels have gained great attention as possible cartilage substitutes when damages are already considerable, due to their biocompatibility and high-water contents. PVA is considered one of the most promising hydrogels for this purpose, however its mechanical properties hinder its application [2]. Reinforcement of the PVA is required and can be achieved through the addition of nanofibres to the hydrogels' polymer network. An interesting polymer for this application is poly(p-phenylene-2,6-benzobisoxazole) (PBO), as this synthetic fibre shows high tensile strength (~5.8 GPa), and a compressive strength of ~0.5 GPa [3]. In this work, a PVA hydrogel, reinforced with PBO nanofibres, obtained by cast-drying, was submitted to three non-conventional sterilization methods (i.e., MW, HHP and PM) in order to avoid problems in polymer properties associated with common sterilization methods (e.g., involving heat or radiation). The efficacy of sterilization was accessed, and the synthesized hydrogels were characterized in terms of their structural, tribological and mechanical properties, wettability, swelling capacity and rheological behavior, to evaluate possible effects due to the sterilization procedures. The biocompatibility of the hydrogels was ascertained via irritability and cytotoxicity assays.

Results and Discussion

The results show that the three sterilization processes ensured sterility in all cases. The treatments did not cause significant changes in the surface' morphology, except PM that suffered an increase in roughness due to the etching effect. FTIR analysis showed that the treatments induced some changes in the materials' chemical structure in terms of crystallinity degree and crosslinking, allowing to explain some differences on its behavior. Samples' equilibrium water content did not suffer significant alteration after the treatments, remaining ~ 74 %. Similarly, hydrophilicity was also not affected (the water contact angle remained ~ 40°). In general, the sterilization treatments did not negatively impact the materials' mechanical properties. MW stood out due to an increase on hardness, stiffness (both on traction and compression at strains) and shear modulus. HHP increased single bonding, improving the mechanical properties, except the compressive stiffness at high loads. The coefficient of friction was significantly

lower for MW and HHP samples, when compared with the non-sterile (Figure 1). PM treatment resulted in breakage of bonds, thus decreasing the material's tribological and load bearing capabilities but improved both the tensile and shear resistance. None of the sterilization methods induced irritability or cytotoxicity.

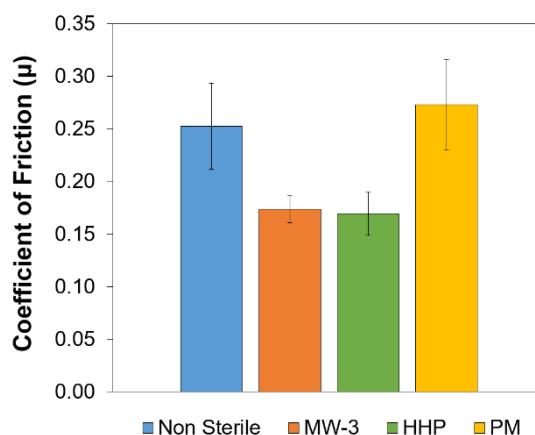


Figure 1. Coefficient of friction for the non-sterile and sterile hydrogels with 30 N of normal load tested against porcine cartilage, using synovial fluid as lubricant.

Conclusions

All the studied methods proved to be able of sterilizing the PVA-PBO hydrogel. PM impaired some of the material's properties and does not allow terminal sterilization, in contrary to HHP and MW. MW proved to be the most promising method, as HHP requires specialized personal and expensive equipment.

References

- [1] A.J. Sophia Fox, A. Bedi, S.A. Rodeo, The basic science of articular cartilage: Structure, composition, and function, *Sports Health*. 1 (2009) 461–468.
- [2] M. Kobayashi, H.S. Hyu, Development and Evaluation of Polyvinyl Alcohol-Hydrogels as an Artificial Articular Cartilage for Orthopedic Implants, *Materials (Basel)*. 3 (2010) 2753–2771.
- [3] M. Chen, Y. Mo, Z. Li, X. Lin, Q. He, Poly(p-phenylenebenzobisoxazole) nanofiber layered composite films with high thermomechanical performance, *Eur. Polym. J.* 86 (2016) 622–630.

3D printing of leucite-based materials reinforced with zirconia for dentistry

A.C. Branco ^{a,b,c*}, M. Polido ^b, R.Colaço ^d, A.P. Serro ^{a,b}, C.G. Figueiredo-Pina ^{b,c,e}

^a Centro de Química Estrutural, Institute of Molecular Sciences, e Departamento de Engenharia Química, Instituto Superior Técnico, Universidade de Lisboa, Lisboa, Portugal;

^b Centro de investigação Interdisciplinar Egas Moniz, Instituto Universitário Egas Moniz, Caparica, Portugal

^c CDP2T e Departamento de Engenharia Mecânica, Escola de Tecnologia de Setúbal, Instituto Politécnico de Setúbal, Setúbal, Portugal

^d IDMEC e Departamento de Engenharia Mecânica, Instituto Superior Técnico, Universidade de Lisboa, Lisboa, Portugal

^e CeFEMA, Centro de Física e Engenharia de Materiais Avançados, Instituto Superior Técnico, Universidade de Lisboa, Lisboa, Portugal

* ana.branco@tecnico.ulisboa.pt

Synopsis

The aim of this study is to produce by 3D, namely by robocasting, leucite-based glass ceramics with suitable tribological performance through the reinforcement with 12.5% and 25% ZrO₂ nanoparticles (%wt). To understand the suitability of the printed samples for dental applications, samples of 100% ZrO₂ coated with glaze were produced for comparison. The samples were evaluated regarding their density, surface roughness and fracture toughness. Also, wear tests were performed in a chewing simulator against dental human cusps in artificial saliva at room temperature with an applied load of 50 N. Then, the counter-faces' wear was quantified.

Introduction

Zirconia has been reported as one of the best materials to be used for dental restorations since it gathers properties that allow supporting the high loads during mastication without fracture, and at the same time does not induce much wear on the opposing teeth. However, these restorations are usually coated with a glass veneer to improve the restorations' optical properties. This type of coating is fragile and therefore increases the wear of the antagonist teeth. To avoid the need of a coating over the zirconia frameworks, the production of glass-ceramic composites may become a good alternative. Although subtractive manufacturing is the most used technique to produce dental materials, additive manufacturing (AM) has been emerging as an alternative technology and so far, there are some works in the literature that show that it presents innumerable advantages [1] and can successfully produce materials with suitable properties for dentistry [2,3]. There are several AM technologies, being robocasting one of them. This is an indirect method that allows obtaining ceramic green pieces through the extrusion of a ceramic paste in a layer-by-layer deposition.

Results and Discussion

Table I presents the results for the produced samples regarding their density, surface roughness and fracture toughness.

Table I. Density, surface roughness and fracture toughness of the produced samples.

	Density (g/cm ³)	Surface roughness (µm)	Fracture toughness (MPa.m ^{1/2})
3D - 12.5% ZrO ₂	2.12±0.02	1.47±0.43	0.79±0.07
3D - 25% ZrO ₂	2.64±0.02	0.86±0.31	1.23±0.12
Glaze	2.05±0.08	0.17±0.02	0.83±0.04

Regarding the samples produced by robocasting, the results showed that although almost no detectable wear was found for 3D-25% ZrO₂, 3D-12.5% ZrO₂ suffered higher wear than 100% ZrO₂+glaze. These results may be explained by the fracture toughness values: 3D- 25% ZrO₂ presented higher toughness values than 100% ZrO₂+glaze. Concerning the cusps wear, 3D-25% ZrO₂ presented lower values than

the ones obtained against 100% ZrO₂+glaze. 3D-12.5% ZrO₂ induced the highest wear on the opposing teeth, which can be explained by its higher roughness combined with its low fracture toughness.

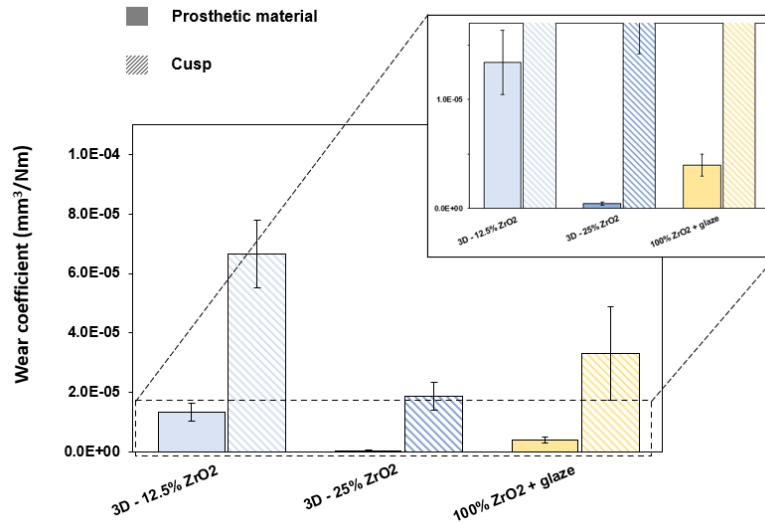


Figure 1. Wear coefficient of prosthetic materials and dental cusps.

Conclusions

This work allowed concluding that robocasting is a potential AM technique to produce 25% ZrO₂ since the prosthetic material wear was almost neglectable and the cusps' wear was lower than the one obtained against the currently used commercial material (100% ZrO₂+glaze). These results may be a starting point to explore alternative vitroc ceramic composite materials that avoid the use of glass-veneer coatings over zirconia prosthesis.

References

- [1] R. Galante, C.G. Figueiredo-Pina, A.P. Serro, Additive manufacturing of ceramics for dental applications: A review, *Dental Materials*, 35 (2019) 825-846.
- [2] I. Rodrigues, M. Guedes, S. Olhero, A. Cheddor, A.C. Branco, M. Leite, A.P. Serro, C.G. Figueiredo-Pina, Development of free binder zirconia-based pastes for the production of dental pieces by robocasting, *Journal of manufacturing processes*, 57 (2020).
- [3] A.C. Branco, R. Silva, T. Santos, H. Jorge, A.R. Rodrigues, R. Fernandes, S. Bandarra, I. Barahona, A.P.A. Matos, K. Lorenz, M. Polido, R. Colaço, A.P. Serro, C.G. Figueiredo-Pina, Suitability of 3D printed nanostructured zirconia pieces for dental applications, *Dental Materials*, 26 (2020) 442-455.

Low friction/wear properties of snake skins: a case study for mimicking nature tribological behavior

Juan Carlos Sánchez-López ^{a,*}, Clemens F. Schaber ^b, Stanislav N. Gorb ^b

^a Instituto de Ciencia de Materiales de Sevilla (CSIC-US), Seville, Spain

^b Functional Morphology and Biomechanics, Zoological Institute, Kiel University, Kiel, Germany

* jcslopez@icmse.csic.es

Synopsis

Snake skins evolved to withstand permanent friction and wear during sliding. Here, the microstructure of ventral scales of the snake *Lampropeltis getula californiae* was analyzed using scanning electron microscopy, and the long-term dynamic friction behavior was investigated by reciprocating sliding friction tests. A smooth epoxy resin with similar elasticity modulus and hardness was used for comparison purposes. Strong differences in frictional and wear mechanisms between the two materials were revealed in spite of similar mechanical properties. Snake skin showed a considerably lower frictional coefficient that kept stable over several thousands of sliding cycles. A reduction of the stick-slip behavior was also denoted by analyzing the variation of the friction coefficient in the forward and reverse motion influencing the wear mechanism. This frictional behavior can be explained by three different but complementary mechanisms: fibrous layered composite material of the skin with a gradient of material properties, surface microstructure, and the presence of ordered layers of lipid molecules at the skin surface.

Introduction

The ventral body side of snakes is almost in continuous contact with the substrate. This has important tribological consequences for the ventral (belly) skin, because it should generate strong friction to support forward motion, and simultaneously low enough friction to enable sliding along the substrate. Microstructures on the skin surface of snakes were suggested to have a high relevance for snake locomotion. Moreover, the study of the textures developed in the nature is being currently the object of multiple investigations for its implementation in real-world product applications [1].

The frictional properties of snake skin were studied in various species using different methods for characterization on the level of single microstructures or single and multiple scales. Most authors showed anisotropic frictional properties along the longitudinal body axis by comparing frictional coefficients for forward and backward direction, based on few sliding cycles. We have used a ball-on-flat tribometer to test the snake skin in reciprocating motion in pure sliding conditions over thousands of cycles and steady-states regimes achieved. The following questions were asked. How does the ventral skin surface behave in long-term friction experiments? How wear resistant is the snake skin under heavy loading conditions? Are the elasticity modulus and the hardness the primary factors for friction reduction and wear resistance?

For this purpose, we compared the snake skin frictional behavior with that of epoxy resin. After the experiments, the samples were inspected using scanning electron microscopy (SEM) to elucidate the frictional properties and wear mechanisms. Study object was the California King Snake (*Lampropeltis getula californiae*). Its skin, similar to other species, has a layered architecture, contains highly ordered embedded fibers, and exhibits a depth gradient in stiffness with a hard, robust outer surface and softer, flexible inner layers.

Results and Discussion

Table I. Average friction coefficient (μ) and standard deviation for the epoxy resin reference and the snake skin at different applied loads.

μ @Loads	0.15 N	0.25 N	1 N	3 N
Resin	0.91±0.68	0.87±0.18	0.79±0.10	0.69±0.10
Snake skin	0.34±0.28	0.29±0.22	0.23±0.09	0.24±0.08

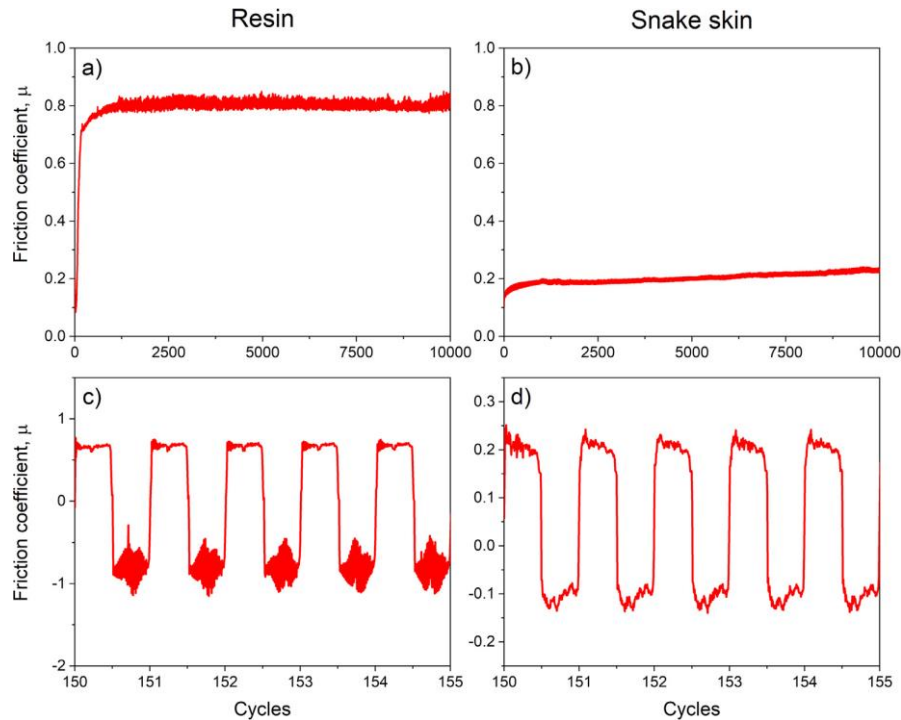


Figure 1. Friction coefficient curves for (a) the epoxy resin reference and (b) the snake skin at 1 N during reciprocating sliding motion. Details of the continuously measured friction coefficient for (c) the epoxy resin and (d) snake skin at 1 N from cycles 150 to 155. Sudden variations correspond to the changes of probe sliding direction.

Conclusions

For the first time the long-term frictional behavior of snake skin using a reciprocating motion in pure sliding conditions was studied (cf. Fig.1 and Table I). The comparative analysis with a flat resin surface of similar mechanical properties has put in evidence the importance of architectural design of biomaterials in preventing friction and wear. Optimized topography and graded mechanical properties enable the modulation of friction forces to ease motion and reduce wear [2]. This study may inspire the design and development of new textured surfaces with enhanced tribological performance.

References

- [1] A.P. Malshe, S. Bapat, K.P. Rajurkar, H. Haitjema, Bio-inspired textures for functional applications, *CIRP Ann. Manuf. Technol.* 67 (2018) 627–650.
- [2] J.C. Sánchez-López, C. F. Schaber, S.N. Gorb, Long-term low friction maintenance and wear reduction on the ventral scales in snakes, *Materials Letters* 285 (2021) 129011.

Torque loss model for axially pre-loaded tandem rolling bearings

Justino O Cruz ^{a,b}, Pedro M T Marques ^b, Jorge H O Seabra ^{a,*}, Jorge D Castro ^c

^a DEMec, Faculdade de Engenharia, Universidade do Porto, Porto, Portugal

^b CETRIB, INEGI, Campus FEUP, Porto, Portugal.

^c DEM, ISEP, Instituto Politécnico do Porto, Porto, Portugal

* jseabra@fe.up.pt

Synopsis

A new torque loss model for tandem Tapered Roller Bearings (TRB) is derived from the loads and torques applied to each rolling element, following the rolling element model proposed by Houpert [3]. The most important novelty of this approach is to consider the static torque, used in the tandem assembly, as an input parameter for the model, instead of the axial pre-load. The comparison of the predictions of the model with experimental measurements in tandem rolling bearings shows an excellent correlation, explained by the accuracy of the static torque used to assemble the bearings and its relevance for the bearing operation.

Introduction

Rolling element bearings (REBs) assembled in tandem, either in “X” and “O” arrangement, are a common design solution for mechanical systems [1, 2], for instance in automotive gear mechanical transmissions.

A common feature of this tandem design is that the rolling element bearings are always assembled with a significant axial pre-load, which assures the proper operation of the system.

One of the consequences of the axial pre-load is that it generates a static torque applied to the REB assembly. In fact, the highest is the static torque the highest will be the power loss generated by the tandem REBs. Figure 1 shows the torque loss measured in a tandem assembly of a pinion shaft, in a passenger car differential [1]. It is clear that, whatever the operating speed, the tandem torque loss increases when the static torque increases.

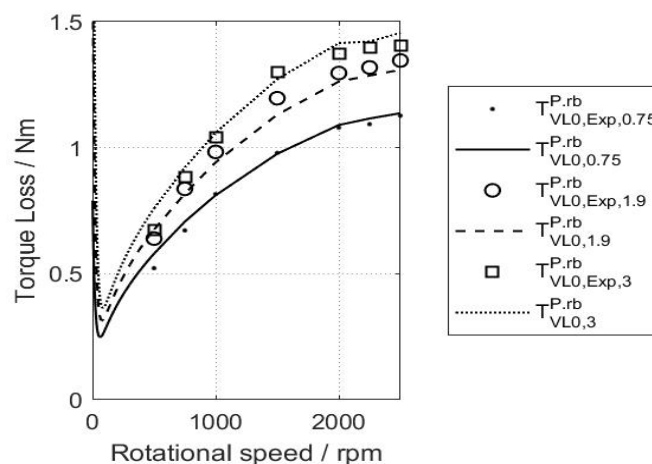


Figure 1. Torque loss in a tandem tapered roller bearing assembly in the differential of a passenger car.

Torque loss models

The torque loss models are derived from the model proposed by Houpert [3] for the torque components applied to each rolling element, that is the torques due to the rolling friction force, dT_{FR} , the friction between the rolling element and the rib of the inner race, dT_{rib} , and the elastic rolling torque,

dT_{MER} , due to the hysteresis losses,

$$dT = dT_{FR} + dT_{rib} + dT_{MER} \quad (1)$$

$$M = dT \cdot Z \quad (2)$$

Developing all these torque components, the overall torque applied to each tapered roller bearing becomes,

$$M = 0.00825 \gamma^* \sin \alpha^* Z^{0.44} E'^{0.19} dm^{1.63} l^{0.63} (\eta \cdot \omega_i)^{0.44} F_a^{0.37} + \quad (3)$$

$$0.424 \cdot B f Z \sin \alpha^* [\phi_{rib} \mu_{bl} + (1 - \phi_{rib}) \mu_{EHD}] F_a + 0.001912 \sin \alpha^* dm \phi_{mer} \mu_{bl} F_a$$

From equation (3) it is possible to define the starting torque, M_{st} , of the tandem TRBs, given by

$$M_{st} = (K_1 \cdot \sin \alpha_1^* \cdot dm_1 + K_2 \cdot \sin \alpha_2^* \cdot dm_2) \cdot \mu_{bl} \cdot F_a \quad (4)$$

$$K_i' = C \cdot \frac{B_i f_i Z_i}{dm_i} \text{ and } K_i = (K_i' + D), \quad i = 1,2 \quad (5)$$

Applying equation (3) it to the tandem TRBs and replacing equations (4) and (5) in (3), the overall torque becomes,

$$M_{tandem}^{TRB} = (1 - \phi) \cdot \frac{\mu_{EHD}}{\mu_{bl}} \cdot A \cdot M_{st} + 0.00825 \cdot B \cdot E'^{0.19} \cdot (\eta \cdot \omega_i)^{0.44} \cdot M_{st}^{0.37} \quad (6)$$

where A and B are defined as,

$$A = \frac{K_1' \cdot \sin \alpha_1^* \cdot dm_1 + K_2' \cdot \sin \alpha_2^* \cdot dm_2}{K_1 \cdot \sin \alpha_1^* \cdot dm_1 + K_2 \cdot \sin \alpha_2^* \cdot dm_2} \quad (7)$$

$$B = \frac{\gamma_1^* \cdot \sin \alpha_1^* \cdot Z_1^{0.44} \cdot dm_1^{1.63} \cdot l_1^{0.63} + \gamma_2^* \cdot \sin \alpha_2^* \cdot Z_2^{0.44} \cdot dm_2^{1.63} \cdot l_2^{0.63}}{[(K_1 \cdot \sin \alpha_1^* \cdot dm_1 + K_2 \cdot \sin \alpha_2^* \cdot dm_2) \cdot \mu_{bl}]^{0.37}} \quad (8)$$

Conclusions

The correlation between the experimental measurements and the predictions of equation (6) is excellent (see Figure 1). Such excellent agreement relies on the fact that the starting torque, M_{st} , as shows equation (5), includes crucial information about the tandem TRB axial load, geometry, contact angle and the rolling element / rib coefficient of friction.

A similar equation has been developed for tandem Angular Contact Ball Bearings.

References

- [1] Justino A O Cruz *et al.*, "No-load power loss of a rear axle gear transmission: Measurement and validation". ASME, Journal of Tribology, September 2022, Vol.144 2020, 091202, 1-13.
- [2] D C Witte, "Operating torque of tapered rolling bearings". ASLE Transactions, Vol. 16 (1973), 161-67.
- [3] Luc Houpert, "Ball bearing and tapered roller bearing torque: Analytical, Numerical and experimental results". Tribology Transactions, Vol. 45 (2002), 3, 345-353.

How can we simulate bio-medical tribological contacts on the lab scale?

D. Drees^{a,*}, L.M. Lopes^a, M.D. Bilde^a, E.P. Georgiou^a

^aFalex Tribology NV, Rotselaar, Belgium

* ddrees@falex.eu

Synopsis

In this work we present an overview on the ‘why’ and ‘how’ we developed and/or modified existing tribological methods to measure the friction and wear of materials for three distinctive bio-medical applications, namely hip joints, surgical sutures, and viscoelastic fluids.

Introduction

Friction and wear are important material characteristics that determine the functionality and lifetime of various applications. Among them, bio-medical tribo-systems stand out, as there is little to no room for error. However, the diversity and uniqueness of each tribological contact, makes it hard to reproduce the same contact conditions and subsequent failure mechanisms on the lab-scale, especially by using simplified test procedures. This is because different set of contact geometries, loads, motions, speeds, and environments are required for different in-vivo conditions. Using a simplified approach poses a great risk, as the obtained results do not necessarily correlate to the actual application and thus cannot be safely transferred/extrapolated.

Results and Discussion

Hip joint simulation: The failure of artificial hip-joints is often a combination of tribo-corrosion of the hip joint materials and inflammations due to wear particles in the body. For this reason, new materials are continuously being developed to prolong the life span of artificial joints. To date, biomaterials are often prescreened with a crude and simplified test such as the dry Taber Abraser (ASTM F 1978 – 00), which does not relate to what happens in the actual tribo-contact. Our proposed prescreening method is to use a multi-station wear approach, which allows to apply a multi-axial motion between 50 tribo-pairs in presence of serum. This motion is called Circular Track Pin on Disk (CTPOD). The method has shown to produce equivalent wear rates and wear particles as a full hip-joint simulator [1,2]. The major advantage is the number of test coupons. With 50 stations, it is easy to compare directly different materials and surface finishes, allowing at least 10 repeats for statistical and confidence level analysis, Figure 1.

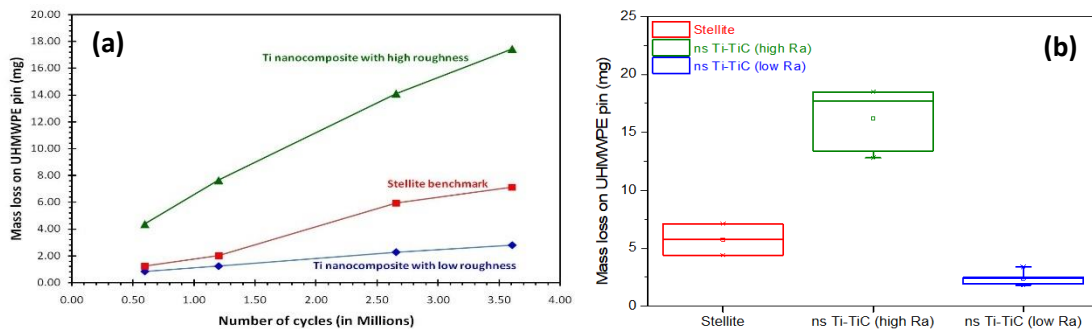


Figure 1. (a) Evolution and (b) statistical analysis of wear loss of UHWPE pins.

Surgical suture friction: Nowadays there is a wide variety of surgical sutures available in the market. They have different shapes, sizes, and thread materials or coatings, whereas they are being used extensively by surgeons, physicians, dentists, podiatrists, eye doctors, and other medical personnel. Up to date, most of the existing ranking and quality control processes are mainly based on mechanical (tensile) properties [3], whereas the frictional behavior is neglected. Thus, we have developed to

measure the friction of sutures with a high precision tribometer under the correct contact conditions. This method also allows for the complete 3D representation (Triboscopy) of the friction throughout the test, Figure 2.

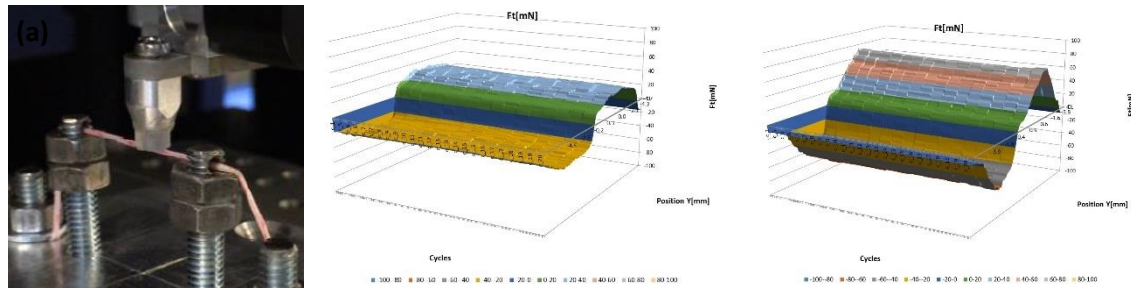


Figure 2. Comparison of 3D friction maps of different sutures, measured direct against silicone rubber countermaterial (50 mN, 5mm/s, vs 5 mm Ø silicone disk).

Adhesion and thread formation of viscoelastic fluids: Viscoelastic fluids are frequently used in biomedical and healthcare fields. Typical examples could be found in hydrogels for treating knee joints, but also in everyday consumer products such as toothpastes, creams or shampoos. Friction and viscosity behavior play as they determine how well these products flow and spread over areas, how they transfer between surfaces or how well they adhere to them. We have developed a new method that is based on indentation/retraction curves [4] with a high precision sensor, operating in the mN range. This approach can measure - in one operation- the adhesive strength, the thread formation (tackiness), the compression and separation energy of a viscoelastic fluid. It also allows to investigate the influence of different test conditions, such as retraction speed and applied load, on these properties. Thanks to the high precision and efficiency of the test method, a relative ranking with high confidence levels of these characteristics can be easily obtained.

Conclusions

- Different/modified tribological approaches are needed to simulate different applications and contacts for biomedical applications.
- Only by reproducing the same contact conditions and failure/wear mechanisms can the obtained results and comparisons are meaningful.

References

- [1] V. Saikko, Analysis of wear produced by a 100-station wear test device for UHMWPE with different contact pressures, *Tribology International*, 171 (2022)
- [2] E.P. Georgiou, D. Drees, S. Dosta, P. Matteazzi, J. Kusinski, J.-P. Celis: Wear Evaluation of Nanostructured Ti Cermets for Joint Reconstruction, *Biotribology*, 11 (2017) 44.
- [3] M. Alsarhan: A Systematic Review of the Tensile Strength of Surgical Sutures, *Journal of Biomaterials and Tissue Engineering*, 9 (2019) 1467.
- [4] E.P. Georgiou, D. Drees, M.D. Bilde, M. Anderson: Can We Put a Value on the Adhesion and Tackiness of Greases?, *Tribology Letters*, 66 (2018) 60.

Traction, Stribeck and scuffing characteristics of lubricants in rolling-sliding contacts using twin disc

Debdutt Patro ^a, Sravan Josyula ^a, Harish Prasanna ^a, Fabio Alemano ^b,
Deepak Halenahally Veeregowda ^{b,*}

^aGlobal Applications Lab, Ducom Instruments, India

^bGlobal Applications Lab, Ducom Instruments, B. V. Netherlands

* deepak.v@ducom.com

Synopsis

Rolling sliding contacts are integral to bearings, power transmission systems, rail-wheel interface and rolling mills are typically subjected to high contact pressures (1.5 to 4 GPa) and slip ratios (0 to 100%). Traction, Stribeck and scuffing characteristics of lubricants, governed by the base oil and additive chemistry respectively, directly affect the efficiency and durability of the machine elements.

Introduction

In this work, twin disc roller on roller with geometry representative of a line contact was used to measure the traction and scuffing performance of a commercial 20W50 oil. The tests were conducted at either room temperature or 100 °C using a heated lubricant recirculation system. Both friction at the contact and the vibration were measured during the test. For the traction test, the load was kept constant (1 to 2 GPa contact pressure) and the % slip varied between 0 and 40%.

Results and Discussion

A peak in the coefficient of friction was observed with % slip indicating the limiting shear stress under EHD conditions. The lubricant temperature also increased at higher % slip denoting the influence of thermal effects due to EHD shearing. Stribeck tests were conducted with decreasing entrainment velocity at constant load. A transition from EHD to boundary lubrication was observed with the friction coefficient increasing from 0.05 to 0.15 representative of non-conformal contacts. During scuffing tests, two different motions were used (a) co-rotation with a finite lubricant entrainment velocity (b) counter-rotation with near zero lubricant entrainment velocity. The load was increased in steps till either a sharp increase in friction (COF > 0.2) and/or vibration were observed. Under co-rotation the coefficient of friction was constant upto loads of 5kN (~2.3 GPa peak contact pressure). With counter-rotation however, there was simultaneous increase in friction coefficient and vibration at ~ 3 kN (1.8 GP contact pressure) indicating scuffing. Microscopy of the disc surfaces post-test indicated severe material transfer and surface damage. Such test methods using twin disc can effectively and quickly screen different base oil and additive chemistries in a repeatable manner and enable development of lubricants for electric vehicles and high-speed railways.

KEYNOTE 3

Corrosion-wear (tribocorrosion) mechanisms of hard coated stainless steels

Peter A Dearnley*

Director, Boride Services Ltd, Blakedown, Worcestershire, UK
Formerly Senior Lecturer, University of Leeds, UK and visiting professor in Surface Engineering, University of Southampton

* p.dearnley@outlook.com

Corrosion-wear (tribocorrosion) can be defined as the surface degradation of a material due to the sequential or simultaneous actions of corrosion and wear. This phenomenon has also been called 'mechanically assisted corrosion' (Jacobs et al, 1998). Laboratory experiments show that whilst such effects can be mitigated by the application of surface coatings, these might become undermined via chemical attack of the substrate. Three basic types of aqueous corrosion-wear mechanisms have been identified that are specific to surface engineered materials engaged in sliding contact with another material. Type I: The mechanical removal of the coating passive film or oxide scale (whichever provides corrosion protection) during sliding contact and its subsequent regeneration; Type II: Galvanic attack of the substrate leading to blistering and then removal of the coating or diffusion compound layer during sliding contact. This phenomenon only afflicts cathodic surface layers applied to anodic substrates and; Type III: Galvanic attack of the opposing sliding contact surface, when it is anodic relative to that of the outer surface of a surface engineered material. When the former is harder and more fracture resistant than the surface engineered material it is sliding against, the latter will become abraded. A series of laboratory investigations led by the author will be reviewed and their relevance to practical applications will be highlighted.

**SESSION D1:
SURFACE
ENGINEERING,
SURFACE TREATMENT
AND COATINGS**

Tribological performance of laser-treated WSC sputtered coatings sliding against NBR rubber

Todor Vuchkov ^{a,b}, Manuel Evaristo ^a, Alexandre Carvalho ^c, Albano Cavaleiro ^{a,b*}

^a University of Coimbra, Department of Mechanical Engineering, SEG-CEMMPRE, Coimbra, Portugal

^b IPN - LED & MAT - Instituto Pedro Nunes, Laboratory for Wear, Testing and Materials, Coimbra, Portugal

^c Physics Department & i3N, University of Aveiro, Campus Universitário de Santiago, Aveiro, Portugal

* albano.cavaleiro@dem.uc.pt

Synopsis

Laser patterning was performed on self-lubricating WSC coating in order to improve their lubricity during sliding against rubber. The patterning conditions allowed to improve the crystallinity of the WS₂ phase. The tribological testing against rubber showed improvement during the initial stages of sliding. During the later stages of sliding, the laser patterned coating performed similarly to the pristine one.

Introduction

Sliding of rubber material against steel can be encountered in many applications, e.g., shaft seals or tire moulding. During dry sliding of rubber against steel the coefficient of friction can be quite high, and lubrication is needed [1]. Conventional liquid/grease lubricants can be used, but in some applications their usage is not optimal due to the constant need of reapplication or extreme operating conditions (e.g., high temperatures). Solid lubricants can be an alternative in these extreme cases as they can operate at higher temperatures, and they can easily be contained on one of sliding interfaces. Tungsten-sulfur-carbon coatings are self-lubricating nanocomposite coatings deposited magnetron sputtering. They consist of an amorphous carbon (a-C) matrix with WS₂ TMD (Transition Metal Dichalcogenide) platelets embedded in it. WSC coatings can provide lubrication during sliding against steel [2]. Nevertheless, during sliding against rubber due to the low contact stresses, these coatings cannot provide the same level of lubrication as the lubricious TMD crystals cannot align in the direction of sliding. Therefore, in an attempt to improve the lubricity of the WSC we performed laser treatment of a W-S-C coating using a UV laser.

Materials and Methods

The W-S-C and a pure WS_x coatings were deposited by magnetron sputtering. Laser treatment on the W-S-C coating was performed using a UV laser. The morphological and structural analysis was performed using scanning electron microscopy (SEM), X-ray diffraction and Raman spectroscopy. The hardness was assessed using nanoindentation. The tribological testing was performed using a unidirectional pin-on-disk device using a NBR rubber ball as a counterbody. Post-test analysis was performed using SEM and 3D profilometry

Results and Discussion

The laser treated sample showed minor swelling (up to 50 nm), which could be related with the graphitization of the a-C phase. The graphitization of the laser treated zones was confirmed through Raman spectroscopy. These treated zones also contained WS₂ with improved crystallinity based on the Raman analysis performed. The untreated coating had a hardness of 5-6 GPa. The measured hardness in the treated zones showed decrease (down to 3 GPa) which could be related to the graphitization of the a-C phase. In this context it should be noted that graphite is inherently softer than a-C.

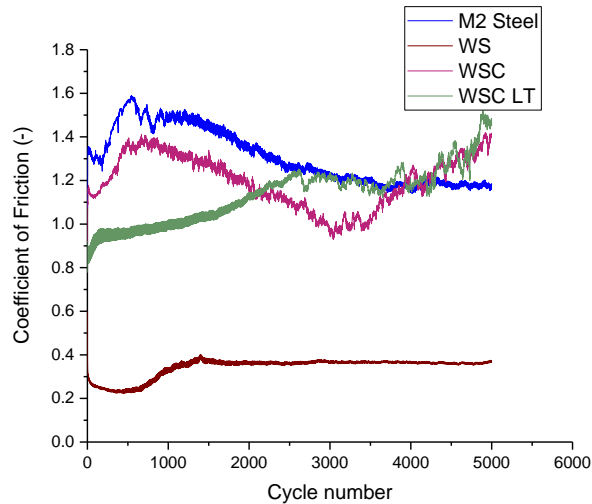


Figure 2. The evolution of the coefficient of friction as a function of the number of cycles

The tribological studies revealed that the laser treatment provided friction reduction during the initial stages of sliding. During the later stages of sliding the response of the untreated and the treated coating was quite similar. These trends are very likely due to depletion of lubricious material from the sliding interface, i.e., depletion/removal of the laser treated lubricious volumes of material. This theory is supported by the fact that the 3D scanning of the wear scar revealed pits (depth size up to 10 nm) in the treated areas. Finally, the pure sputtered WS_x coating showed the highest level of friction reduction due to its highly lubricious nature. Nevertheless, it should be noted that this coating suffered wear ($5 \times 10^{-5} \text{ mm}^3/\text{Nm}$), unlike the other samples where no measurable wear was detected.

Conclusions

Laser patterning can successfully be used for localized improvement of the crystallinity of coatings containing a-C and TMDs. The improvement of the crystallinity is often coupled with graphitization of carbon phase and a subsequent hardness reduction. During sliding against rubber counterbodies, the treatment can lower the coefficient of friction during the initial stages of sliding. The level of friction reduction is highest for single-phase sputtered WS_x coatings, but they suffer from excessive wear.

References

- [1] Caessa J, Vuchkov T, Yaqub TB, Cavaleiro A. On the Microstructural, Mechanical and Tribological Properties of Mo-Se-C Coatings and Their Potential for Friction Reduction against Rubber. *Mater* 2021;14.
- [2] Yaqub T Bin, Vuchkov T, Bruyère S, Pierson J-F, Cavaleiro A. A revised interpretation of the mechanisms governing low friction tribolayer formation in alloyed-TMD self-lubricating coatings. *Appl Surf Sci* 2022;571:151302.

Study of 2D Nano-coated Steel Surfaces for Wear Reduction

María J.G. Guimarey ^{a,b,*}, Mark Hadfield ^a, Amor Abdelkader ^a

^a Department of Design and Engineering, Faculty of Science & Technology, Bournemouth University, United Kingdom

^b Laboratory of Thermophysical and Tribological Properties, Nafomat Group, Department of Applied Physics, Faculty of Physics and Institute of Materials (iMATUS), University of Santiago de Compostela, Santiago de Compostela, Spain

* mariajesus.guimarey@usc.es

Synopsis

To explore the potential of two-dimensional (2D) nanomaterials as friction, wear, and hardness improvers, films of 2D hexagonal boron nitride (h-BN), graphene nanoplatelets (GNP), and the combination of both nanomaterials (h-BN/GNP) were deposited on mild steel by spray coating method followed by post-heat treatment. The mechanical and tribological properties of the coatings compared with bare steel were performed and analyzed using a Vickers micro-hardness testing, ball-on-disc tribometer, and a 3D optical profilometer, respectively.

Introduction

Reducing friction losses and thus wear between moving mechanical parts in contact with each other remains one of the significant industrial challenges of recent years [1]. The synergy between nanomaterials and industrial lubricant has shown great promise in addressing this challenge with reported excellent friction and wear performance [2]. However, liquid lubricants may not be used under certain operating conditions or applications: high temperature or vacuum. Therefore, the solid self-lubrication of two-dimensional (2D) nano-additives as metal reinforcement coatings presents itself as a very interesting alternative [3]. Moreover, nano-coatings would be a solution to the current demand for energy efficiency and help reduce the production of waste oil.

Among the 2D nanomaterials, graphene (GNP) and hexagonal boron nitride (h-BN) stand out as protective coatings due to their layered structure and excellent chemical resistance, barrier properties, impermeability together with thermal stability. Thus, to explore their potential in improving steel's friction and wear resistance, films of GNP, h-BN and a heterogeneous structure of both (h-BN/GNP) were deposited on mild steel by spray coating method combined with post-heat treatment.

Results and Discussion

The hardness results showed a greater improvement in this property for substrates coated with a post-heat treatment at 300°C, with increases of 2.5, 3.3 and 2.6 % being achieved for the 200-layer GNP, h-BN and h-BN/GNP coatings compared to the uncoated steel substrate, respectively (Figure 1a).

Sliding friction tests were performed on substrates uncoated and coated with 200 layers of each nanomaterial (GNP, h-BN and h-BN/GNP) and post-heated to 300°C for 4h first in dry conditions and then using a commercial oil as lubricant (5W-30). For dry lubrication conditions, excellent antifriction behavior is revealed for all coatings applied on the substrate compared to the bare one, reaching a coefficient of friction (COF) reduction of 22% for the steel sample coated with 200 layers of h-BN. This is not the case when an oil (5W-30) is used as a lubricant between the contact surfaces during sliding friction tests. Only the GNP-coated substrate produces a 15% improvement in COF over the bare sample, the h-BN and hybrid coatings do not achieve this antifriction effect when 5W-30 lubricant is used.

After the friction tests, the wear scars produced on the substrates were optically analyzed. Thus, excellent anti-wear performance was revealed for the nano-additive based coated substrates, especially for the h-BN/GNP based hybrid coating, reaching 44% reduction in wear area under dry lubrication. The GNP and h-BN coatings similarly managed to reduce the wear area on the steel substrate by 31% and 28% respectively (Figure 1b).

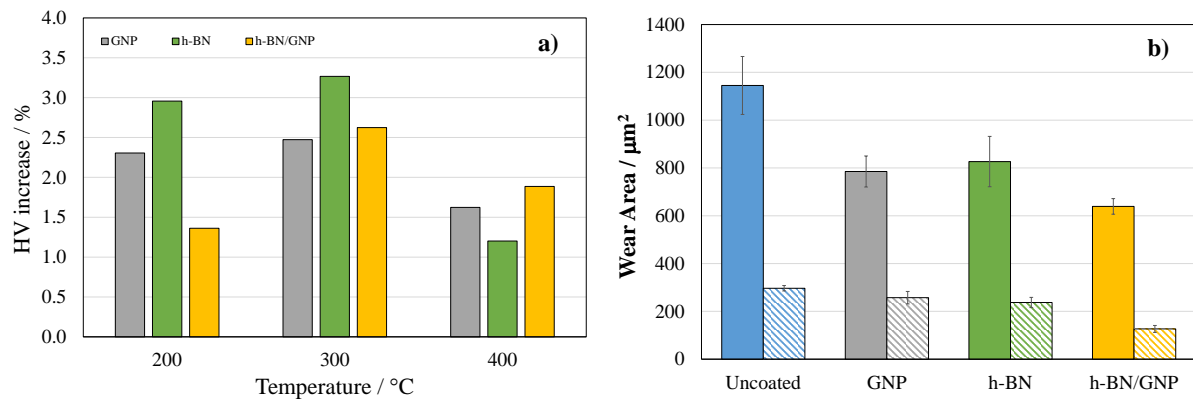


Figure 1. a) Increase in Vickers hardness of steel substrates coated with 200 layers of different 2D materials at different temperatures and b) wear cross-sectional area for uncoated and coated substrates in two different lubrication conditions: dry (filled bar) and lubricated (grated bar).

Conclusions

In this work, different 2D nano-coated steel surfaces were tribologically studied. In friction tests with sliding steel-steel tribo-pairs under dry conditions, graphene-containing ethanol solution coating decreased the coefficient of friction and wear area by 21% and 31%, respectively. Interestingly, it is revealed that under dry and lubricated conditions, h-BN-graphene heterostructure exhibits outstanding anti-wear properties synergistically compared to stand-alone 2D materials. This research suggests that this sort of nano-coating has the potential to improve the tribological performance of steel-steel tribo-pairs.

Acknowledgments

The financial support of the State Research Agency (AEI) of Spain and the European Regional Development Fund through the PID2020-112846RB-C22 project, and of Xunta de Galicia through ED431C 2020/10 is acknowledged.

References

- [1] K. Holmberg, P. Kivikytö-Reponen, P. Härkisaari, K. Valtonen, A. Erdemir, Global energy consumption due to friction and wear in the mining industry, *Tribology International*, 115 (2017) 116–139.
- [2] M.J.G. Guimarey, A. Abdelkader, M.J.P. Comuñas, C. Alvarez-Lorenzo, B. Thomas, J. Fernandez, M. Hadfield, Comparison between thermophysical and tribological properties of two engine lubricant additives: electrochemically exfoliated graphene and molybdenum disulfide nanoplatelets, *Nanotechnology*, 32 (2020) 025701-025714.
- [3] T.W. Scharf, S.V. Prasad, Solid lubricants: a review, *Journal Material Science*, 48 (2013) 511–531.

Plasma Electrolytic Oxidation coatings on a secondary cast Al-Si alloy for brake applications

Patricia Fernández-López ^{a,b,c,*}, Aleksey B. Rogov ^b, Sofia A. Alves ^a, Aleksey Yerokhin ^b, Raquel Bayón ^a

^a TEKNIKER, Basque Research and Technology Alliance (BRTA)

^b The University of Manchester (UoM)

^c University of the Basque Country (UPV/EHU)

* patricia.fernandez@tekniker.es

Introduction

Cast aluminium-silicon (Al-Si) alloys have been increasingly employed in different industrial sectors for the development of novel lighter components. In the automotive industry, the application of cast Al-Si components, among which engine parts and brake discs stand out, is envisaged as a strategic approach towards vehicle weight reduction, thereby minimizing fuel consumption [1]. The main interest in cast Al-Si alloys resides in their excellent castability, high mechanical properties and strength-to-weight ratio. Nevertheless, poor wear resistance and tribo-corrosion properties hamper the application of cast Al-Si alloys for critical components with stringent requirements [2].

Plasma Electrolytic Oxidation (PEO) is an environmentally friendly surface technology for the development of protective coatings on light alloys, e.g., aluminum, titanium, or magnesium alloys. The main advantages of PEO coatings are their high adhesion to the substrate, thickness and hardness, together with their excellent tribological and tribocorrosion performance. Despite the versatility of PEO technology, formation of PEO coatings with proper mechanical properties on cast Al-Si alloys represents a challenge, mainly due to the p-semiconducting behavior of the silicon phases as well as the presence of complex intermetallic compounds that hinder the initiation of plasma microdischarges [3].

The present study is focused on the development of PEO coatings on a heterogeneous secondary cast Al-Si alloy for brake disc related applications. PEO treatments have been carried out using a bipolar pulsed power supply, with variable pulse frequency and cathodic-to-anodic current density ratio. The electrolyte was specifically formulated for deposition of dense coatings with uniform thickness. Obtained PEO coatings were characterized in terms of thickness, roughness, phase composition and required energy consumption (Figure 1). Based on these results, potential candidates have been selected for further SEM/EDS characterization, hardness measurement and wear testing.

Tribological and intermittent tribocorrosion tests have been developed with the aim of validating the application of PEO coatings on brake discs. The tribological tests have been performed using a special tribometer that mimics the brake pad to disc contact pair. In order to assess coating feasibility for this application, the tribological behavior of PEO-coated Al-Si discs have been compared against that provided by cast iron which is commonly applied in brake discs. Furthermore, in real applications, brake pad-disc wear often occurs under adverse weather conditions or water-based lubricants promoting corrosive environments. Therefore, tribocorrosion tests have been also carried out for performance evaluation of the PEO coatings developed for brake application.

Conclusion

The present study presents new insights for the development of PEO coatings with high tribological performance on a secondary cast Al-Si alloy. From the results obtained, PEO technology is envisaged as an efficient alternative to extend the service life of cast Al-Si automotive components, making them competitive against the use of heavy cast iron parts.

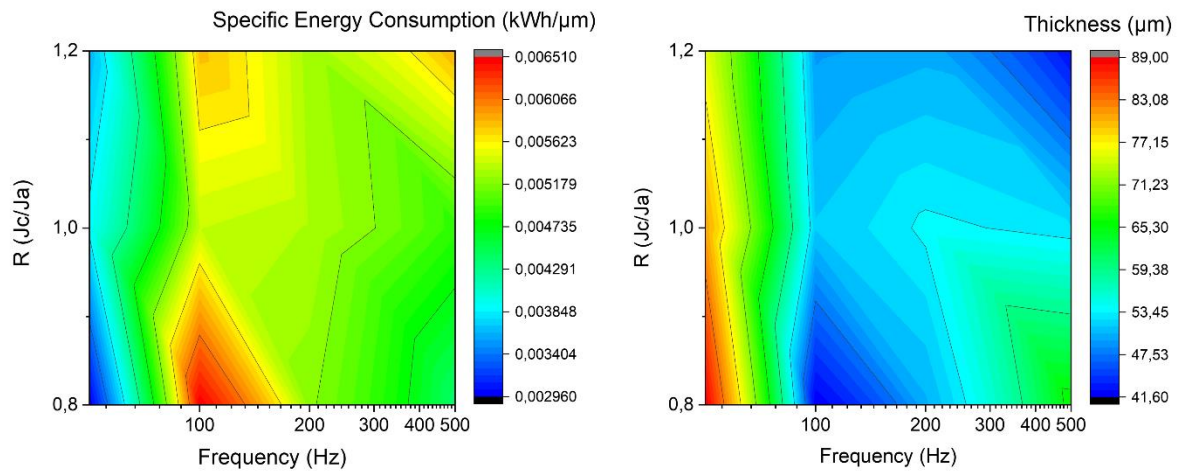


Figure 1. Dependence of specific energy consumption (kWh/μm) and thickness (μm) of the PEO coatings with the frequency and current ratio applied.

References

- [1] P. Fernández-López, S.A. Alves, A. López-Ortega, J.T. San José-Lombera, R. Bayón, High performance tribological coatings on a secondary cast Al–Si alloy generated by Plasma Electrolytic Oxidation, *Ceramics International*, 47 (2021) 31238.
- [2] S.A. Alves, P. Fernández-López, A. López-Ortega, X. Fernández, I. Quintana, J.T. San José-Lombera, R. Bayón, Enhanced tribological performance of cylinder liners made of cast aluminum alloy with high silicon content through plasma electrolytic oxidation, *Surface and Coatings Technology*, 433 (2022) 128146.
- [3] A.B. Rogov, H. Lyu, A. Matthews, A. Yerokhin, AC plasma electrolytic oxidation of additively manufactured and cast AlSi12 alloys, *Surface and Coatings Technology*, 399 (2020) 126116.

Enhancing the lubrication effect on tribological response of laser textured PH stainless steel surfaces

J.M. Vazquez-Martinez ^{a,*}, I. Del Sol ^a, M. Batista ^a, J. Salguero ^a

^a University of Cadiz, Av. Universidad de Cádiz 10, Puerto Real, Cádiz, Spain

* juanmanuel.vazquez@uca.es

Introduction

The UNS S17400 stainless steel, also identified as Grade 630 or 17-4 PH, is an extensively used engineering alloy in aerospace, automotive, energy or biomedical industry. In addition, this alloy is considered as strategic material for additive manufacturing applications. The excellent mechanical properties of the Precipitation-Hardening (PH) steel make it one of the most recommended materials for dynamic contact components. However, under lubricated sliding conditions this type of alloys may show limitations and unstable friction coefficient values [1,2].

This study is focused on the increase of performance, based on laser texturing modification procedures, of 17-4 PH steel surfaces under tribological wear. The development of a micro-dimple topography allows to improve the lubrication effect on the sliding contact, decreasing the wear damage and extending the lifetime of the surface.

In this research Commercial 17-4 PH steel samples of 60 mm diameter and 6 mm thickness, with an initial hardness of 380 HV were grinded to a surface finish of $R_a < 0,05 \mu\text{m}$ / $R_z < 0,15 \mu\text{m}$. Under these conditions, samples were irradiated using a 20 W Ytterbium fiber infrared laser system with 60 μm spot diameter and 100 ns pulse duration. Laser texturing was performed at 0.354 J/mm² of pulse energy density (E_d), in a range of 6 different scanning speeds (V_s), Table 1. Pulse distribution and density of dimples from the laser treatments was altered by selecting different pulse rates, separation between laser tracks (L_s) and scanning speeds. This allows to generate textures with a wide range of irradiated surface percentage (ISP), resulting on different nature and properties based on equidistant dimples. All the textures were irradiated in an open-air atmosphere.

Table I. Laser texturing conditions

ISP	98%	79%	55%	25%	14%	9%
P (W)	20					
F (kHz)	20					
Ls (μm)	80	100	120	180	240	300
Vs (mm/s)	1600	2000	2400	3600	4800	6000

Each texture was developed on a 5 mm thickness circular ring with 55, 45 and 30 mm external diameter.

Laser textured effects on steel samples were characterized with SEM/EDX, evaluating the size and shape of the dimple density by optical microscopy techniques and roughness measurement. The examination of the lubrication retention was carried out by the study of wetting behavior through contact angle measurement. Finally, pin-on-disc tribological tests were performed over the 6 different textured surfaces and an untreated sample. All tests were performed with a load of 25 N, a sliding distance of 500 m and a sliding speed of 27 m/min (0.45 m/s), using a tungsten carbide pin with 3.0 mm diameter. Sliding tests were carried out under lubricated conditions using 100 μl volume of Fuchs Renolin MR 3 VG 10 lubricating oil (DIN 51502).

Results and Discussion

Through laser texturing processes on 17-4PH steel surfaces, the development of modified layers with special topographies for specific applications have been achieved. Lubricant absorption has been improved through equidistant micro-dimples textures, improving the wear and friction resistance in sliding conditions compared to non-textured samples. A reduction of approximately 90% of friction coefficient (μ) have been obtained for lower activated areas (density of dimples), Figure 1. This improvement is also related to wear track volume, were adhesion and abrasion phenomena were identified as the main mechanism involved in the wear process of the tribological pair WC-Co / 17-4PH steel.

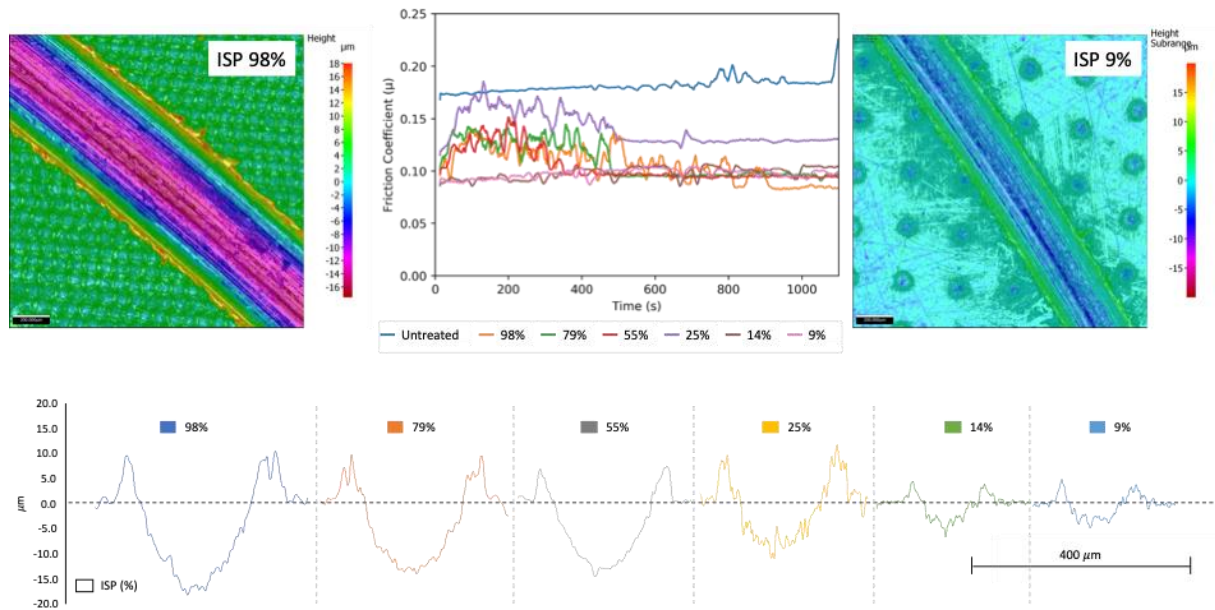


Figure 1. Wear and friction behavior of textured specimens

Conclusions

The percentage of irradiated surface shows a significant influence on the friction and sliding behavior of steel surfaces by the development of specific topographies that achieves a decrease in the μ values for all the laser treatments, mainly due to decreasing the wear debris on sliding track and stick-slip phenomena. By decreasing the ISP, average reductions higher than 50% and 70% were reached between higher and lower of the irradiated percentage surfaces.

References

- [1] N.S. Mahesha, R. Hanumantharaya, M.B. Davanageri, P.R. Devananda and K.M. Shivakumar, Tribological Wear Behavior of AISI 630 (17-4 PH) Stainless Steel Hardened by Precipitation Hardening, American Journal of Materials Science 6 (2016) 6-14.
- [2] H.R. Lashgari, Y. Xue, C. Onggowarsito, C. Kong, S. Li, Microstructure, tribological Properties and Corrosion Behaviour of Additively Manufactured 17-4PH Stainless Steel: Effects of Scanning Pattern, Build Orientation, and Single vs. Double scan, Materials Today Communications 25 (2020) 101535.

Study on the effect of LST atmosphere on the tribological wear behavior of Ti6Al4V

Irene Del Sol^{a,*}, Moises Batista^a, Jorge Salguero^a, Juan Manuel Vazquez-Martinez^a

^a University of Cadiz, Av. Universidad de Cádiz 10, Puerto Real, Cádiz, Spain

* irene.delsol@uca.es

Introduction

Ti6Al4V is the most common titanium alloy in the industry. Used in several fields, such as aerospace, automotive or medical, its engineering applications are uncountable. Among them, friction and wear situations may appear, being critical to improve the wear behavior of this alloy. In particular, the advantages of Laser Surface Texturing (LST) for surface modification have already been proven [1], among which we may find the control of the morphology, color and oxidation layer as a function of the processing parameters [2].

The LST parameters mainly used to control the morphology are the energy density (Ed) and the scanning speed (Vs). However, wear behavior is highly related to the formation of an oxidation layer for process under air atmosphere. Additionally, it should be noticed that the ablation environment has an impact on the material removal rate and laser ablation, which changes the microcracks geometry and the heat affected zone [3]. Nevertheless, far too little attention has been paid to the differences between inert and oxygen atmospheres effects on the LST surfaces of titanium. Therefore, this research is focused on the comparative study of the different atmosphere environments LST and its effects on the wear behavior.

For this purpose, titanium samples were textured under three different Vs values, with 4.04 J/cm² Ed, using air and protective (Ar) atmosphere (table I). Then, the samples were tested using a pin on disk tribometer to characterize the effect of the textures at different environments LST conditions. After testing, friction coefficient, pin and samples wear rates and wear mechanisms were studied.

Table I. Laser texturing conditions

Energy density (J/cm ²)	4.04	
Atmosphere	Air	Argon
Scanning speed (mm/s)	40-80-150	40-80-150

Results and Discussion

The atmosphere of the textures presented different aspects due to oxidation depending on the process atmosphere. Under oxygen, the scanning speed also changes the color of the textured area due to the oxidation, while argon samples did not modify the superficial color.

Regarding the tribology tests, the textures performed under an inert atmosphere generally increased the friction coefficient due to the roughness of the surface, Figure 1. Argon samples presented lower friction coefficients than oxygen with closer values to untextured surfaces, obtaining the same value (0.28) for 150 mm/s.

The main wear mechanisms detected for the samples were adhesion and abrasion. There is a significant reduction of the abrasion for both argon and oxygen tests. The weight variation of the pins is smaller for argon samples, being mainly related to a reduction of the adhesion and abrasion wear mechanisms. Oxidative treatments showed the formation of adhered multilayer deposition on the pin, Figure 2. Similarly, the scanning speed also affects the effect of the protective layer for oxygen samples, where at 40 mm/s the oxidation layer is unstable, and it is detached from the surface.

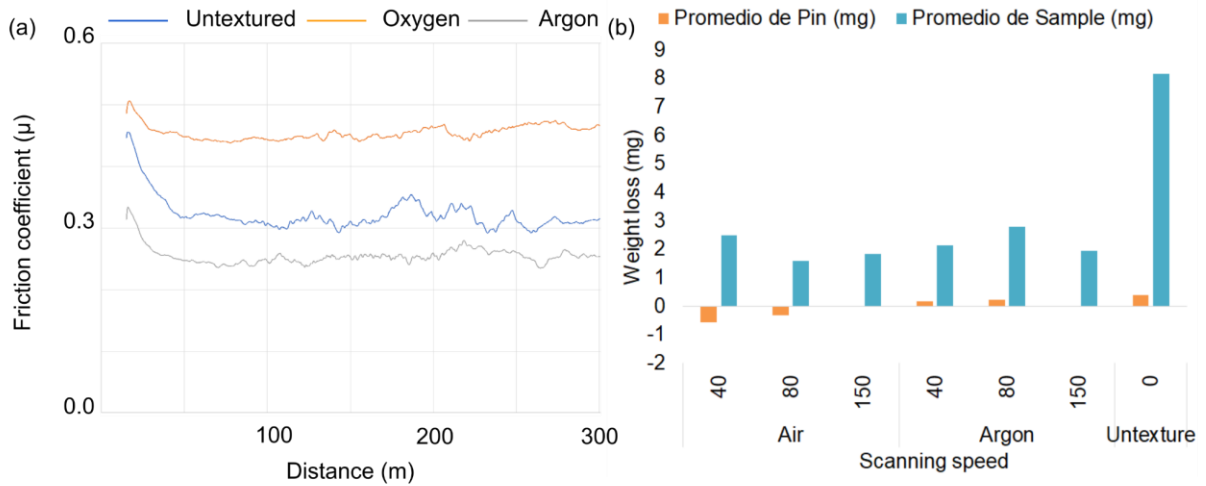


Figure 1. (a) Average Friction coefficient for $V_s=80$ mm/s (b) average weight loss for pin and samples.

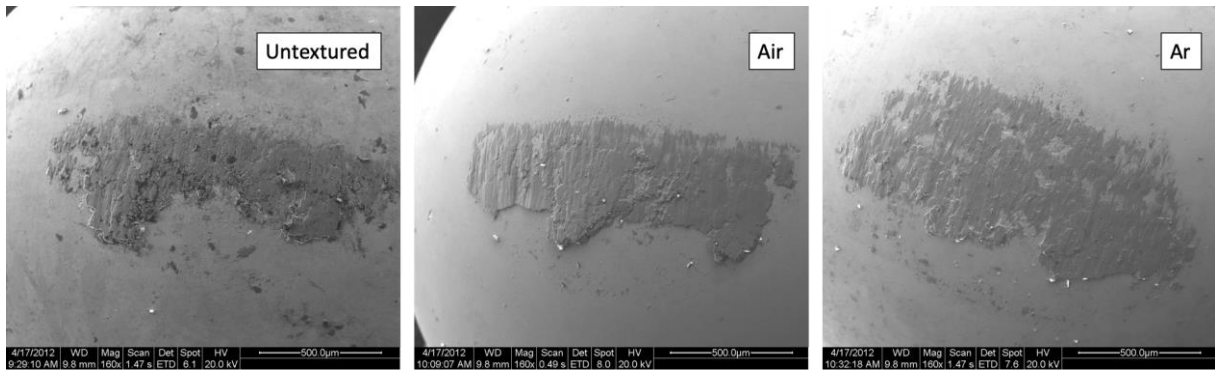


Figure 2. Adhesive effects of wear on pins for $V_s=40$ mm/s under different irradiation conditions

Conclusions

The friction coefficient is highly influenced by the V_s and the environmental atmosphere. Textures presented low variability between the LST treatments, and they reduced the wear of the samples which isolated the effect of the texture from the oxide layer. Oxidative environment increases the adhesion on the pins.

References

- [1] H. qiang Dou, H. Liu, S. Xu, Y. Chen, X. Miao, H. Lü, X. Jiang, Influence of laser fluences and scan speeds on the morphologies and wetting properties of titanium alloy, *Optik*, 224 (2020) 165443.
- [2] J.M. Vazquez-Martinez, J. Salguero, E. Blanco, J.M. González-Leal, Nanosecond Pulsed Laser Irradiation of Titanium Alloy Substrate: Effects of Periodic Patterned Topography on the Optical Properties of Colorizing Surfaces, *Coatings*, 9 (2019) 658.
- [3] Y. Wang, X. Zhao, C. Ke, J. Yu, R. Wang, Nanosecond laser fabrication of superhydrophobic Ti6Al4V surfaces assisted with different liquids, *Colloid Interface Sci. Commun*, 35 (2020) 100256.

Dry sliding wear of a laser-clad NiCrBSi-WC composite coating

I. Rodrigues^{a,b,*}, B. Nunes^{b,c}, R. Vilar^{b,c}, C.G. Figueiredo-Pina^{a,b}, A. Almeida^{b,c}

^a CDP2T and Department of Mechanical Engineering, School of Technology of Setúbal, Instituto Politécnico de Setúbal, Setúbal, Portugal;

^b CeFEMA, Center of Physics and Engineering of Advanced Materials, Instituto Superior Técnico, Universidade de Lisboa, Lisboa, Portugal;

^c Department of Chemical Engineering, Instituto Superior Técnico, Universidade de Lisboa, Lisboa, Portugal

* ivan.rodrigues@tecnico.ulisboa.pt

Synopsis

The wear behavior of an advanced hardfacing NiCrBSi-60%WC (wt.%) composite coating deposited by laser cladding is assessed in dry sliding conditions, under reciprocation motion against an alumina sphere. The microstructure of the coatings consists in WC particles dispersed in a matrix of primary γ -Ni dendrites and γ -Ni+Ni₃B interdendritic eutectic, with a fraction of other Cr and W carbides and borides particles formed due to some dissolution of the WC particles in the liquid during deposition. However, only minor dissolution of WC has occurred during deposition, leading to the formation of other carbide and boride phases that strongly contribute to its high hardness and good wear behavior, particularly by limiting adhesion phenomena at the softer matrix during sliding.

Introduction

Laser cladding is an established process for producing hardfacing coatings that increase the wear resistance of components, extending their service life [1]. NiCrBSi alloys reinforced with a high fraction of WC particles are among materials recently designed for laser deposition [2], with various applications in the mining and oil drilling industries and in cutting, metal forming and machining tools [3,4]. However, a careful control of the deposition parameters is critical to avoid excessive dissolution of the carbide and the consequent formation of brittle phases that often impair the coatings properties and wear behavior [2,5,6]. This study is a contribution to understand the effects of laser deposition on the microstructure and wear behavior of the coatings under dry sliding conditions.

Results and Discussion

Coatings of NiCrBSi-60%WC were deposited by laser assisted deposition on plates of 316L steel, using a diode laser system, at a laser power of 1200 W, scanning speed of 10 mm/s and a powder flow rate of 0.23 g/s (Figure 1a). The microstructure of the coatings consists of WC particles dispersed in a matrix of primary γ -Ni dendrites and γ -Ni+Ni₃B interdendritic eutectic (Figure 1b). Other phases, such as small faceted W₂C particles and M₇C₃ carbides, formed due to the partial dissolution of WC during solidification. Cr₅B₃, Fe₃B borides and Fe₂C, may have also precipitated in low fractions.

Reciprocating sliding wear tests were made under a sphere-on-plate configuration, using a 6 mm diameter alumina sphere, at a normal load of 2 N, a stroke length of 3 mm, at 2 Hz for 2 h. After a short initial transient, the friction coefficient remains relatively constant (0.5 ± 0.02) during sliding. The wear craters are very shallow and the wear coefficient is low (1.3 ± 0.4) $\times 10^{-7}$ mm³N⁻¹m⁻¹), as expected, due to the coating's high average hardness (1260 \pm 60 HV₂), resulting from the presence of a high volume fraction of the hard carbide and boride phases in the microstructure.

The wear surfaces show few traces of light abrasion (Figure 2a) and some evidence of carbide fracture and pull-out (Figure 2b) as main material removal mechanisms. Chemical analyses show oxide debris accumulated at the pulled carbide cavities (Figures 2b and c) and some alumina fragments from the counterbody (Figures 2b and d).

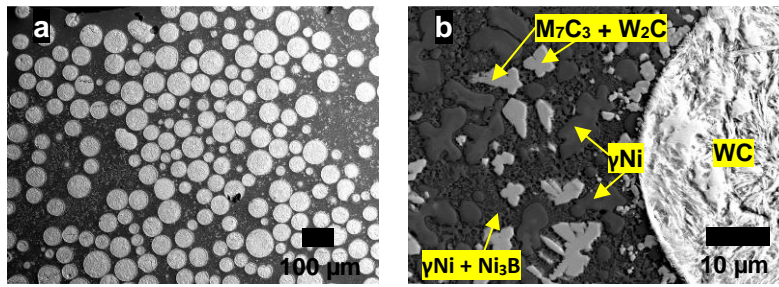


Figure 1. Coating cross-section (a) and microstructure (b).

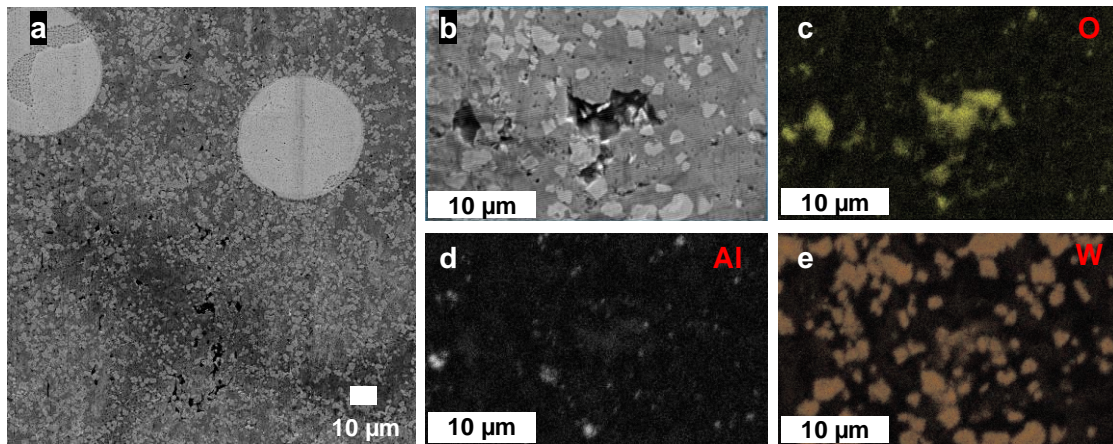


Figure 2. SEM analyses of the wear surface: secondary electron (SE) image (a); cavities due to carbide pull-out (b); EDS distribution map of O (c); EDS distribution map of Al (d); EDS distribution map of W (e).

Conclusions

The results show that the laser deposited coating presents a very high hardness and wear resistance. Only minor dissolution of WC has occurred during deposition, leading to the formation of other carbide and boride phases. Furthermore, the presence of a high volume fraction of hard phases strongly contributes to its good wear behavior, particularly by limiting the tendency for adhesion at the softer matrix during sliding.

References

- [1] B. Maroli, C. Liu, Overlay welding of NiSiB mixes with tungsten carbides, in: APMA 2017, Hsinchu, Taiwan, 2017.
- [2] S. Al-Sayed et al., Laser Powder Cladding of Ti-6Al-4V α/β Alloy, *Mat.* 10 (2017) 1178.
- [3] C. Guo et al., Effects of WC–Ni content on microstructure and wear resistance of laser cladding Ni-based alloys coating, *Surf. Coat. Tech.* 206 (2012) 2064–2071.
- [4] K. Bonny et al., Dry Reciprocating Sliding Friction and Wear Response of WC–Ni Cemented Carbides, *Trib. Let.* 31 (2008) 199–209.
- [5] D. Youssef et al., New 3D model for accurate prediction of thermal and microstructure evolution of laser powder cladding of Ti6Al4V alloy, *Alex. Eng. J.* 61 (2022) 4137–4158.
- [6] M. Vostřák et al., Comparison of Mechanical properties of laser clad WC and (TiW)C_{1-x} Ni based alloy coatings, in: METAL 2020, Proceedings: pp. 717–722.

KEYNOTE 4

Tribocorrosion Aspects of Biomedical Implant Failures: Progresses and New Directions

M.T. Mathew*

Regenerative Medicine and Disability Research lab, Department of Biomedical Science, UIC School of Medicine, Rockford, IL-61107

Dept of Restoratory Dentistry & Department of Bioengineering, UIC, Chicago, Department of Orthopedics, Rush University Medical Center, Chicago

* mathewtmathew@gmail.com

Ti/CoCrMo based Biomedical Implants are commonly used in clinical management and medical practices, to replace or repair malfunctioned or failed body parts or joints. The challenge of a clinician is to have an implant which satisfies the functional requirements of the patients, and it should have minimum side effects on the patient's body. Several clinical reports and studies showed the early failure of such implants and release of the metal ions/particles to the surrounding tissues, which become a serious clinical concern. Such processes are mainly caused by the mechanical movements of the implants coupled with the effect of body environment. The effect can be the biochemical or electrochemical response of the implant metals to the surrounding solution, which is called as corrosion. Furthermore, the combined effect of such mechanical/tribological factors and chemical and electrochemical factors is known as tribocorrosion.

This talk will address the basics and recent progress in the tribocorrosion (sliding/fretting) studies on the biomedical implant in vitro simulations, as a function of mechanical, biochemical and biological variables. Last 10 years, the research from our own lab, on corrosion, tribology and tribocorrosion aspects of biomedical implants (minimizing and early predictions) will be discussed and summarized. Through the combination of hip simulator, incubator/bioreactor and micro-fluidic system, a patient in lab (PiL) can be facilitated to investigate the potential risk associated with tribocorrosion processes from the implants.

**SESSION D2: SURFACE
ENGINEERING,
SURFACE TREATMENT
AND COATINGS/
LUBRICANTS AND
ADDITIVES/ MICRO AND
NANOTRIBOLOGY/
TRIBOCORROSION**

Wear resistance of laser cladded 25NiCr – 75CrC coatings

B.J. Diniz^{a,b,*}, C.G. Figueiredo-Pina^{a,b} A. Almeida^{a,b}

^a CeFEMA, Instituto Superior Técnico, Universidade de Lisboa, Lisboa, Portugal;

^b Department of Chemical Engineering, Instituto Superior Técnico, Universidade de Lisboa, Lisboa, Portugal;

^c Department of Mechanical Engineering, ESTSetúbal, Instituto Politécnico de Setúbal, Setúbal, Portugal

* bernardo.diniz@tecnico.ulisboa.pt

Synopsis

This work aimed at investigating the possibility of producing highly reinforced 25NiCr–75CrC composite coatings by laser deposition and to study their structure and wear behavior under dry sliding conditions.

Introduction

In many industries, such as the aerospace, metal forming, energy production and in mining machinery parts, the surface properties of the materials employed are of major importance. Metal matrix composites (MMC's) show excellent wear and corrosion resistance. These coatings are usually deposited by thermal spraying technologies that may lead to defects like porosity, microcracks, unmelted particles and low bonding to the substrate. Laser deposition enables coatings with a metallurgical bond to the substrate, low porosity and high microstructure control [1]. However, laser assisted deposition of coatings with high fractions of reinforcement phases present difficulties and cracking is frequent. St. Noworny *et al.* [2] have reported when laser cladding with particle loadings higher than 50wt%, it is increasingly harder for material to flow, leading to melt pool instabilities that result in a tooth edge appearance and poor coating quality, suggesting that an intrinsic upper limit in the amount of reinforcement phase should exist for the process.

Results and Discussion

The coatings were deposited by laser cladding on 304 stainless steel substrates, using a 1.5KW diode laser system and powders of NiCr–75CrC. The deposition parameters that allowed the production of coatings with optimized general characteristics are summarized in table 1.

Table 1. Laser processing conditions

Laser Power (W)	Scanning speed (mm/s)	Powder feed rate (g/s)	Overlap (%)
800	10	0.15	53

The coating has an average thickness of 1.1 ± 0.1 mm and presents a homogeneous microstructure and little porosity. The microstructure consists of elongated faceted Cr_3C_2 and Cr_7C_3 carbide particles dispersed in and matrix of (Ni,Cr)- $\text{Cr}_3\text{C}_2/\text{Cr}_7\text{C}_3$ eutectic (Fig. 1).

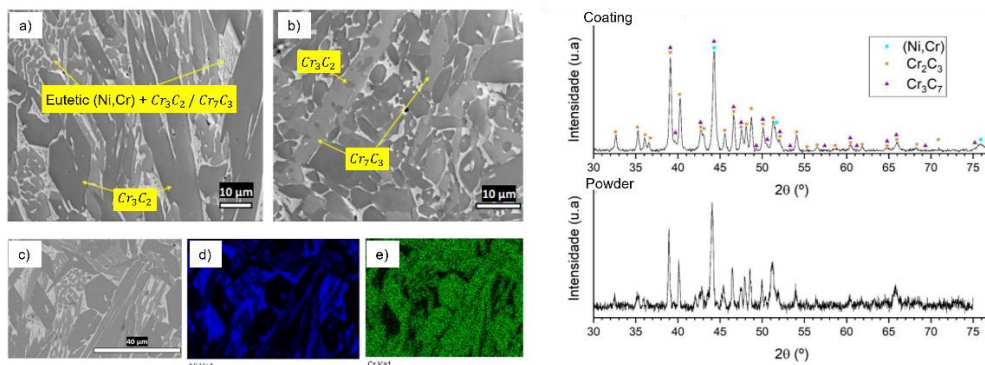


Figure 1. Microstructure of the coating (BSE) and corresponding XRD pattern.

The coatings present an average hardness of 1120 ± 20 HV1, constant throughout the coating thickness. The dynamic friction coefficient was measured during reciprocal sphere-on-plane sliding tests, against a 6 mm diameter alumina sphere, under a 2N load, a cycle distance of 3mm, a 2Hz frequency, for 2h. After an initial transient, the friction coefficient stabilizes at a relatively low value (0.1 ± 0.02). Wear tests performed in more severe dry-sliding conditions, against an alumina sphere (25.4 mm), under a load of 3N, a speed of 130 mm/s and a linear distance of 2500 m. The wear coefficient, calculated from measurements of the average crater diameter, yielded an average value of $(1.9 \pm 0.15) \times 10^{-5}$ mm³/(Nm). The wear surfaces show evidence of an oxide-rich tribolayer formation (Fig. 2), confirming that wear occurs in the mild oxidative regime and there is little tendency for adhesion.

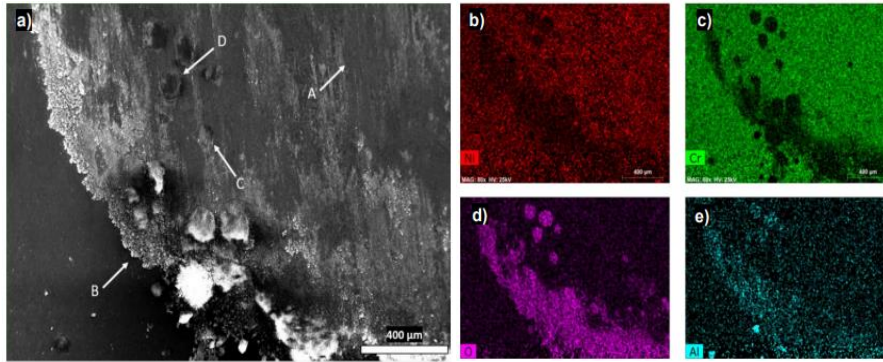


Figure 2. Wear crater surface micrograph after severe wear test. a) A –Light abrasion marks; B – Oxide accumulation; C and D – tribolayer formation; b) Ni EDS map; c) Cr EDS map; d) O EDS map e) Al EDS map.

Conclusions

High reinforced NiCr–75CrC coatings were successfully deposited by laser cladding. The coatings microstructure is formed of elongated chromium carbide particles and (Ni,Cr)+Cr₃C₂/Cr₇C₃ eutectic. The high carbide volume fraction is responsible for the coatings' high hardness and high wear resistance that occurs mainly in the mild oxidative regime.

References

- [1] Rui M. Vilar, Laser cladding, Proc. ALT'02 International Conference on Advanced Laser Technologies, 5147 (2003) 385-392.
- [2] St. Noworny, A.Techel, A.Luft and W. Reitzenstein, Microstructure and wear properties of laser clad carbide coatings, ICALCO 1993, 985-993.
- [3] J. P. Angle, Z. Wang, C. Dames, and M. L. McCartney, Comparison of two-Phase Thermal conductivity Models with experiments on Dilute Ceramic Composites, Journal of American Ceramic Society, 96 (2013) 1–8.
- [4] K. Wiczerzak and G. Cios, The characterization of cast Fe-Cr-C alloy, Archives of Metallurgy and Materials, 60 (2015) 779–782.

Performance assessment of different base oils for e-thermal fluids applications in BEVs

Vicente Macián ^a, Bernardo Tormos ^a, Jorge Alvis-Sánchez ^{a,*}

^a Instituto Universitario CMT-Motores Térmicos, Universitat Politècnica de València, Spain.

* jalvsan@mot.upv.es

Synopsis

The main purpose of this study was to characterize physical, chemical, and thermal properties of 4 low viscosity base oils before and after 120 hours of thermal aging at 150°C with a copper catalyst in order to determine the best option as a potential e-thermal fluid for immersion cooling application in Battery Electric Vehicles (BEVs).

Introduction

With the rise of electrification in the transport sector, an important topic of interest regarding thermal management and tribology arises: e-fluids [1]. With no standards and no extensive research, and with only a few products on the market, studying these fluids will help us understand, evaluate, and optimize current and future products.

Despite the lack of standardized tests, we can measure the most relevant properties for different specimens and provide ranking before and after degradation processes as well as detect advantages and limitations.

Results and Discussion

In order to determine how thermal aging affects the test fluids, thermal, physical, and chemical characterization should be done before and after degradation, following international standards shown in Table 1:

Table I. Standards used for properties measured

Properties	Equipment/Method	Standard
Viscosity & Density	Viscodensimeter	ASTM D7042, D4052, D287, D1298
Water content	Karl Fischer Titration	ASTM D6304
Particle content	ICP	ASTM D5185 / ISO 4406
Acid Number	TAN	ASTM D8045
Oxidation, Nitration & Sulfation	FT-IR	ASTM E2412, D7214, D7414
Thermal conductivity & c_p	Transient hot wire method	ASTMD7896

In addition to the 4 base oils used in this study, water and a fully formulated synthetic engine oil SAE 5W30 were used as references.

Table II. Thermal properties of test fluids at 20°C

Thermal properties	Water	SAE 5W30 Syn	Polyalphaolefin	Group 3 Paraffin	Diester	Polyol-ester
k [W/m K]	0,594	0,14	0,145	0,138	0,146	0,149
c_p [kJ/kg k]	4,167	2,174	2,314	2,21	2,076	2,052

Test fluids were subjected to thermal degradation at 150°C for 120 hours with a copper catalyst to boost the oxidation process. Although thermal conductivity and specific heat capacity can suggest a certain amount of cooling/heating potential, are not enough to determine the best candidate for e-fluid

applications, that is why a Figure of merit known as the Mouromtseff number (Mo) was used to determine the heat transfer capabilities of each fluid before and after thermal aging.

$$M_o = \frac{k^a * \rho^b * c_p^d}{\mu^e}$$

Where k is the thermal conductivity, ρ density, c_p specific heat capacity, and μ the dynamic viscosity. The exponents a , b , d , and e are values for a specific type of application; 0.8, 0.67, 0.33, 0.47 respectively for internal turbulent flow [1].

The following figures represent the Mo as a function of temperature for each aged fluid (Figure 1), and Mo Water/Fluid correlation (Figure 2):

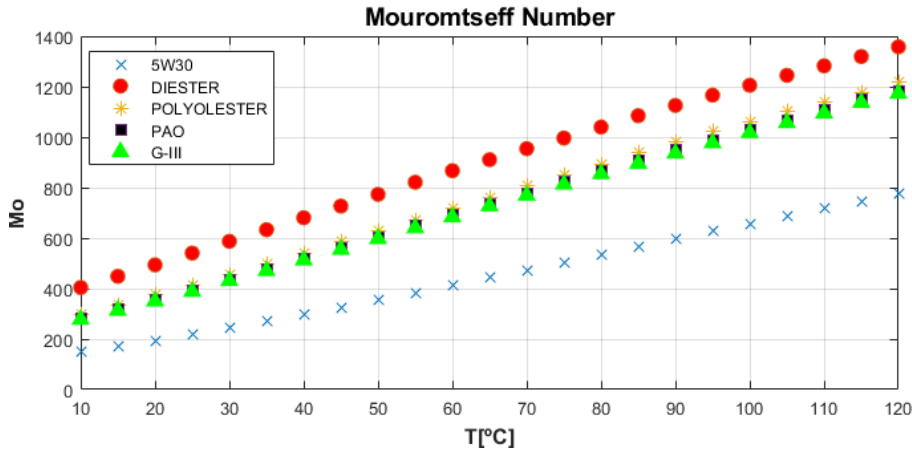


Figure 1. Mouromtseff number of aged fluids

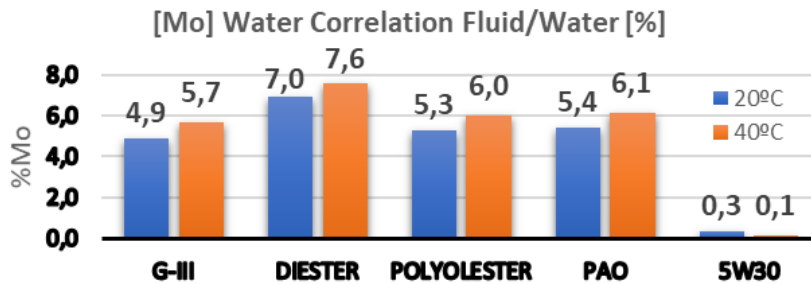


Figure 2. Fluid/Water Mo Correlation

Conclusions

From a thermal point of view, the properties of all test fluids didn't suffer any significant changes (less than 1%), indicating thermal endurance under adverse conditions. However, considering other chemical factors such as oxidation and acidification, there were some changes that can reduce their service life.

The best suitable base oil for immersion cooling applications in this experiment is the Diester, which has better heat transfer capabilities than the rest of the test fluids as well as better potential against oxidation.

References

- [1] J. Van Rensselar, «Driveline Fluids For Electric Vehicles» *TLT - Tribology & Lubrication Technology*, August 2021.
- [2] R. Simons, «Comparing Heat Transfer Rates of Liquid Coolants Using the Mouromtseff Number», *Electronic cooling*, 1 May 2006.

Oxidation influence on the electrical conductivity of transmission fluids in electric vehicles

R. González^{a,c,*}, N. Rivera^a, E. Rodríguez^b, A. García Tuero^b, A. Hernández Battez^{b,c}

^a Department of Marine Science and Technology, University of Oviedo;

^b Department of Construction and Manufacturing Engineering, University of Oviedo;

^c Department of Design and Engineering, Bournemouth University.

* gonzalezruben@uniovi.es

Synopsis

This work studies the influence of factors like temperature, time, and air exposition on the oxidation of three automatic transmission fluids (ATFs) and their changes in electrical conductivity. Results showed that electrical conductivity of the oils with higher additive content was less affected by oxidation. Electrical conductivity measurements are better than FT-IR ones for monitoring oil thermo-oxidative degradation at initial periods. Conventional ATFs could maintain good electrical compatibility in electrified drivelines, although their materials compatibility and copper corrosion protection of electrical components should be also tested.

Introduction

Currently, the lubrication of the electrified vehicles drivelines is carried out mainly by ATFs, but this solution is not optimized for the performance of the hybrid electric vehicles (HEVs) and electric vehicles (EVs) [1]. ATFs can also lubricate the electric motors (EMs) which requires compatibility with the copper in the coils and the polymers used in sensors and seals, an improved thermal conductivity, as well as electrical and magnetic compatibility [1-4]. Electrical conductivity of the oils should be low for avoiding current leaks and possible electric shock and short-circuits in the EMs. On the contrary, the oil cannot be an insulator because static buildup followed by static discharges can occur [5]. Tribology could contribute with formulation of new lubricants [6], which not only reduce both friction and wear, but also fulfil new requirements from systems like the EVs. Formulation of ATFs should contribute to reduce the oil degradation and its influence on different properties of interest for the EVs. The aim of this work is to study the influence of temperature, time, and air flow on the degradation (oxidation) of three commercial ATFs, using as response variable the electrical conductivity of the oil.

Results and Discussion

Lubricants were aged through a controlled process of oxidation. Two temperatures (150 and 170 °C), two air flow ratios (20 and 40 l/h) and two ageing times (168 and 216 h) were combined to create eight different oxidation states. Electrical conductivity was measured at different temperatures between 45 and 150 °C. All the lubricant samples can be classified as dissipative ones. In general, the aged lubricant samples have higher electrical conductivity than the fresh samples. An analysis of variance (ANOVA) was performed. The factor with the higher influence on the response was the temperature, followed by the time and the air flow. Viscosity of the aged lubricant samples increased a little compared to the ones of the fresh lubricant samples, so the variations in electrical conductivity can be associated to the oxidation. The Walden plot was used to evaluate the ionicity of the lubricant samples (Fig. 1). Results obtained show that all lubricant samples are considered "non-ionic" liquids. These results are very important for potential application of these ATFs in an electrified driveline. The molecular changes occurred in the lubricant samples after the oxidation process were measured by using the Fourier Transform Infrared (FT-IR) Spectroscopy technique. The ATFs showed an increase in oxidation, which was related to the corresponding antioxidant additive depletion. These experiments allow to conclude that the temperature in every case and the air flow rate in two cases induce chemical changes in the oils, which are translated into changes in the electrical conductivity.

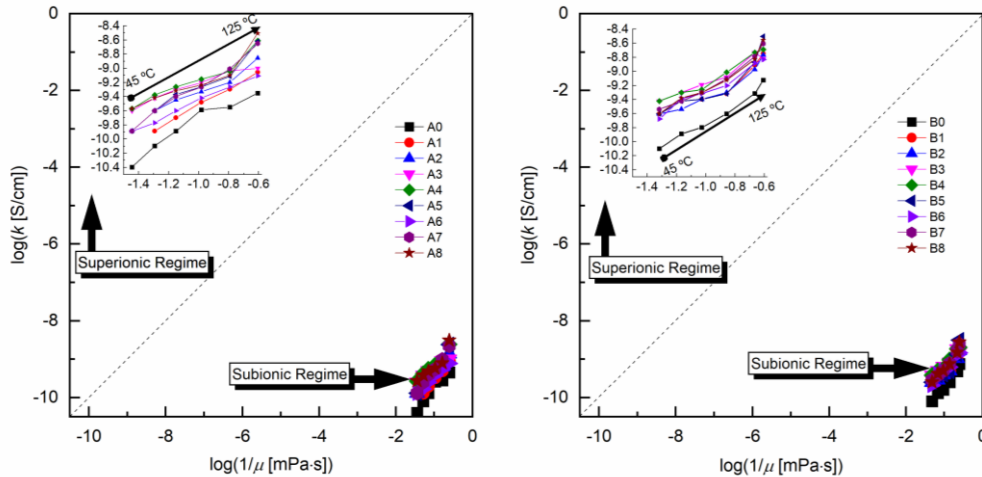


Figure 1. Walden plot of fresh and aged lubricant samples.

Conclusions

- Higher contents of additives in the oil formulation minimize the variations of electrical conductivity with the oxidation.
- Electrical conductivity is a good parameter for monitoring the degradation of ATFs and has greater resolution than FT-IR at initial periods of thermo-oxidative degradation.
- The variation of viscosity was small in the aged ATFs and then the variation in their electrical conductivity was attributed mainly to the oxidation, even at levels not clearly determined by FT-IR.
- All ATFs (fresh and aged) could be considered as dissipative and thus adequate to be used in EV with respect to the electrical conductivity.
- Principal component analysis shows a clear clustering of the oils depending on the aging conditions.

References

- [1] B. McCoy, Next generation driveline lubricants for electrified vehicles, *Tribology & Lubrication Technology*, 77(3) (2021) 38-40.
- [2] E. Becker. Gear lubricants in electric vehicles. *Tribology & Lubrication Technology*, 77(4) (2021) 80.
- [3] L.I. Farfan-Cabrera, Tribology of electric vehicles: A review of critical components, current state and future improvement trends, *Trib. Int.*, 138 (2019) 473-486.
- [4] A. Gangopadhyay, P.D. Hanumalagutti, Challenges and opportunities with lubricants for HEV/EV vehicles, *STLE Annual Meeting* (2019), USA.
- [5] Lubes'n'Greases, Perspective on Electric Vehicles Annual Report, LNG Publishing Company, Inc. 23-27, 2019.
- [6] K. Holmberg, A. Erdemir, Influence of tribology on global energy consumption, costs and emissions, *Friction*, 5(3) (2017) 263–284.

A molecular dynamics study of adhesion in metallic contacts

S. González-Tortuero ^a, M.A. Garrido ^a, C. Múnez ^a, J. Rodríguez ^{a,*}

^aDIMME, Grupo de Durabilidad e Integridad Mecánica de Materiales Estructurales.
Universidad Rey Juan Carlos, Madrid, Spain.

* jesus.rodriguez.perez@urjc.es

Synopsis

In this work, the effect of adhesion on metallic nanocontacts has been studied by means of molecular dynamics simulations. Simulations of nanoindentation tests with spherical tips on plane substrates in Cu-C, Cu-Cu, Ni-C and Ni-Ni systems have been carried out. Different contact models have been evaluated from the results obtained by molecular dynamics.

Introduction

The reliability and durability of micro and nanodevices (MEMS and NEMS) is highly conditioned by surface interactions that depends on the forces that can occur on a surface at small scale, such as friction, adhesion, meniscus forces and surface tension. Therefore, adhesion can be of great significance in metallic nanocontacts. The interaction between the bodies that come into contact is controlled by the asperities of their surfaces. At small scales, adhesion can alter forces and displacements fields around the contact leading to variations in stiffness contact, area of contact and other relevant quantities that are used to describe the surface interaction between solids.

Nanoindentation is a method that allows mechanical properties to be extracted from the continuous measurement of force and displacement at the contact between a tip and a substrate. Adhesion energy can also be obtained from the results of an indentation test if a suitable contact model is available. In the scientific literature, the best-known contact models are those of Johnson, Kendall and Roberts (JKR) and Derjaguin, Muller and Toporov (DMT). However, these models are only strictly applicable in situations where adhesion forces dominate over elastic ones or vice versa. Maugis proposed a contact model that could also describe intermediate situations.

In this work, simulations of nanoindentation tests with spherical tips on plane substrates in Cu-C, Cu-Cu, Ni-C and Ni-Ni systems have been carried out. Molecular dynamics simulations have been performed by using the open-source code Large-scale Atomic Molecular Massively Parallel Simulator (LAMMPS), developed by Sandia National Laboratories. The interactions between atoms in the substrates were described by the embedded atom method (EAM) potential, while the interactions between tip and substrate atoms were described by the Lennard-Jones potential.

Results and Discussion

The force-displacement curves obtained from molecular dynamics simulations of the indentation process onto Cu and Ni are the main results of this work. These curves were formed by a loading and unloading branches and from them, mechanical properties such as the modulus of elasticity and the adhesion energy can be determined if a suitable contact model is used for each system. In this case the Maugis model has been used to fit the molecular dynamics results.

At very shallow penetration depths for both cycles, the load showed negative values (arrows in Figure 1), signifying tensile forces because of an evident adhesion effect. These forces were higher for Cu samples than on Ni, in its interaction with spherical diamond tips. Consequently, a higher adhesion energy is expected for Cu than for Ni.

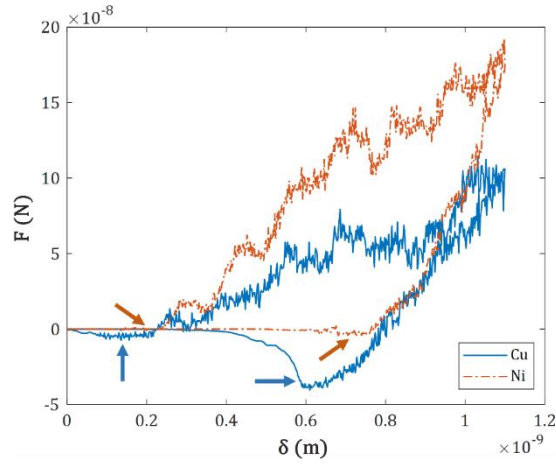


Figure 1. On the left, Force-displacement curves obtained from molecular dynamics simulations of indentation on Ni and Cu with spherical diamond tips; on the right, A contact model map: normalized indentation force versus λ parameter.

Figure 2 shows an adhesion map in which the total force applied during indentation (normalized with the adhesion energy and the effective radius of the contact) is plotted against the Tabor parameter. With this map it is possible to evaluate the most appropriate contact model for each situation.

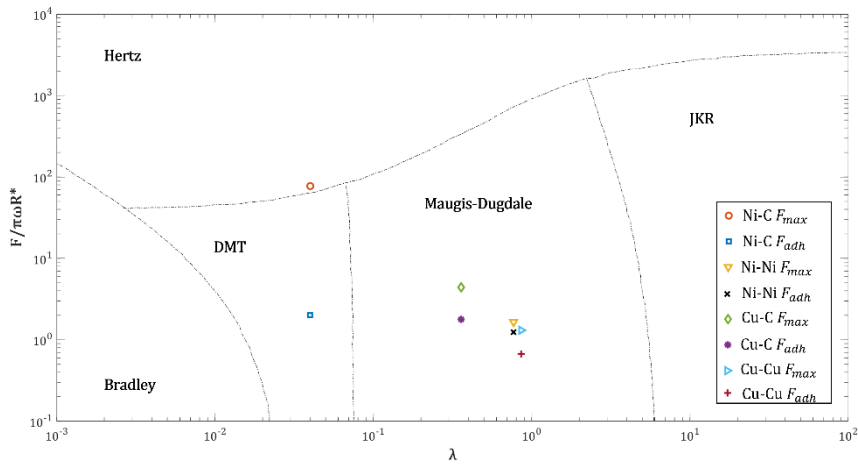


Figure 2. A contact model map: normalized indentation force versus λ parameter.

Conclusions

In this work, the applicability of the different contact models in the case of very small-scale metallic contacts has been evaluated. In most of the cases analyzed, the Maugis-Dugdale model is the most appropriate.

References

- [1] D. Maugis, Adhesion of Spheres: The JKR-DMT Transition Using a Dugdale Model. *J Colloid Interface Sci* 1992;150:243–69.
- [2] Ciavarella M, Joe J, Papangelo A, Barber JR, Bari P, Japigia V. The role of adhesion in contact mechanics. *J R Soc Interface* 2019;16.

Influence of swirl number and incidence angle on erosion-corrosion behavior of API steel pipe under swirling jets

Daniel E. Ramírez-Arreola ^a, Manuel Vite-Torres ^b, Francisco J. Aranda-García ^a, Ezequiel A. Gallardo-Hernández ^b, Jesus G. Godínez-Salcedo ^c, César Sedano-de la Rosa ^{a,b,*}

^a Departamento de Ingenierías, Centro Universitario de la Costa Sur, Universidad de Guadalajara, Jalisco, México;

^b Instituto Politécnico Nacional, SEPI-ESIME-UZ, Grupo de Tribología Col. Lindavista, Ciudad de México;

^c Instituto Politécnico Nacional, ESIQIE, Ciudad de México

* cesar.sedano@academicos.udg.mx

Synopsis

In this work, the effect of swirl velocity on erosion-corrosion damage was studied into the context of pipeline elbows and bends transporting slurries, focusing on axial velocity and incidence angle. Tests were conducted on API X-52 steel pipe coupons as target material and carried out at four different swirling intensities. The corrosive slurry consisted of a brine solution with suspended aluminum oxide particles. The impinging angles employed were 30°, 45°, 60° and 90°. Corrosion rates were obtained from LPR measurements. Pitting corrosion and corrosion products were characterized by means of SEM/EDS techniques. The experimental results showed that the swirl intensity enhances the pit growing, and the angle of incidence is not a relevant factor on pitting corrosion behavior.

Introduction

The American Petroleum Institute specification (API) covers seamless and welded steel line pipe. API X52 steel is suitable for conveying hydrocarbons, gas, water and oil in the petroleum and natural gas industries due to its high resistance against corrosive solutions; such as, H₂S [1], H₂SO₄ [2], alkaline electrolytes [3], and solutions with CO₂ [4]. Nowadays, in Mexico there are more than 17,000 km of pipelines made of this type of steel [5]. However, X52 steel is sensitive to the erosion-corrosion phenomenon when swirl flows are present in pipelines, particularly when transported hydrocarbons are forced to change direction.

This work is part of a series of studies that deal with the understanding of erosive-corrosive wear against pipeline steels, under impinging jets at different swirl numbers. Although there is information on the effects of the flow swirl number, there are no studies that combines both phenomena with different angles of incidence in order to observe which of these has a greater effect on the erosion-corrosion behavior of steel. In this study, the samples were exposed to a higher flow velocity of 5 m s⁻¹ and four angles of incidence (30°, 45°, 60° and 90°).

Results and Discussion

Figure 1(a) displays a radial path of corrosion products from the center of impact region towards the edge of the sample, which is aligned with the flow of the corrosive fluid. Figure 1(b) shows a 400X magnification bright-field image of the impingement region of Figure 1(a), exhibiting a localized corrosion due to pitting attack on the impinged surface. Besides, it can be seen some micropits surrounded by colored halos also observed by other researchers [6], as well as larger pits surrounded by brown corrosion products. Figure 1(c) presents an output flow path different from that observed at 90° of incidence, Figure 1(d) illustrates the corrosion products coming from dissolved metal into the pits leaving a trail along the flow direction. Regarding the distribution of the pits, it is also observed that some pits are so close together join to form a single larger pit.

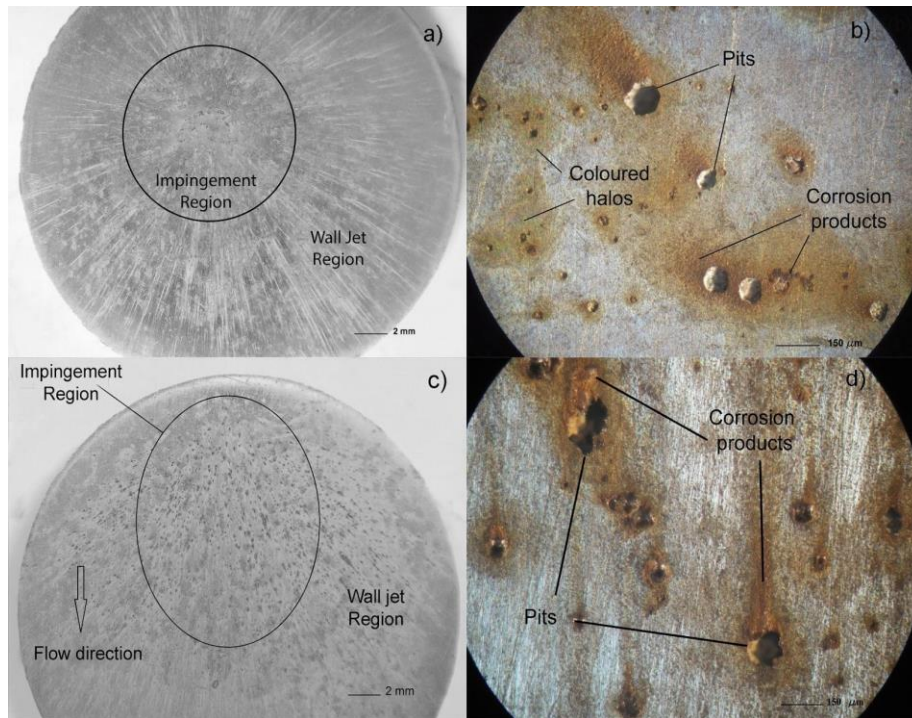


Figure 1. (a) Wear scar after 4 hours of erosion-corrosion at 90° of incidence and swirl intensity of $S=0.1$, (b) 400X magnification of impingement region at 4 hours of erosion-corrosion at $S=0.1$, (c) Image of surface damaged after 4 hours of erosion-corrosion at swirl intensity of $S=0.1$ and 30° of incidence, (d) Bright-field image of surrounding area of incident region of figure (c), after 4 hours of erosion-corrosion.

Conclusions

The swirl intensity accelerates the removal of corrosion products enhancing the pit growth, and promotes the API X-52 steel dissolution exposed to NaCl solution. Based on the conditions used, metal dissolution was the predominant metal degradation in erosion-corrosion process. The maximum corrosion rate was observed at high swirl intensities, making clear the severity of swirl conditions. Pitting nucleation was affected by the angle of incidence rather than the swirl intensity. Thus, for grazing angles minor pitting densities were observed. The incidence angle is not a determining factor that influences the pit depth behavior. The swirl intensity enhances the pit depth growing promoted by abrasive particles suspended into the corrosive solution.

References

- [1] D. G. Lilley, Swirl flows in combustion: a review, *AIAA J* 15 (8) (1977) 220 1063–1078.
- [2] Facciolo, Luca. A study on axially rotating pipe and swirling jet flows. Diss. KTH, 2006.
- [3] Zhang, K., Dybe, S., Shen, Y., Schimek, S., Paschereit, C. O., & Duwig, C. (2021). Experimental and Numerical Investigation of Ultra-Wet Methane Combustion Technique for Power Generation. *Journal of Engineering for Gas Turbines and Power*, 143(5)
- [4] S. V. Alekseenko, A. V. Bilsky, V. M. Dulin, D. M. Markovich, Experimental study of an impinging jet with different swirl rates, *International Journal of Heat and Fluid Flow* 28 (6) (2007) 1340–1359.
- [5] A. Nozaki, Y. Igarashi, K. Hishida, Heat transfer mechanism of a swirling impinging jet in a stagnation region, *Heat Transfer—Asian Research* 32 (8) (2003) 663–673.
- [6] W. Wang, X. Zhang, J. Wang, Pits with coloured halos formed on 1cr18ni9ti stainless steel surface after ennoblement in seawater, *Materials Science and Engineering: C* 29 (3) (2009) 851–855.

POSTER PRESENTATIONS

Characterization of cavitation corrosion behavior of different copper systems in artificial seawater

M. V. Biezma-Moraleda ^{a,*}, P. Linhardt ^b

^a Departamento de Ciencia e Ingeniería del Terreno y de los Materiales, Universidad de Cantabria, Spain;

^b Institute for Chemical Technologies and Analytics, Technische Universität Wien, Austria.

* Maria.Biezma@unican.es

Synopsis

This study is related to the behavior of various copper-based alloys and electrolytic copper against cavitation corrosion. A test was designed using an ultrasound (US) bath to create cavitation conditions in artificial seawater environment and monitoring the corrosion response via the free corrosion potential. It was observed that the low-alloyed copper systems, including pure copper, do not respond significantly on the impact of US, while the higher alloyed systems, nickel aluminum bronze, NAB, and manganese aluminium bronze, MAB, exhibit a pronounced electrochemical response. Based on mixed potential theory, this fact is explained based on the roles of kinetics, mass transport, and protective layers.

Introduction

Numerous marine components, as propellers, pumps, heat exchangers, etc., are based on copper alloys. Many of them are by the strong influence of the synergism of corrosion and cavitation, i.e., coupled electrochemical and mechanical phenomena. There are numerous studies that dealt mainly with the tribological properties of NAB [1-2], but only few systematic studies address the effect of passive/protective layers in this interactive phenomenon [3].

For this study, specimens made from (1) CuNiFe welded, (2) CuNiFe, (3) electrolytic Cu, (4) CuAlFe, (5) MAB and (6) NAB, were contacted to a wire, embedded in resin and the surface was prepared by grinding, final grit #1000. A glass beaker, filled with artificial seawater according to DIN EN 50905-4(2018) was placed in the water filled US bath, and a reference electrode (Ag/AgCl) was placed in the center of the beaker via a Luggin-electrolyte bridge. The specimens were immersed face-down in the beaker, Figure 1 presents this setup. The free corrosion potentials (E_{OC}) of all 6 specimens were scanned and recorded each second by a data acquisition system while the US was turned on and off repeatedly.



Figure 1. Setup of the corrosion cavitation test, before (left), and during the test (right)

Results and Discussion

Figure 2 presents the evolution of E_{OC} for all specimens during the test and Figure 3 provides views on the surfaces after the test. There appears no significant US effect on E_{OC} of specimens 1-4, which also did not exhibit any surface damages. By contrast, potential increase during US was observed for specimen 5 (MAB) with significant impacts on the surface (detail in Figure 3), while E_{OC} dropped during US for specimen 6 (NAB), but without notable impacts on its surface.

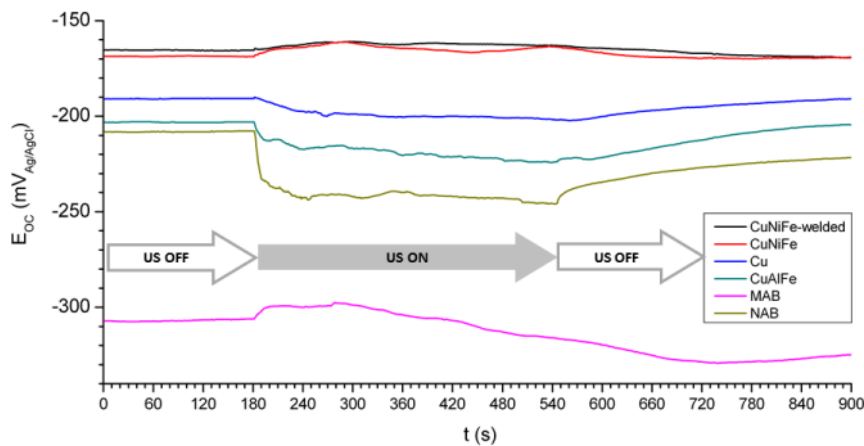


Figure 2. Evolution of E_{OC} of the specimens immersed in artificial seawater, with and without US

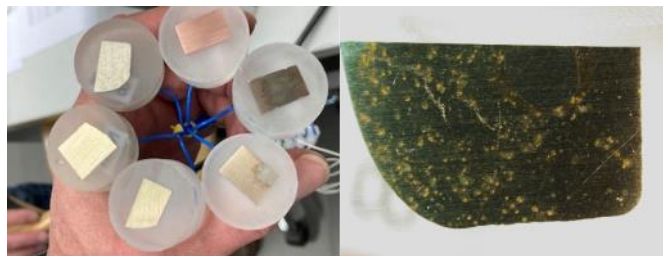


Figure 3. General view of tested specimens (left) and close-up view of cavitated MAB surface (right)

The NAB alloy is rather reactive but has a well protecting, conductive passive layer resulting in relatively positive E_{OC} without US with negligible anodic/cathodic reactions. Under US cavitation, E_{OC} of NAB drops significantly due to local removal of passivity and fast dissolution of the reactive metal. MAB corrodes actively, there is (almost) no protective layer and diffusion limited oxygen supply controls the corrosion process without US. The US enhanced mass transport for oxygen shifts E_{OC} of MAB to positive, which gets compensated by time by the increased metal dissolution due to cavitation impacts. The other metals (1-4) follow these basic principles to different degrees, showing less impact on their E_{OC} from the US effect.

Conclusions

The effect of cavitation conditions on the corrosion processes of various copper-based materials can be assessed by the free corrosion potential applying mixed potential theory and considering mass transport, kinetics of anodic metal dissolution and the role of protective layers.

Acknowledgements

To Wärtsila and Weldcopper S.A., Spain, for providing specimens, and project SUBVTC-2021-0024, Gobierno de Cantabria, for financial support.

References

- [1] R. Cottam, et al., The role of microstructural characteristics in the cavitation erosion behaviour of laser melted and laser processed Nickel–Aluminium Bronze, *Wear*, 317 (2014) 56.
- [2] B. Zhang, J. Wang, F. Yan, Load-dependent tribocorrosion behaviour of nickel-aluminium bronze in artificial seawater, *Corrosion Science*, 131 (2018) 252.
- [3] Al-Hashem, A. Hameed and H. Tarish. The Effect of Ultrasonically Induced Cavitation Conditions on the Behavior of Copper and Nickel Based Alloys in Seawater. *CORROSION 2006*, San Diego, California, March 2006. (paper 06299).

Electrochemically exfoliated 2D materials as lubricant additives

María J.G. Guimarey ^{a,b,*}, Jose Luis Viesca ^{b,c}, Amor M. Abdelkader ^{b,d}, A. Hernández Battez ^{b,c},
Mark Hadfield ^b

^a Laboratory of Thermophysical and Tribological Properties, Nafomat Group, Department of Applied Physics, Faculty of Physics and Institute of Materials (iMATUS), University of Santiago de Compostela, Santiago de Compostela, Spain;

^b Department of Design and Engineering, Faculty of Science & Technology, Bournemouth University, United Kingdom;

^c Department of Construction and Manufacturing Engineering, University of Oviedo, Asturias, Spain;

^d Department of Engineering, University of Cambridge, Cambridge, United Kingdom

* mariajesus.guimarey@usc.es

Synopsis

In the present work, lubrication properties (friction and wear) of a commercial engine oil 5W-30 doped with electrochemically exfoliated 2D materials, molybdenum disulfide nanoplatelets (MSNP) and graphene nanoplatelets (GNP), were investigated under two configurations (pure sliding and rolling/sliding). Thus, six 5W-30 nanolubricants were formulated: 5W-30 + 0.05 wt% GNP, 5W-30 + 0.1 wt% GNP, 5W-30 + 0.2 wt% GNP, 5W-30 + 0.05 wt% MSNP, 5W-30 + 0.1 wt% MSNP and 5W-30 + 0.2 wt% MSNP showing all of them an excellent stability for 6 months. Lubrication mechanisms of GNP and MSNP dispersed in engine oil for improving its antifriction, and anti-wear capabilities are proposed. The traction coefficient determination was performed at a 50% of slide-to-roll ratio and at different temperatures.

Introduction

Recent studies suggest that 33% of the fuel energy in passenger cars is dissipated to overcome frictional losses [1]. Similar energy losses are also observed in other moving parts, such as electric motors and transmission systems. These significant frictional losses have generated a growing demand for more efficient lubricants to fulfil low carbon emissions and fuel economy requirements in automotive engines. These systems operate under various lubrication regimes: boundary (BL), mixed (ML), elastohydrodynamic (EHL), or hydrodynamic (HL). Therefore, it is important to analyze the friction properties of engine lubricants under different test conditions and lubrication regimes using Stribeck curves. Nanoparticles as lubricant additives have attracted great interest as they play an essential role in tribology [2]. The selection of nanomaterials with suitable properties is a crucial step towards improving the tribological performance and enhancing the overall performance of engine oils. Adding nanomaterials to lubricating oils improves the tribological properties by forming a protective film on surfaces and creating a polishing effect between friction surfaces. In this respect, the emerging 2D materials have shown promising results as effective surface lubricants by offering interlayer sliding interfaces with phenomenally low interfacial shear strength [3].

Results and Discussion

1. Nanolubricants preparation

A novel electrochemical exfoliation method [4] was used for producing few-layer of GNP and MSNP in a single-step. Both nano additives were added to the commercial engine oil 5W-30 at concentrations of 0.05, 0.1 and 0.2 wt% by two-step method using an ultrasonic disruptor.

2. Sliding tests

The sliding tests were performed using an UMT-3 tribometer in a reciprocating ball-on-disc configuration for steel-steel contact at 363.15 K (optimum operating temperature of an internal combustion engine) and under a 20 N load. The nanolubricants with the lowest concentrations showed better antifriction behavior than the engine oil. However, when the concentration of additives increases, the friction coefficient worsens compared to the base oil (Figure 1a). Both nanolubricants, GNP and MSNP, showed very similar behavior at low and high concentrations but differed significantly at 0.1 wt%.

3. Rolling/sliding tests

The Stribeck curves were recorded for the engine oil and for all nanolubricants at three different temperatures (303.15, 333.15 and 363.15 K) and a slide-to-roll ratio (SRR) of 50%. All the nanolubricants changed to a ML at lower speeds and to EHL at high speeds under all tested temperatures. The traction behavior of the MSNP nanolubricants revealed a noticeable reduction of the traction coefficient for nanolubricants of 0.05 and 0.2 wt% MSNP concentration, both under mixed and elastohydrodynamic lubrication regimes (Figure 1b).

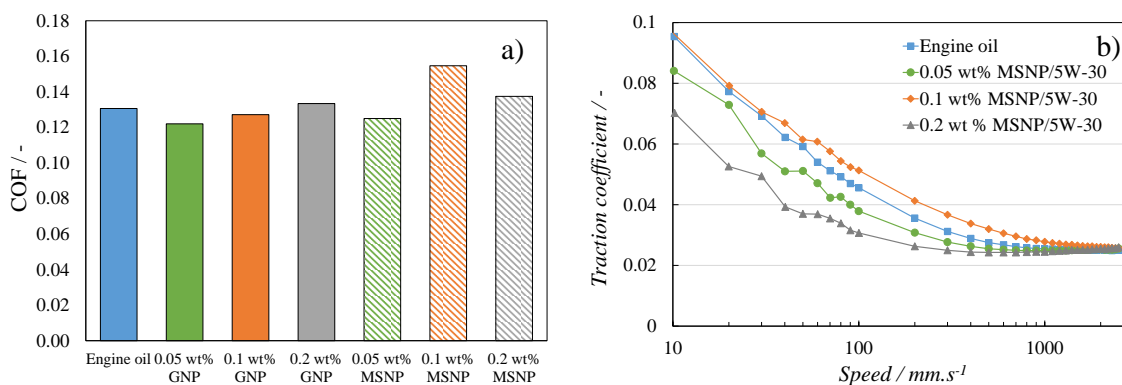


Figure 1. a) Coefficient of friction (COF) at 363.15 K during sliding tests and b) Stribeck curves of the engine oil and the different nanolubricants of MSNP at 363.15 K during rolling/sliding friction tests.

Conclusions

In this work, well-dispersed and surfactant-free nanolubricants with 2D materials showed an improvement in the antifriction and anti-wear properties of engine oil in different contact conditions, both through sliding friction tests and Stribeck curves. In particular, a remarkable tribological improvement of the formulated oil modified with GNP and MSNP was revealed at low concentrations (0.05 wt%) under pure sliding conditions. This enhancement was produced by tribofilm formation and mending/polishing mechanisms of both nano additives.

Acknowledgments

Ministry of Economy and Competitiveness of Spain (grant number: ENE2017-86425-C2-2-R project), Foundation for the Promotion of Applied Scientific Research and Technology in Asturias (grant number: IDI/2018/000131), and Xunta de Galicia in Spain (grant numbers: AEMAT ED431E 2018/08, GRC ED431C 2020/10 and ED481B-2019-015).

References

- [1] K. Holmberg, P. Andersson, A. Erdemir, Global energy consumption due to friction in passenger cars, *Tribology International*, 47 (2012) 221–234.
- [2] A.P. Singh, R.K. Dwivedi and A. Suhane, Influence of nano particles on the performance parameters of lube oil – a review, *Materials Research Express*, 8 (2021) 102001.
- [3] M.J.G. Guimarey, J.L. Viesca, A.M. Abdelkader, B. Thomas, A.H. Battez, M. Hadfield, Electrochemically exfoliated graphene and molybdenum disulfide nanoplatelets as lubricant additives, *Journal of Molecular Liquids*, 342 (2021) 116959.
- [4] A.M. Abdelkader, I.A. Kinloch, R.A.W. Dryfe, Continuous electrochemical exfoliation of micrometer-sized graphene using synergistic ion intercalations and organic solvents, *ACS Applied Material Interfaces*, 6 (2014) 1632–1639.

Effect of grooves and their geometry on the wear behavior of structured grinding wheels

P. Capela ^{a,b}, S.M. Costa ^{a,b,e}, M.S. Souza ^a, S.F. Carvalho ^a, L. Carvalho ^c, M. Pereira ^d,
J.R. Gomes ^{a,b,e,*}, D. Soares ^{a,b,e}

^a Departamento de Engenharia Mecânica, Universidade do Minho, Guimarães, Portugal

^b CMEMS – UMinho, Universidade do Minho, Guimarães, Portugal

^c Dragão Abrasivos Lda, Paços Brandão, Portugal

^d Centro de Física das Universidades do Minho e do Porto, Braga, Portugal

^e LABBELS – Associate Laboratory, Braga/Guimarães, Portugal

* jgomes@dem.uminho.pt

Synopsis

The dry and wet wear behavior of different structured abrasive grinding wheels, with different grooves geometry, were investigated and compared with an unstructured abrasive composite. It was found that the grooves, as well as their geometry, play a decisive role in the wear behavior of abrasive composites.

Introduction

Grinding wheels are the most used tools in manufacturing industry for roughing operations and surface finishing of components through a chip removal process. However, to achieve this goal, the wear resistance of the grinding wheel materials and their ability to promote wear on the opposing surface determine the performance of these tools. During these operations, very high cutting forces are required and the friction between the tool and the part to wear generates a high heat effect in the contact zone: this may induce thermal damages to the workpiece and a decrease in the grinding wheel performance [1,2]. The surface structuring/texturing of abrasive wheels has been a proposal to reduce the operating temperature [3]. In this work, two different kinds of grooved abrasive discs were produced, with spiral and hexagonal geometry. The structured grinding wheels were evaluated for their dry and wet wear behavior, being compared with an unstructured one.

Methods

Vitreous grinding wheels, made of alumina abrasive grains, were tested. All grinding discs under study were produced with $\varnothing 62 \times 8$ mm. Fig. 1 shows the difference between the unstructured abrasive disc (R) and the two structured discs with spiral grooves (S) and hexagonal grooves (H). The grooves were produced with 4 mm depth and 0.5 mm width.

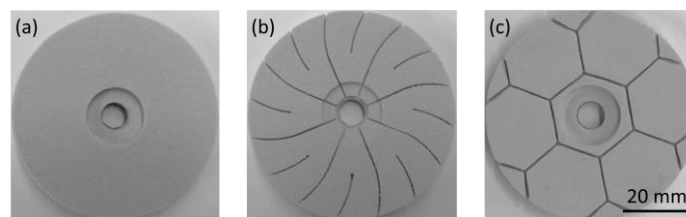


Figure 1. Abrasive discs tested surface: (a) unstructured, structured with (b) spiral and (c) hexagonal grooves.

Wear tests were carried out in a pin-on-disc geometry. Each type of abrasive disc was tested with and without distilled water flow (6 ml/min) as a coolant fluid (CF). Alumina pins were used as counterface ($\varnothing 5$ mm), creating particularly hard contact conditions. The normal applied load, the sliding speed and the sliding distance were kept constant at 20 N, $0.5 \text{ m}\cdot\text{s}^{-1}$ and 1800 m, respectively. The wear rate of mating samples was measured by gravimetric method.

Results and Discussion

Fig. 2 shows the wear rate of the discs (Fig. 2(a)) and of the corresponding alumina pins (Fig. 2(b)), as well as the grinding ratio (pin/disc wear rates) for each tested tribopair (Fig. 2(c)). When comparing wear tests with and without CF, results show that the CF contributes to a significant reduction in the wear rates of abrasive discs (up to 91 % for H) and of alumina pins (up to 67 % for H), increasing the grinding

wheel durability. The presence of the CF during wear tests increases the grinding ratio of the tested pairs, i.e. performance of the grinding wheels. This effect is significantly enhanced for structured grinding wheels (Fig. 2(c)). On the other hand, the beneficial effect of abrasive wheel structuring on its performance depends on the design of the wheel grooves. The hexagonal grooves (H) seems to have a coolant reservoir effect allowing better lubrication of the pin-disc contact, which significantly reduces the wear rates of the disc and of the pin. However, the spiral grooves (S) may allow a greater fluid flow favoring the removal of wear debris. In this way, the spiral geometry provides better grinding wheel performance than hexagonal geometry structure (H).

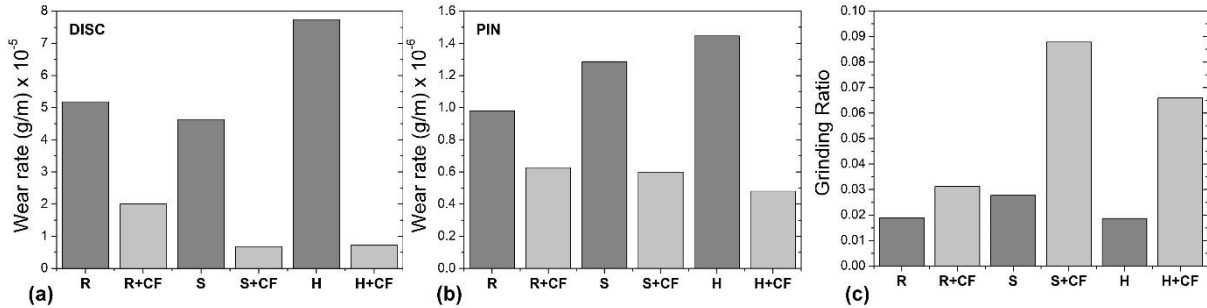


Figure 2. Wear rate of the (a) abrasive discs, (b) alumina pins counterface and (c) grinding ratio of the tribopairs.

Conclusions

The use of coolant fluid always results in a reduction of the wear rate of the grinding wheels. The coolant increases the performance of the grinding wheels (grinding rate) and this effect is more noticeable for the structured wheels. The beneficial effect of wheel structure depends on the wheel grooves geometry. Spiral grooves allow for increased fluid flow and better removal of wear debris. Spiral grooved grinding wheels outperform hexagonal grooved grinding wheels.

References

- [1] R.L. Paiva, R.S. Ruzzi and R.B. Silva, An approach to reduce thermal damages on grinding of bearing steel by controlling cutting fluid Temperature, *Metals*, 11(2021)1660.
- [2] H. El-Hofy, "Fundamentals of machining processes: conventional and nonconventional processes," Boca Raton: CRC press, 2018.
- [3] H.N. Li and D. Axinte, "Textured grinding wheels: a review", *International Journal of Machine Tools and Manufacture*, vol. 109, 2016, 8-35.

Acknowledgements: This work is within the scope of the Sharlane Costa Ph.D. degree in progress, financially supported by the Portuguese Foundation for Science and Technology (FCT) through the PhD grant reference 2021.07352.BD; this work is also supported by FCT national funds, under the national support to R&D units grant, through the reference project UIDB/04436/2020 and UIDP/04436/2020.

Effect of SiO₂ and coated SiO₂-SA nanoparticles on the lubricant properties of a paraffinic base oil

José M. Liñeira del Río ^{a,b,*}, Arturo Castro Currás ^a, Vanesa Somoza ^a, Fátima Mariño ^a, María J.G. Guimarey ^{a,c}, María J.P. Comuñas ^a, Josefa Fernández ^a

^aLaboratory of Thermophysical and Tribological Properties, Nafomat Group, Department of Applied Physics, Faculty of Physics and Institute of Materials (iMATUS), Universidade de Santiago de Compostela, Santiago de Compostela, Spain;

^bUnidade de tribologia, vibrações e manutenção industrial, INEGI, Universidade do Porto, Porto, Portugal

^cDepartment of Design and Engineering, Faculty of Science & Technology, Bournemouth University, UK

*fatima.marino.fernandez@usc.es

Synopsis

This work analyzes the effect of two types of silicon dioxide nanoparticles, one uncoated, SiO₂ and the other coated with stearic acid SiO₂-SA on the lubricant properties of a paraffinic base oil (Yubase 6) supplied by Repsol with a dynamic viscosity at 313.15 K of 28.9 mPa s and a viscosity index of 133. Two-step method with ultrasonic disruptor was used to prepare eight nanolubricants of Yubase 6 + SiO₂ or of Yubase 6 + SiO₂-SA at 0.15 wt%, 0.30 wt%, 0.45 wt% and 0.60 wt% nanoparticle mass concentrations. Some lubricant properties (viscosity, viscosity index, friction coefficient and wear) are reported. The morphology of nanoparticles was analyzed by electron microscopy. Visual observation, and temporal evolution of refractive index were used to analyze the stability of the nanolubricants. Viscosity and viscosity index data were obtained from a rotational viscometer. Finally, tribological tests were performed at pure sliding conditions at 383.15 K and the wear was quantified with a 3D optical profilometer.

Introduction

Automotive industries have recently switched development trends from the traditional powertrain mechanical components into the digital transformation of the electrification components in advanced propulsion vehicles. This industrial impact on global development trend into automotive electrification designs has created an emerging technology for new propulsion systems such as hybrid electrical vehicles or electrical vehicles (EVs) [1]. From an environmental point of view, the rise of EVs can reduce both noise and air pollutions, especially in the cities. From a technological point of view, the development of new fluids and materials or the evolution of batteries can be promoted. Although EVs present a substantial high efficiency in terms of energy consumption, there is a challenge to improve the efficiency even more. Tribology can contribute to improve the efficiency of EVs by reducing friction in components such as wheel bearings and gears [2]. New formulations of electric transmission fluids that fulfil all the requirements respect to electrical, thermal and tribological properties, and compatibility with copper and other materials in presence of electric and magnetic fields are necessary.

Results and Discussion

The variation of the viscosity index due to the presence of nanoparticles is plotted in Figure 1a. It can be observed an increase of this property with both nanoparticles, being the biggest values obtained for SiO₂-SA, thus at the highest nanoparticle concentration (0.60 wt%) an increase of 15% is obtained. From Figure 1b, it can be concluded that SiO₂-SA nanoparticles lead to the biggest increase in viscosity. Hence, for the same composition, at 0.30 wt% for example, the increase obtained with SiO₂ is 4.5% whereas for SiO₂-SA is 18.4%. Friction coefficients obtained with SiO₂-SA nanolubricants are much smaller than those observed for SiO₂ nanolubricants and unadditivated Yubase 6 oil for all tribological

tests. Thus, the greatest reduction (46%) on the friction coefficient was observed when SiO₂-SA coated nanoparticles are used as additives of Yubase 6.

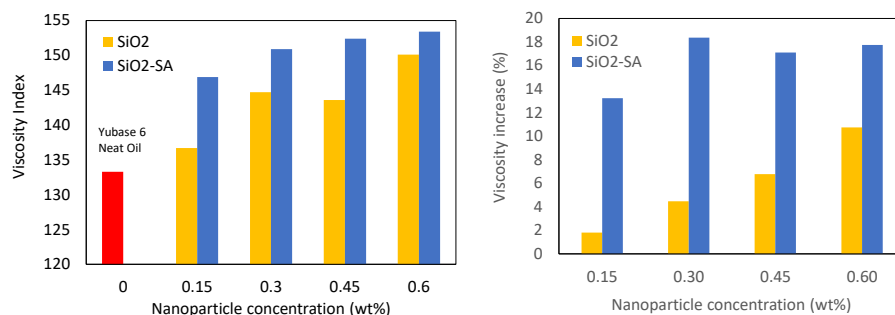


Figure 1. (a) Viscosity Index and (b) relative viscosity increase due to the presence of the nanoparticles.

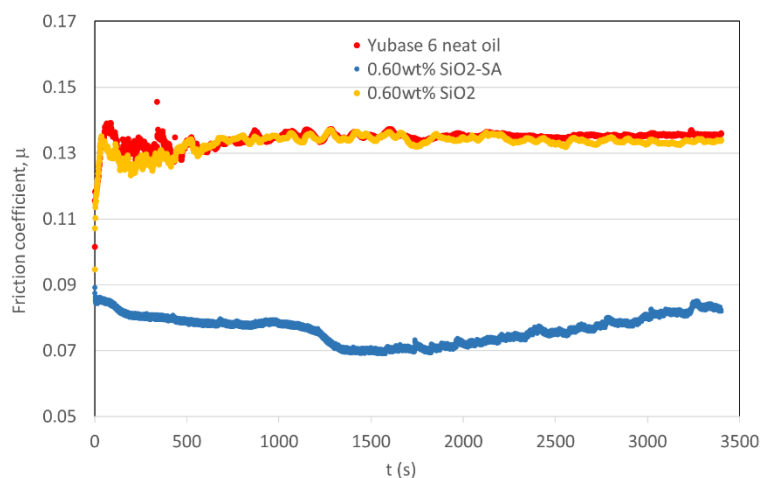


Figure 2. Friction coefficient evolution with time for Yubase 6 neat oil and nanolubricants at 0.60wt% nanoparticle concentration.

Conclusions

The viscosity index increases as the nanoparticle concentration increases, especially in the case of coated SiO₂-SA nanoparticles. The same effect is caused by the addition of nanoparticles on the viscosity of the designed nanolubricants, except for the nanolubricant containing 0.30 wt% SiO₂-SA. It was also observed that the use of coated (SiO₂-SA) nanoparticles clearly improves the tribological performance of the Yubase 6 neat oil. The lowest friction coefficient was obtained for the 0.60 wt% SiO₂-SA nanolubricant, leading to a 46% reduction in comparison to base oil.

Acknowledgments

The financial support of the State Research Agency (AEI) of Spain and the European Regional Development Fund through the PID2020-112846RB-C22 project, and of Xunta de Galicia through ED431C 2020/10 is acknowledged.

References

- [1] L.I. Farfan-Cabrera, Tribology of electric vehicles: A review of critical components, current state and future improvement trends, *Tribol. Int.* 38 (2019) 473–486.
- [2] K. Holmberg, A. Erdemir, The impact of tribology on energy use and CO₂ emission globally and in combustion engine and electric cars, *Tribol. Int.* 135 (2019) 389–396.

Protic Ionic Liquids for Lubrication in Nanotechnology

Mariana T. Donato ^{a,b}, Jonas Deuermeier ^c, Mónica Antunes ^d, Rogério Colaço ^d, Luís C. Branco ^{b*}, Benilde Saramago ^{a,*}

^a Centro de Química Estrutural (CQE), Institute of Molecular Sciences, Departamento de Engenharia Química, Instituto Superior Técnico, Universidade de Lisboa, Portugal;

^b LAQV-REQUIMTE, Departamento de Química, Faculdade de Ciências e Tecnologia, Universidade Nova de Lisboa, Caparica, Portugal

^c CENIMAT|3N and CEMOP/UNINOVA, Departamento de Ciência dos Materiais, Faculdade de Ciências e Tecnologia, Universidade Nova de Lisboa, Caparica, Portugal

^d IDMEC-Instituto de Engenharia Mecânica, Departamento de Engenharia Mecânica, Instituto Superior Técnico, Universidade de Lisboa, Lisboa, Portugal

*l.branco@fct.unl.pt; b.saramago@tecnico.ulisboa.pt

Synopsis

Protic ionic liquids (PILs) are a subclass of ILs that have recently been considered as potentially good lubricants of metallic surfaces. They possess the capacity of establishing dense hydrogen bonding due to the presence of proton-donor and proton-acceptor sites. In this work, we report the use of PILs, based on S-containing anions, as additives to the commonly used base oil PEG 200 and assess the tribological performance, namely friction and wear, using steel and silicon spheres against Si surfaces. All the prepared lubricant formulations were characterized in terms of their water content, viscosity and wettability. The most promising PIL, 4-picolinium hydrogen sulfate ([4-picH][HSO₄]), showed excellent tribological performance, both in terms of friction and wear reduction comparing to the model lubricant, making it a very good candidate for future applications in micro and nanoelectromechanical systems (MEMS/NEMS), which are traditionally made of Si.

Introduction

Ionic Liquids (ILs) are a class of materials with peculiar properties to be used as good alternative lubricants, such as high chemical and thermal stability, almost negligible vapor pressure, high ionic conductivity and non-flammability.

Protic Ionic Liquids (PILs) are ILs formed by proton transfer from a Brønsted acid to a Brønsted base that have recently been considered as particularly efficient lubricants.[1]. They have the advantage of being easily synthesized, with relatively low cost, and reduced toxicity. Besides that, they exhibit low viscosity when compared to the conventional aprotic ionic liquids. These type of compounds have been applied to lubricate several metallic contacts.[2] but, to the best of our knowledge, they were never tested as lubrication solutions for silicon surfaces. Lubrication of silicon contacts is an emerging field as it is of extreme importance to find efficient lubricants for nano and microelectromechanical devices (NEMs and MEMs), made of silicon, a hard and brittle material. NEMs and MEMs are a set of new devices that will significantly change our day-to-day lives in the next few decades.

In this work, we prepared and characterized a set of new ten PILs. Their tribological performance on silicon contacts was evaluated and will be discussed in the next section.

Results and Discussion

Ten PILs containing five different organic cations and the same two anions, hydrogen sulfate [HSO₄]⁻ and methanesulfonate [MeSO₃]⁻ were synthesized. The PILs were used as additives to the commonly used base oil PEG 200 (2% w/w) and the tribological properties of the mixtures, namely friction and wear, were assessed. The water content of the mixtures was smaller than 500 ppm, the viscosities varied between 49 and 64 mPa·s⁻¹ and the contact angle on Si from 18 to 28°. The friction coefficients (CoFs) were measured for steel/Si contacts, and the PILs containing the cation 4-picolinium [4-picH]⁺ revealed to be the best ones, while those based on the cation 1,8-diazabicyclo(5.4.0)undec-7-ene, [DBUH]⁺, were the worst. This behavior may be attributed to the higher adsorption capacity of [4-picH]⁺,

which is a small and symmetric cation comparing to [DBUH]⁺ which is a large and not symmetric structure.

For the best and worst lubricants a study in Si/Si contacts was performed. The CoF values and the wear volumes obtained at different loads are presented in Figure 1A and 1B, respectively. The best lubricant mixture was [4-picH][HSO₄] 2%PEG, which allowed the formation of a protective film on the Si surfaces, leading to a reduced friction and wear at high loads.

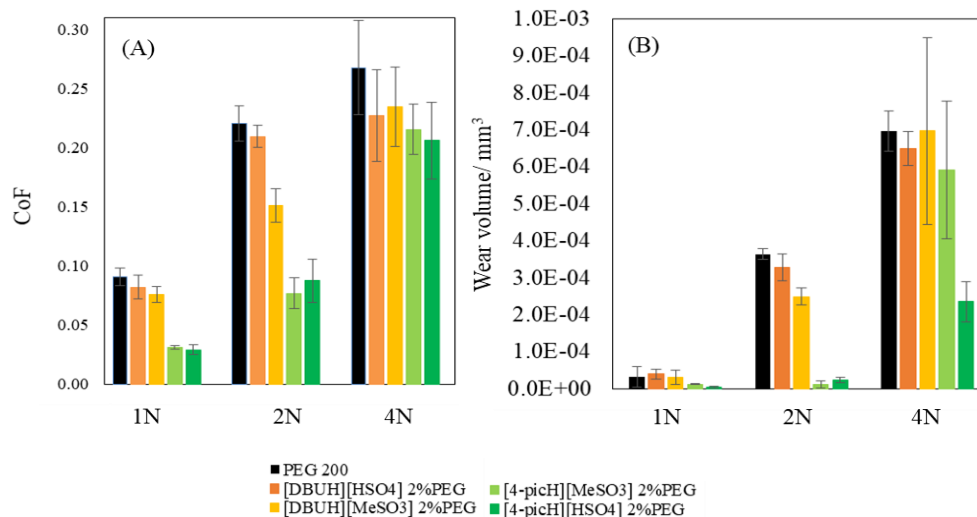


Figure 1. Average CoF (A) and wear volumes (B) obtained with the pair Si sphere/Si substrate using neat PEG200 and the mixtures PEG200+PIL 2% as lubricants under the load of 1N, 2N and 4N.

Conclusions

The tribological properties of ten PILs based on the anions [HSO₄]⁻ and [MeSO₃]⁻, as additives to model lubricant PEG200, were evaluated in steel/Si contacts. From the initial screening, two cations were chosen, which led to the best and the worst lubrication, respectively [4-picH]⁺ and [DBUH]⁺. The lubrication capacity of these four PILs was assessed for Si/Si contacts and the best additive was [4-picH][HSO₄], which revealed excellent lubrication capacity. We concluded that this PIL might be a very promising additive for efficiently lubricate MEMs and NEMS.

Acknowledgements

The work was funded by the Portuguese Foundation for Science and Technology (FCT-MCTES) through the projects UIDB/00100/2020, UIDP/00100/2020 and IMS-LA/P/0056/2020 and through the PhD grant SFRH/BD/140079/2018.

References

- [1] H. Guo, A. R. Adukure, P. Iglesias, Effect of Ionicity of Three Protic Ionic Liquids as Neat Lubricants and Lubricant Additives to a Biolubricant, *Coatings*, 9 (2019), 713.
- [2] H. Kondo, Protic Ionic Liquids with Ammonium Salts as Lubricants for Magnetic Thin Film Media, *Tribol. Lett.* 31 (2008) 211-218.

Tribological enhancement using Mn₃O₄-Graphene nanocomposites as additives for potential transmission fluids of electric vehicles

José M. Liñeira del Río ^{a,b}, Enriqueta R. López ^a, Josefa Fernández ^{a,*}

^a Laboratory of Thermophysical and Tribological Properties, Nafomat Group, Department of Applied Physics, Faculty of Physics and Institute of Materials (iMATUS), Universidade de Santiago de Compostela, Santiago de Compostela, Spain;

^b Unidade de Tribologia, Vibrações e Manutenção Industrial, INEGI, Universidade do Porto, Porto, Portugal

*josefa.fernandez@usc.es

Synopsis

This work describes the antifriction and antiwear properties of Mn₃O₄-Graphene nanocomposites (Mn₃O₄-G) as additives of a paraffinic base oil generally used in the lubrication of electric vehicles (EVs) drivelines, Yubase6. Firstly, four Yubase6 based nanodispersions have been designed: Yubase6 + 0.025 wt% Mn₃O₄-G, Yubase6 + 0.050 wt% Mn₃O₄-G, Yubase6 + 0.075 wt% Mn₃O₄-G and Yubase6 + 0.100 wt% Mn₃O₄-G, to find the optimal concentration of additive. Tribological tests were carried out at pure sliding conditions, with the previous described transmission nanofluids and with Yubase6 base oil under a working load 9.43 N and at temperature of 393.15 K. The wear produced during friction tests was analyzed by means of a 3D optical profilometer measuring different geometrical parameters of the 3D profile of the worn scars. Finally, in order to know the role that nanocomposites play in the wear reduction, Raman mapping and roughness measurements were performed.

Introduction

Electric vehicles (EVs) have gained high regard in recent years around the world as a viable response to reduce greenhouse gas emissions by limiting the antagonistic effect produced using vehicles with internal combustion engines (ICEs). With the inclusion of EVs in automotive industry, different conditions appear, with transmission gears being one the largest sources of friction losses in EVs. Therefore, the development of a new generation of transmission fluids is needed to overcome the challenges created by the latest technology, such as these fluids must also lubricate the electrical motor. For this purpose, the use of nanoparticles as additives of transmission fluids may be a possible solution to meet the new requirements [2]. For this reason, new research on transmission nanofluids is needed.

Results and Discussion

Graphene (purity >99.5%, thickness between 0.35 nm and 1.2 nm and diameter in the range 1-10 μm) and Mn₃O₄ (purity >99.5%, average particle size 30 nm) are in a proportion of Mn₃O₄: graphene in the nanocomposite of 1:1. The use of any of the Mn₃O₄-G based nanofluids leads to a slight reduction of the coefficient of friction with respect to Yubase6 oil. Specifically, the minimum friction coefficient (0.129 versus 0.135 achieved with Yubase6 oil, which evidences a 4 % friction reduction), was obtained with Yubase6 + 0.075 wt% Mn₃O₄-G nanolubricant (Figure 1). The wear produced using any one of the Mn₃O₄-G based nanofluids is much lower than that obtained with Yubase6 oil. It is obvious that the concentration of additives in the nanolubricant considerably affects the antiwear behavior. The highest reductions in width, depth and transversal area of the worn scars were found with the Yubase6 + 0.075 wt% Mn₃O₄-G nanolubricant with decreases of 25, 50 and 64 %, respectively (Figure 2). Finally, after mapping Raman analysis, it was found that synergetic effect, tribofilm formation and rolling mechanisms occur.

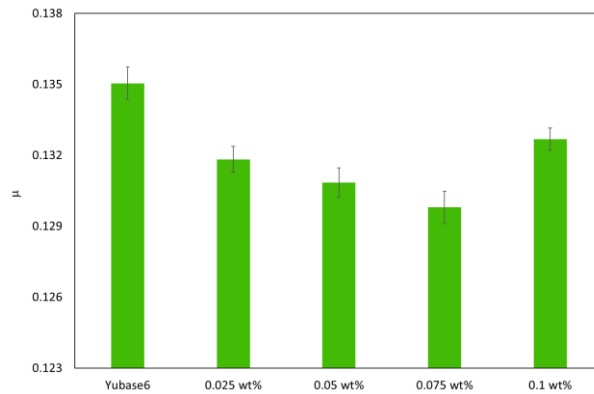


Figure 1. Coefficients of friction (μ) obtained with Yubase6 and Yubase6 + $\text{Mn}_3\text{O}_4\text{-G}$ based nanolubricants.

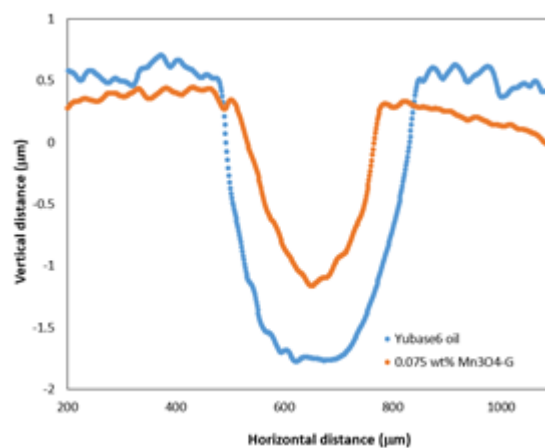


Figure 2. Cross section profiles comparison of worn scars lubricated with Yubase6 oil and Yubase6 + 0.075wt% Mn_3O_4 based nanolubricant.

Conclusions

Friction coefficients obtained with the $\text{Mn}_3\text{O}_4\text{-G}$ nanolubricants are slightly lower than that observed for the neat Yubase6 oil. For all the $\text{Mn}_3\text{O}_4\text{-G}$ nanolubricants, the wear generated in pins is lower than for Yubase6 oil being the highest reductions of 25, 50 and 64% in width, depth, and transversal area of the worn scar respectively (Yubase6 + 0.075 wt% $\text{Mn}_3\text{O}_4\text{-G}$ nanolubricant). Raman mappings confirm that tribological lubrication mechanisms can be described by both the rolling effect and the synergistic effect of the adsorbed tribofilm.

Acknowledgements

The authors acknowledge the financial support of the State Research Agency (AEI) of Spain and the European Regional Development Fund (ERDF, FEDER in Spanish) through the PID2020-112846RB-C22 project, and of Xunta de Galicia through ED431C 2020/10.

References

- [1] W. Ahmed Abdalgilil Mustafa, F. Dassenoy, M. Sarno, A. Senatore, A review on potentials and challenges of nanolubricants as promising lubricants for electric vehicles, *Lubrication Science*, 34 (2022) 1-29.
- [2] S.C. Tung, M. Woydt, R. Shah, Global Insights on Future Trends of Hybrid/EV Driveline Lubrication and Thermal Management, *Frontiers in Mechanical Engineering*, 6 (2020).

Transmission fluids based on a low-viscosity polyalphaolefin and ZrO₂ and CeO₂-ZrO₂ nanoparticles as additives

José M. Liñeira del Río ^{a,b,*}, Arturo Castro Currás ^a, María J.G. Guimarey ^{a,c}, María J.P. Comuñas ^a, Josefa Fernández ^a

^a Laboratory of Thermophysical and Tribological Properties, Nafomat Group, Department of Applied Physics, Faculty of Physics and Institute of Materials (iMATUS), Universidade de Santiago de Compostela, Santiago de Compostela, Spain

^b Unidade de tribologia, vibrações e manutenção industrial, INEGI, Universidade do Porto, Porto, Portugal

^c Department of Design and Engineering, Faculty of Science & Technology, Bournemouth University, UK

*josemanuel.lineira@usc.es

Synopsis

The antifriction and anti-wear behaviour of ZrO₂ and CeO₂-ZrO₂ nanoparticles as additives of a low-viscosity polyalphaolefin, PAO8 are reported. For this aim, eight PAO8 based nanodispersions were formulated: PAO8 + 0.05 wt% ZrO₂, PAO8 + 0.075 wt% ZrO₂, PAO8 + 0.10 wt% ZrO₂, PAO8 + 0.20 wt% ZrO₂ and PAO8 + 0.05 wt% CeO₂-ZrO₂, PAO8 + 0.075 wt% CeO₂-ZrO₂, PAO8 + 0.10 wt% CeO₂-ZrO₂, PAO8 + 0.20 wt% CeO₂-ZrO₂ to achieve the nanoadditive and its mass concentration with the optimal tribological performance. The characterization of nanopowders was carried out by scanning electron microscopy, FTIR, Raman and XRD. Tribological tests were performed at pure sliding conditions at 393.15 K at a load of 20 N, with the previous designed nanolubricants and with PAO8. After friction tests, the produced wear was quantified with a 3D optical profilometer.

Introduction

There is a need to develop new ultra-low viscosity lubricants to meet the requirements of the transmission fluids for new electric vehicles (EVs) [1,2]. Some of these requirements are: low viscosity, improved wear protection, high thermal conductivity and stability, appropriate electrical properties and non-corrosive to electronics and copper. To reach all these needs for coming EVs lubricants, high-performance additives are needed [3]. Nanoparticles (NPs) have larger surface area and can help enhance the thermal cooling properties of the transmission fluids, increase its antifriction and antiwear capabilities as well as to modulate its electric properties. This work is focused on the study of the effect of ZrO₂ (30 – 60 nm) and CeO₂-ZrO₂ (15 nm) nanoparticle concentrations on the lubricating properties of a low-viscosity base oil, PAO8 (dynamic viscosity at 313.15 K of 39.47 mPa).

Results and Discussion

The friction coefficients found with ZrO₂ and CeO₂-ZrO₂ nanolubricants are smaller than that observed for the unadditivated PAO8 oil except at 0.20 wt% for both nanoparticles (Figure 1). This fact can be explained, because at high concentrations nanoparticles tend to agglomerate and can cause an increase in the coefficient of friction. The best antifriction capabilities were found for the 0.05 wt% ZrO₂ and 0.075 wt% CeO₂-ZrO₂ nanofluid, with reductions of 13% for both nanolubricants. The produced wear in pins is lower for all nanolubricants than for the base oil (Figure 2), being the best performance for the 0.05 wt% ZrO₂ with reductions of 37%, 66% and 76% in width, depth, and area of pins, respectively. Regarding the CeO₂-ZrO₂ nanolubricants the optimal wear value was obtained for 0.10 wt% with decreases of 31%, 52% and 62% in width, depth, and area respectively.

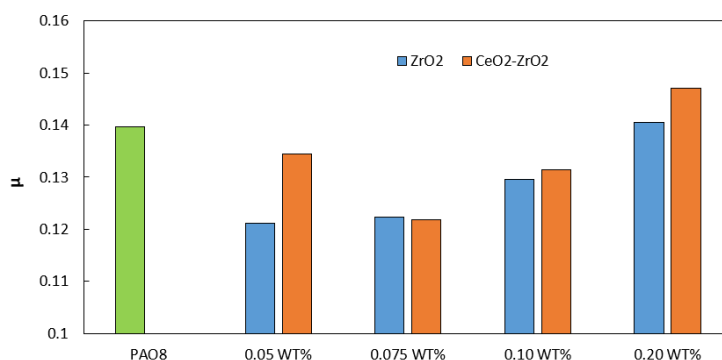


Figure 1. Mean friction coefficient, μ , obtained with the PAO8 oil and with the ZrO₂ and CeO₂-ZrO₂ nanolubricants.

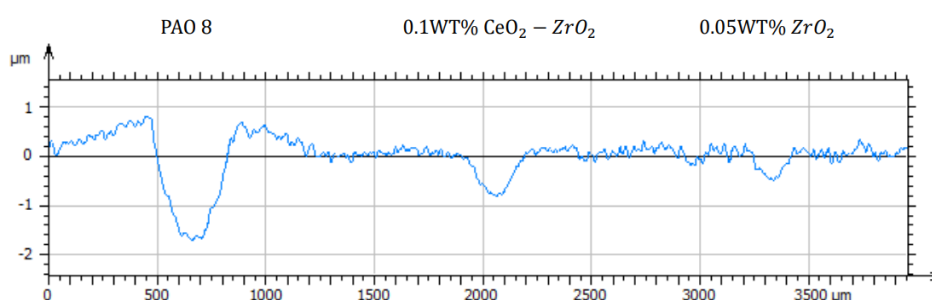


Figure 2. Cross section profiles of worn pins for the all the PAO8 base oil and optimal anti-wear nanolubricants containing CeO₂-ZrO₂ and ZrO₂ NPs.

Conclusions

In the present work, eight nanolubricants based on PAO8 polyalphaolefin doped with ZrO₂ and CeO₂-ZrO₂ nanoparticles were tribological characterized. All of them showed a considerable improvement in terms of friction and wear compared to the neat base oil, PAO8, except for the highest concentrations (0.20 wt%). The optimum concentration of antifriction and anti-wear performance was found to be 0.05 wt% ZrO₂ achieving a 13 % reduction in coefficient of friction and 76 % reduction in wear area. Thus, the tribological improvement of a low-viscosity lubricant has been demonstrated without affecting its thermophysical properties.

Acknowledgments

The financial support of the State Research Agency (AEI) of Spain and the European Regional Development Fund through the PID2020-112846RB-C22 project, and of Xunta de Galicia through ED431C 2020/10 is acknowledged.

References

- [1] G.B. Calderon Salmeron, Enabling More Efficient E-Mobility: Grease Development by a Novel Bearing-Grease Test Machine, (2019): 569 MSc Thesis TRITA-ITM-EX 2019:569, KTH Industrial Engineering and Management Machine Design.
- [2] K. Holmberg and A. Erdemir, The impact of tribology on energy use and CO₂ emission globally and in combustion engine and electric cars, *Tribology International*, 135 (2019) 389-396.
- [3] S.C. Tung, M. Woydt, R. Shah, Global Insights on Future Trends of Hybrid/EV Driveline Lubrication and Thermal Management, *Frontiers in Mechanical Engineering*, 6 (2020).

Multifunctional TiO₂ coatings by Plasma Electrolytic Oxidation on TiNbZrTa alloy for dental applications

A. López-Ortega^{a,*}, G. Mendoza^a, A. Cimpean^b, R. Bayón^a

^a Tekniker, Basque Research and Technology Alliance (BRTA), Eibar, Spain

^b University of Bucharest, Department of Biochemistry and Molecular Biology, Bucharest, Romania

* ainara.lopez@tekniker.es

Synopsis

A multifunctional ceramic-like TiO₂ coating with superior tribocorrosion (wear and corrosion) resistance and biocompatibility has been developed on a newly developed β -Ti alloy based on the Ti-Nb-Zr-Ta system (Ti₂₀Nb₂₀Zr₄Ta). The chemical composition and morphology of the TiO₂-PEO coating was characterized, and its multifunctionality was addressed.

Introduction

The current survival rate of dental implants ranges from 90% to 96.5% [1]. The durability of implants is deeply affected by the metal ion release from the implant as wear debris or corrosion products during the implantation process [2], which can promote infections that could eventually lead to implant rejection and a need of substitution in a new surgical operation. Therefore, the improvement of the wear, corrosion resistance of an alloy and, thus, their synergistic interaction (tribocorrosion), is of great interest to improve durability and clinical success of the implants. Thus, the objective of this work was the development of a multifunctional TiO₂ coating by PEO technique on a β -Ti alloy for dental applications with improved wear, corrosion and tribocorrosion resistances, as well as low cytotoxicity and adequate biocompatibility. Different elements were incorporated into the TiO₂ layers to obtain a multifunctionality, i.e., bactericide to avoid infections and bioactive to improve osteointegration.

Results and Discussion

The multifunctional TiO₂ coating was formed on the surface of the Ti₂₀Nb₂₀Zr₄Ta alloy by PEO treatment in a KERONITE KT 20-50 equipment with a 20KW AC power supply. The electrolyte used contained calcium acetate and β -glycerol-phosphoric acid as sources of Ca and P, respectively, to be incorporated into the oxide layer as bioactive promoters, and Ag nanoparticles (NPs) as biocide elements.

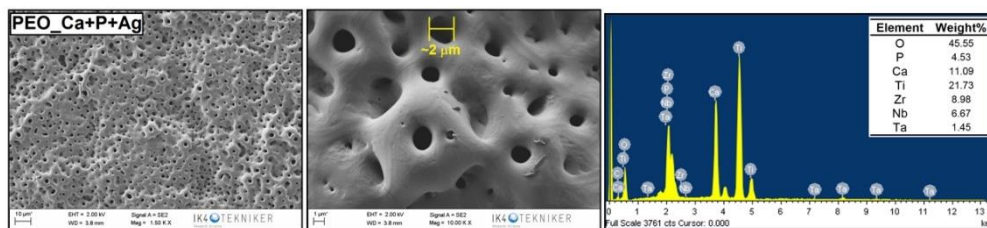


Figure 1. SEM images of the surface morphology of the PEO layer, and EDS analysis

The coatings morphology was assessed by SEM. The coating presented the typical morphology of a PEO coating consisting of a highly porous surface (Figure 1). The small pores on the oxide layer are generated during the process due to the gas evolution that takes place when the material is molten [3,4]. Interestingly, according to literature, different *in vitro* tests revealed TiO₂ coatings with small pore sizes (~2 μ m) to present suitable surface for cell anchoring [5,6], suggesting an adequate morphology of the coatings developed in this work for biomedical purposes. The chemical composition of the coating consisted of oxygen, titanium, the main elements present in the alloy (Zr, Nb, and Ta), and the Ca and P incorporated into the electrolyte as bioactive promoters. Ag NPs were detected on the surface of the coating, located preferentially near the pores.

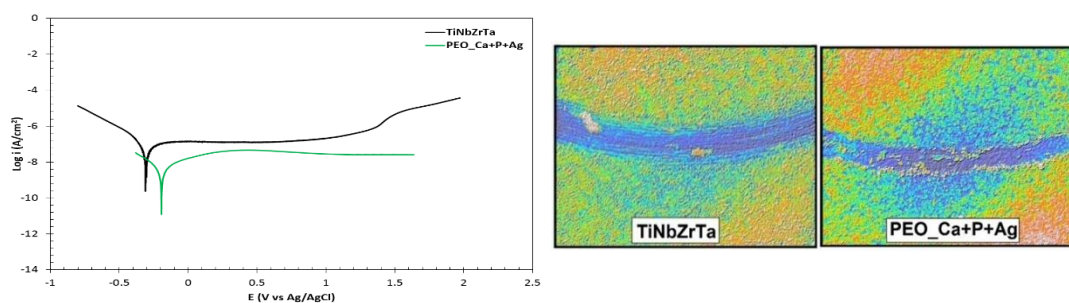


Figure 2. Potentiodynamic polarization curve obtained in the corrosion tests (left) and wear scar profiles obtained in the tribocorrosion tests (right).

The results obtained in the corrosion tests in Ringer's solution (Figure 2, left) clearly show lower current densities for the coating in the whole anodic domain, which remain practically constant in values close to 30 nA/cm², indicating a higher electrochemical stability on the dynamic nature of corrosion processes for the TiO₂ coatings. The results of the tribocorrosion tests (Figure 2, right) evinced the improvement of the PEO coating on the performance of the alloy. The material loss of the uncoated Ti alloy ($81.5 \pm 2 \times 10^{-3} \text{ mm}^3$) was reduced in a 95% after the PEO treatment ($4.5 \pm 1 \times 10^{-3} \text{ mm}^3$).

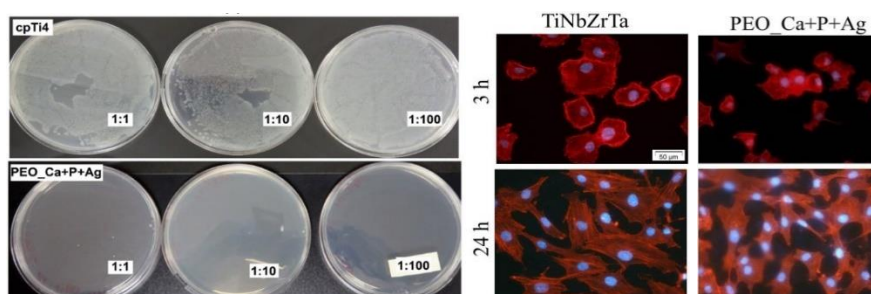


Figure 3. Bacterial growth after 24 hours on the cpTi4 reference and PEO_Ca+P+Ag layer at 1:1, 1:10, and 1:100 dilutions (left) and morphological appearance of MC3T3-E1 cells grown in contact with the Ti20Nb20Zr4Ta and PEO_Ca+P+Ag samples after 3 h and 24 h of culture (right).

The antibacterial activity assessment tests confirmed the high bactericide character of the functionalized layer against the *E. coli* bacterium (reduction of 99.99%) (Figure 3, left). And the MC3T3-1 preosteoblast response showed a good cell proliferation on the coating at 24 h post-seeding, showing a predominantly polygonal shapes and less organized actin cytoskeleton compared to the bare alloy (Figure 3, right).

Conclusions

The developed coating presented enhanced corrosion and tribocorrosion resistance, antibacterial ability with low cytotoxicity, and adequate biocompatibility, able to sustain MC3T3-E1 preosteoblast viability/proliferation and osteogenic differentiation. Altogether, the results obtained demonstrate the potential of the TiO₂ coating incorporating Ca, P, and Ag NPs to be used for dental applications.

References

- [1] Y. Kirmanidou, *et al.* New Ti-Alloys and Surface Modifications to Improve the Mechanical Properties and the Biological Response to Orthopedic and Dental Implants: A Review, *BioMed Res. Int.* (2016) Article ID 2908570
- [2] E. Fuentes, *et al.* Advanced Surface Treatments on Titanium and Titanium Alloys Focused on Electrochemical and Physical Technologies for Biomedical Applications, *Biomaterial-supported Tissue Reconstruction or Regeneration* (2019), IntechOpen.
- [3] J. Martin, *et al.* Effects of electrical parameters on plasma electrolytic oxidation of aluminium, *Surf. Coat. Technol.* 221 (2013) 70–76.
- [4] M. Treviño, *et al.* Wear of an aluminium alloy coated by plasma electrolytic oxidation, *Surf. Coat. Technol.* 206 (2012) 2213–2219
- [5] K.R. Shin, *et al.* In vitro biological response to the oxide layer in pure titanium formed at different current densities by plasma electrolytic oxidation. *Appl. Surf. Sci.* 314 (2014) 221–227.
- [6] D. Buser, *et al.* Interface shear strength of titanium implants with a sand blasted and acid-etched surface: a biomechanical study in the maxilla of miniature pigs. *J. Biomater. Res.* 45 (1999) 75–83.

Functionalization of CoCr surfaces with graphene oxide

L. Sánchez-López ^{a,b}, G. Mellado ^a, C. Abarca ^a, B. Chico ^a, I. Llorente ^a, M.L. Escudero ^a, R.M. Lozano ^c, M.C. García-Alonso ^{a,*}

^a Centro Nacional de Investigaciones Metalúrgicas (CENIM), Consejo Superior de Investigaciones Científicas (CSIC), Madrid, Spain;

^b PhD Program in Advanced Materials and Nanotechnology, Doctoral School, Universidad Autónoma de Madrid, Ciudad Universitaria de Cantoblanco, Madrid, Spain;

^c Centro de Investigaciones Biológicas-Margarita Salas (CIB-MS), Consejo Superior de Investigaciones Científicas (CSIC), Madrid, Spain

*crisga@cenim.csic.es

Synopsis

Improvements regarding durable lubrication together with minimized wear are mandatory for obtaining long-term, functioning metallic joint prostheses. For this goal, CoCr surface was functionalized with Graphene Oxide (GO), characterized by FTIR and XPS, and tested at tribocorrosion. Deposition of GO was carried out by consecutive steps: alkalization of CoCr; intermediate coupling via 3-aminopropyltriethoxysilane (APTES) which was cured at 45 °C for 24 h; and final assemble of GO layers at 60 °C for 24 h upon exposure with silane-coated CoCr. Tribocorrosion test was performed by using a pin-on-disk tribometer with an integrated cell that contains the hyaluronic acid (HA) solution 3 g/l. GO incubated on silane-coated CoCr (CoCr-OH-Si-GO) and CoCr disks were submitted to tribocorrosion against alumina balls, applying a normal load of 5 N and a rotation rate of 120 rpm for 500 m.

Introduction

CoCr alloy for total hip and knee arthroplasties is widely extended due to, among others, the excellent tribocorrosion behavior. Nevertheless, it is unavoidable that the continuous sliding between the contact areas shorten prosthesis durability. In fact, the released degradation products as wear particles and metal ions cause inflammatory and immune reactions, as well as systemic toxicity and genotoxicity.

All the efforts addressed to decrease wear-corrosion on contacting areas are welcomed. In particular, the aim of this study is to simulate the carbon-enriched chemical composition found on the surface of the retrieval prosthesis associated with the lowest wear rate [1]. The strategy described in this work tries to take advantage of the mechanical properties of graphene to generate biocompatible carbon-enriched layers on CoCr surfaces.

Experimental

Biomedical grade CoCr alloy supplied by International Edge was immersed in 5 M NaOH for 2 h for surface hydroxylation. After that, activated surfaces were soaking in hydrolyzed APTES (2 vol % in isopropanol-water (200: 1 v/v) and stirred for 1 h at room temperature for 1 min. Then, silane-coated samples were cured at 45 °C for 24 h. Final step was the incubation of silane-coated samples in 4 g/l graphene oxide aqueous suspension at 60 °C for 24 h [2]. Tribocorrosion response was studied by using a pin-on-disk tribometer with an integrated cell that contains the hyaluronic acid (HA) solution 3 g/l. The wear-corrosion tests were performed on GO incubated on silane-coated CoCr (CoCr-OH-Si-GO) and CoCr disks against alumina balls. A normal load of 5 N was applied at a rotation rate of 120 rpm for 500 m.

Results and Discussion

Table 1 shows the % peak area from high-resolution XPS spectra. After incubation of GO on silane-CoCr, a reduction of the primary amine peak areas together with an increase in the secondary amine is observed. C-O-C peak area decreased in GO incubated silane-surfaces compared to epoxy contribution in Reference GO. Finally, C=O peak area is significantly increased and COOH slightly diminishes in comparison with Reference GO [2].

Table 1. % peak area from high-resolution XPS spectra for multilayer system on CoCr.

Spectrum	O 1s		N 1s		C 1s					
	OH ⁻	NH ₂	NH	C sp ²	C sp ³	C-N	C-O	C-O-C	C=O	COOH
BE (eV)	(532.1)	(399.61)	(401.34)	(284.5)	(285.4)	(285.9)	(286.19)	(286.83)	(288)	(289.01)
% peak area										
CoCr	56,76									
CoCr-OH	94,21									
CoCr-OH-Si	90,20	85,78	14,22							
CoCr-OH-Si-GO		40,43	59,57	55,58	2,01	2,79	16,77	11,35	6,84	4,66
Reference GO				53,2	0,5		2,0	34,42	2,61	7,27

Figure 2 shows the coefficient of friction (COF) versus distance for CoCr and CoCr-OH-Si-GO surfaces in HA solution. The presence of GO modifies the surface performance decreasing the coefficient of friction (lower than 0.20) from the beginning to the end of the test with respect to CoCr disks.

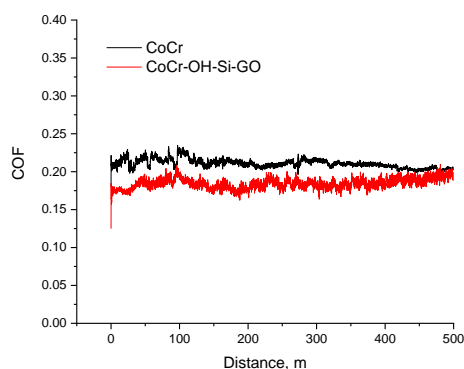


Figure 1. COF versus distance for CoCr and CoCr-OH-Si-GO in HA.

Conclusions

- Covalent silane/GO reactions occurred mainly between primary amines of APTES silane and epoxy groups of GO.
- Graphene oxide on silane-CoCr decreases COF values.

References

- [1] A. García-Arguménez, et al. Electrochemical Reduction of Graphene Oxide on Biomedical Grade CoCr Alloy. *Appl. Surf. Sci.* 465 (2019) 1028.
- [2] L. Sánchez-López, et al. Covalent immobilization of Graphene Oxide on biomedical grade CoCr alloy by an improved multilayer system assembly via Silane/GO bonding. *Materials Chemistry and Physics.* (2022) Under revision.

Dynamic aspects of oral processing of curcumin-loaded solid lipid nanoparticles yoghurts by rheology and soft tribology assessment

Gonçalves R.F.S.^a, Abreu C.S.^{b,c,*}, Gomes J.R.^{b,d}, Vicente A.A.^a, Pinheiro A.C.^a, Vieira J.M.^a

^a Centre of Biological Engineering (CEB), University of Minho, Portugal;

^b Microelectromechanical Systems Research Unit (CMEMS), University of Minho, Portugal;

^c Dept. of Physics, Instituto Superior de Eng. do Porto (ISEP), Portugal;

^d Dept. of Mechanical Engineering, University of Minho, Portugal

* csa@isep.ipp.pt

Synopsis

Mouthfeel and consistency originating from the consumption of yoghurts represent decisive factors for the consumers' acceptability [1]. The present work aims to identify potential differences in the sensory perceptions of yoghurts with curcumin-loaded solid lipid nanoparticles (SLN) incorporation. Thus, rheology coupled with tribology were considered to simulate the dynamic aspects of oral processing. Similar values for the elastic (G') and viscous (G'') parameters were obtained for both control yoghurt and yoghurt with curcumin-loaded SLN, as well as flow index (n) and consistency index (k) around 0.56 and 1.50 Pa.sⁿ, respectively. However, the friction behavior was characterized by significant differences in all tribological regimes, suggesting that the incorporation of nanoparticles in yoghurts could potentially affect the after-feel upon swallowing, whilst not directly impacting on yoghurt's structure.

Introduction

The ever-growing awareness from consumers regarding the link between food and wellness/health has led to an increasing interest in the development of new functional food products. The bright yellow chemical curcumin present in the flowering plant turmeric is a polyphenol with many benefits, such as antioxidant, anti-inflammatory, anti-microbial and anti-tumoral properties. Despite such beneficial attributes, curcumin exhibits low solubility in aqueous solutions, sensitivity to light and low bioavailability, therefore limiting its usage in functional foods [2]. A possible strategy to overcome some of the shortcomings consists in encapsulating curcumin particles. That said, several properties in the functional food development have impact on the consumer's acceptance. The relationship between rheological and tribological properties has been increasingly studied and constitute a valuable tool to achieve indicatives of in-mouth sensory perceptions.

Experimental Techniques

The rheological properties of plain yoghurts and curcumin-loaded SLN samples were assessed from flow curves acquired with an up-down-up step program and subsequently fitted with Herschel-Bulkley's equation. The oscillatory measurements were carried out within the linear viscoelastic domain. The tribological behaviour of the functional foods was studied using a ball-on-disc contact configuration. Polydimethylsiloxane (PDMS) polymeric hemispheres and discs, sliding with relative velocities up to 105 mm/s under constant applied load (1 N), were used to mimic oral soft tissues and confine the food samples during tribotesting.

Results and Discussion

Experimental results regarding the effects of incorporating curcumin-loaded SLN on the rheological properties of yoghurts are showed in Tab. 1 and Fig. 1. As can be seen, curcumin incorporation did not noticeably alter the apparent and complex viscosity, pseudoplasticity and viscoelasticity of the original yoghurt matrix. Therefore, the newly established molecular bonds between the matrix and SLN particles did not change the consistency, firmness, smooth texture and microstructure of the functional foods. Nevertheless, as the particles' size of the yoghurt systematically decreases due to sliding, the tribological nature of the interactions starts to dominate and noticeable differences can be observed between the friction behavior of normal and functionalized yoghurts (fig. 2).

Table I. Rheological properties (k , n and $\eta^*_{50 \text{ rad/s}}$) of control yoghurt and yoghurt with curcumin-loaded SLN.

Sample	k (Pa.s ^{n})	n	$\eta^*_{50 \text{ rad/s}}$ (Pa.s)
Yoghurt	1.51 ± 0.02	0.567 ± 0.005	1.89 ± 0.26
Yoghurt-curcumin SLN	1.50 ± 0.10	0.568 ± 0.005	1.85 ± 0.30

Curcumin incorporation potentially increased the creaminess, fattiness and slipperiness of yoghurts, which reflected itself in a significant increase of yoghurts' lubricating capacity.

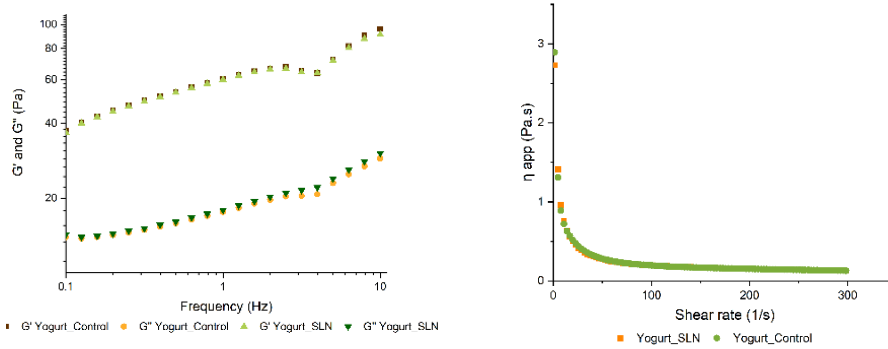


Figure 1. Storage modulus (G') and loss modulus (G'') as a function of frequency (left); Apparent viscosity profile of control yoghurt and yoghurt with curcumin-loaded SLN (right).

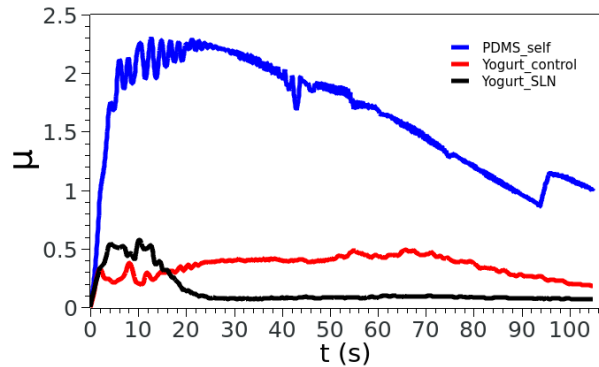


Figure 2. Representative friction coefficient curves as a function of sliding time for control yoghurt, yoghurt with curcumin-loaded SLN and self-mated PDMS.

Conclusions

The lubricating properties of functionalized yoghurts cannot be entirely related to their viscosity, since the friction coefficient observed for yoghurts incorporating curcumin-loaded SLN is significantly lower than yoghurts, despite having similar rheological parameters.

References

- [1] Stokes, J.R. et al., "Oral processing, texture and mouthfeel: From rheology to tribology and beyond" *Curr Opin Colloid Interface Sci*, 18, 4, 2013, 349-359.
- [2] Chang, C., Meikle, T. G., Su, Y., Wang, X., Dekiwadia, C. et al., "Encapsulation in egg white protein nanoparticles protects anti-oxidant activity of curcumin" *Food Chemistry*, 280, 2019, 65–72.

Effect of Normal Load and Rotational Rate on the Coefficient of Friction of CoCr Alloy in Hyaluronic Acid as Lubricant

J. Carnero ^a, L. Sánchez-López ^{a,b}, M.C. García-Alonso ^a, M.L. Escudero ^a, R.M. Lozano ^c, B. Chico ^{a,*}

^a Centro Nacional de Investigaciones Metalúrgicas (CENIM), Consejo Superior de Investigaciones Científicas (CSIC), Madrid, Spain;

^b PhD Program in Advanced Materials and Nanotechnology, Doctoral School, Universidad Autónoma de Madrid, Ciudad Universitaria de Cantoblanco, Madrid, Spain;

^c Centro de Investigaciones Biológicas-Margarita Salas (CIB-MS), Consejo Superior de Investigaciones Científicas (CSIC), Madrid, Spain

*bchico@cenim.csic.es

Synopsis

The effect of normal load and rotational rate on the coefficient of friction (COF) of CoCr sliding against alumina was evaluated using a pin on disk tribometer. Tribological tests were carried out by using CoCr disks of 38 mm diameter and alumina balls of 6 mm diameter as counterpart (pin). An aqueous solution containing 3g/L of HA, concentration equivalent of that found in the synovial fluid, was used as lubricant and it was in continuous recirculation throughout the test. The COF values for two normal loads, 1N and 5N, and two rotational rates, 60 rpm and 120 rpm, have been obtained for a constant sliding distance of 500 m. The tribological tests were performed in duplicate in order to verify the reproducibility of the results. The results show that the COF varies with the load and with the rotational rate, so that, for the same load, the COF increases as the rotational rate decreases. This effect is more significant at lower loads. Meanwhile, the COF values are higher for loads of 1N than for 5N regardless of the rotational rate. The wear tracks were observed by optical microscopy and the images revealed the widest tracks at 5N and 60 rpm.

Introduction

Cobalt-chrome alloys (CoCr) are commonly used for the MoM hip joints, due to their substantially low corrosion and wear rates. Nevertheless, it is unavoidable that the continuous sliding between the contact areas shorten prosthesis durability.

The friction between two surfaces depends on multiple factors such as lubrication, type of material, surface cleanliness, etc., but perhaps the ones that play a more important role in the variation of the friction are the normal load and the sliding rate [1]. Therefore, in this research an attempt is made to study the effect of both factors on frictional behavior of CoCr sliding against alumina in a hyaluronic acid (HA) solution as a lubricant.

Results and Discussion

- Effect of rotational rate on the coefficient of friction

Figure 1 (a, b) shows the COF versus distance for CoCr/alumina in HA solution: (a) for load of 1N and (b) for load of 5N. This figure reveals the increase in COF with the decrease in rotational rate from the beginning to the end of the test. In the case of 5N the effect of rotational rate is less significant exhibiting a less stable COF along the test.

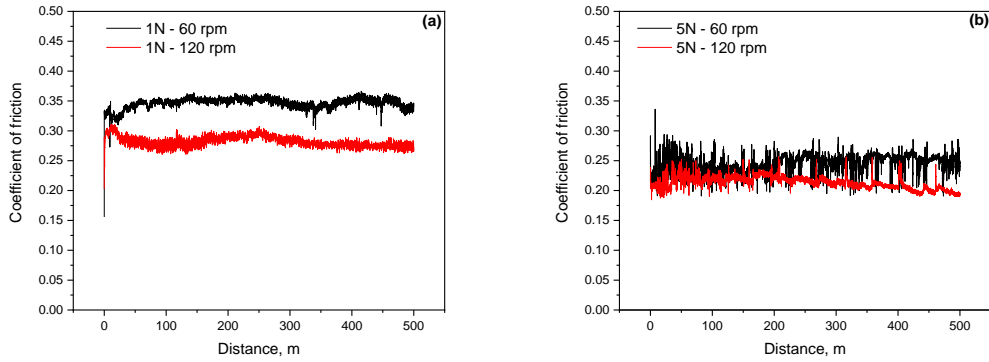


Figure 1. COF versus distance for CoCr/alumina in HA for 60 rpm and 120 rpm rotational rates. Normal load: (a) 1N and (b) 5 N.

- Effect of normal load on the coefficient of friction

The COF data obtained for each condition and replicate were represented in a box-whisker type graph (Figure 2), which shows the statistical data as separate box that indicates the middle 50% of the data (box) and with markings that indicate the 25 (bottom line), 50 (horizontal line in the box) and 75 (top line) percentiles. The lines that go from the box correspond to the standard deviation and the black and red dot correspond to the mean. This figure shows that the COF increases with the decrease in normal load at both 60 and 120 rpm. Optical microscopy images revealed wider tracks at 5N than at 1N.

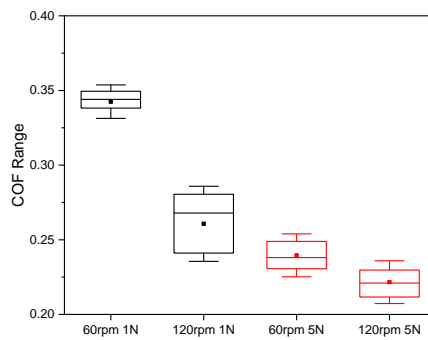


Figure 2. Variation in the COF values with the normal load and rotational rate.

Conclusions

The COF values of CoCr alloy sliding against alumina in HA vary with the load and with the rotational rate, increasing as the rotational rate decreases and normal load decreases.

References

[1] D.M. Nuruzzaman and M.A. Chowdhury, Effect of Normal Load and Sliding Velocity on Friction Coefficient of Aluminium Sliding Against Different Pin Materials, American Journal of Materials Science, 2 (2012) 26.

Wear performance of 3D printed PLA, PC and PEI

C.G. Figueiredo-Pina^{a,b,*}, D. Pereira^a, J. Josefa^a, A. C. Branco^{a,c}, R. A. Cláudio^{a,d}

^a CDP2T, Escola Superior de Tecnologia de Setúbal, Instituto Politécnico de Setúbal, Portugal

^b CeFEMA, Instituto Superior Técnico, Universidade de Lisboa, Lisboa, Portugal

^c CQE, Instituto Superior Técnico, Universidade de Lisboa, Lisboa, Portugal

^d IDMEC e Departamento de Engenharia Mecânica, Instituto Superior Técnico, Universidade de Lisboa, Portugal

*celio.pina@estsetubal.ips.pt

Synopsis

In this work, fused filament fabrication (FFF) technique was used to produce polylactic acid polyetherimide (PLA) from Real-Filaments, polycarbonate (PC) K7 from Kexcelled and polyetherimide (PEI) from Statasys/Sabic ULTEM™ 1010 samples in order to select the material with the highest wear resistance to be used in the production of dies for stamping aluminum sheet metal parts. For this, hardness measurements were carried out and then the samples were submitted to reciprocating pin-on-plate wear tests against steel (AISI 2100) and aluminum (AL 1070) balls. The tests were carried out under dry conditions applying a vertical load of 2.7 N, sliding distance of 6 mm and frequency of 2 Hz.

Introduction

Additive manufacturing (AM) is a production technology whose market increased substantially during the past years. The rapid rise of this technology is attributed to the advances in hardware, materials and software that increased rapidly the maturity in multiple applications of high-tech industries like aerospace, medical, transportation, energy and others. Additive manufacturing is playing a major role in the manufacturing of parts, being able to produce disruptive products, not possible by traditional techniques, opening new opportunities in terms of production paradigm. One of the most popular processes is fused filament fabrication (FFF), because is the most affordable process, flexibility and the wide variability of materials available. In the FFF, the most common material is thermoplastic. The material is fed from a spool with filament to a heated printer head and is deposited on the part to be built, layer by layer [1]. Most of these materials have interesting properties in terms of thermal, electrical, mechanical or biocompatible characteristics, being used for prototyping and the production of high-performance functional components. However, mechanical properties of parts produced by FFF process are extremely anisotropic and lower than produced by conventional process. Even that, some materials like polylactic acid (PLA), polyetherimide (PEI) and polycarbonate (PC) have potential to be used in some demanding functional applications, like for example to stamp sheet metal parts made from aluminum ([2], [3]) For such applications, apart from mechanical resistance and tolerances, the resistance to wear is an important factor to be considered.

Results and Discussion

The hardness of the produced materials was determined and was found that PEI presented the highest hardness (29 ± 1 HV), followed by PC (17 ± 0.5 HV) and PLA (16 ± 0.7 HV).

The results showed that there is no relationship between the wear coefficient and the friction coefficient. On the other hand, the wear coefficient was influenced by the used counterbody (see Figure 1). Even tough steel presents a higher hardness (812 HV) than aluminum (170 HV), it induced the lowest wear on the three tested materials. This may be explained by the wear mechanisms. Scanning electron microscopy (SEM) analysis showed that for all tested materials, aluminum balls present high plastic deformation with some polymeric material adhesion. In addition, aluminum was also extensively detected on the wear tracks. Concerning steel balls, no wear was detectable, being just accumulation of polymeric material found on their surface. This accumulation was more significant for tests carried out against PEI samples, followed by PLA. PC showed insignificant transference.

Regarding to the wear coefficient, while PC was the material that showed the lowest value, PEI showed the highest. These results show that there is no direct relation between hardness and wear. For all materials, SEM analysis showed that there is formation of a tribolayer which is made of wear debris accumulation and their compaction. It was found a correlation between the extent of the tribolayer observed by SEM and the wear coefficient: the thicker the tribolayer, the higher the wear. Adhesive wear was considered the predominant wear mechanism.

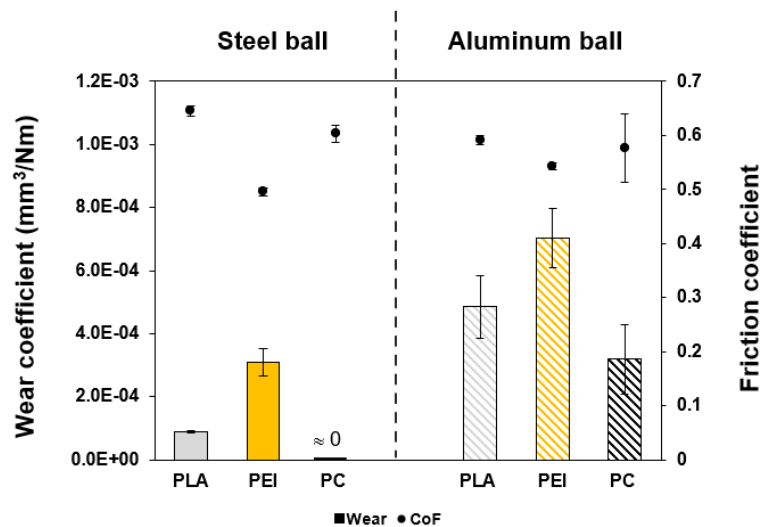


Figure 1. Wear coefficient of PLA, PEI and PC against steel and aluminum ball.

Conclusions

Samples of PLA, PEI and PC were successfully produced by fused filament fabrication. Among the three materials, PC revealed to be the most promising material for stamping aluminum parts die, showing the highest resistance to wear. For all tested materials, adhesive wear was the main wear mechanism.

References

- [1] S. Singh, G. Singh, C. Prakash, and S. Ramakrishna, "Current status and future directions of fused filament fabrication," *J. Manuf. Process.*, vol. 55, no. January, pp. 288–306, 2020.
- [2] P. Frohn-Sörensen, M. Geueke, T. B. Tuli, C. Kuhnhen, M. Manns, and B. Engel, "3D printed prototyping tools for flexible sheet metal drawing," *Int. J. Adv. Manuf. Technol.*, vol. 115, no. 7–8, pp. 2623–2637, 2021.
- [3] R. A. Cláudio, P. Cardoso, H. Ferreira, V. Alcácer, and J. Simões, "Behaviour of 3D Printed PLA dies for Rubber Pad Forming," 2021.

The influence of glaze on the tribological properties of zirconia dental pieces obtained by subtractive and additive manufacturing

A.C. Branco ^{a,b,c,*}, M. Polido ^b, R.Colaço ^d, C.G. Figueiredo-Pina ^{b,c,e}, A.P. Serro ^{a,b}

^a Centro de Química Estrutural (CQE), Institute of Molecular Sciences, Departamento de Engenharia Química, Instituto Superior Técnico, Universidade de Lisboa, Portugal;

^b Centro de investigação Interdisciplinar Egas Moniz, Instituto Universitário Egas Moniz, Caparica, Portugal;

^c CDP2T e Departamento de Engenharia Mecânica, Instituto Politécnico de Setúbal, Setúbal, Portugal

^d IDMEC e departamento de Engenharia Mecânica, Instituto Superior Técnico, Universidade de Lisboa, Portugal;

^e CeFEMA, Centro de Física e Engenharia de Materiais Avançados, Instituto Superior Técnico, Lisboa, Portugal;

* ana.branco@tecnico.ulisboa.pt

Synopsis

The aim of this study is to evaluate the potential of additive manufacturing (AM) to produce reliable zirconia dental pieces and the influence of glazing on the tribological performance of the obtained samples. To validate the possibility of using AM, the results were compared with those obtained with samples produced by a conventional subtractive manufacturing (SM) method.

Zirconia samples produced by both methods were sintered at 1500°C, polished to obtain the same surface finishing and some of them were glazed. Density, porosity, Vickers hardness, toughness and roughness measurements were performed. Also, chewing simulation tests against dental human cusps were carried out in artificial saliva at room temperature, before and after glazing. The wear tests were carried out with an applied load of 50 N, vertical speed 40 mm/s, horizontal speed 20 mm/s, vertical movement 2 mm, horizontal movement 0.7 mm and frequency ~1 Hz. The counter-faces' wear was quantified, and the wear mechanisms investigated.

Introduction

Ceramic based prosthetic materials are highly used for the repairing/replacing of a damaged/missing tooth, due to their suitable mechanical and aesthetic properties, chemical stability and biocompatibility [1-2]. Additive manufacturing (AM) has emerged as new methodology to obtain long term 3D dental pieces at low cost, decreasing the materials' waste and production time relatively to the conventional manufacturing methods [3]. Generally, ceramic restorations are coated with a ceramic glaze paste to improve aesthetics.

Results and Discussion

AM and SM samples have similar density and surface roughness, but AM samples show a higher surface porosity and lower hardness and toughness than SM samples. After the chewing simulation tests, no wear was found for both unglazed SM and AM samples, but the cusps suffered a significant volume reduction, especially in the tests against SM samples. Concerning the glazed samples, the wear tests revealed that both the cusps and the coated surfaces suffered wear. The cusps' wear was significantly higher than with unglazed samples. Although glaze presents a lower surface hardness than zirconia (similar to enamel), the delamination of glaze leads to three body abrasion which increases the cusps wear. Dental material adhesion occurred both on glazed and unglazed samples.

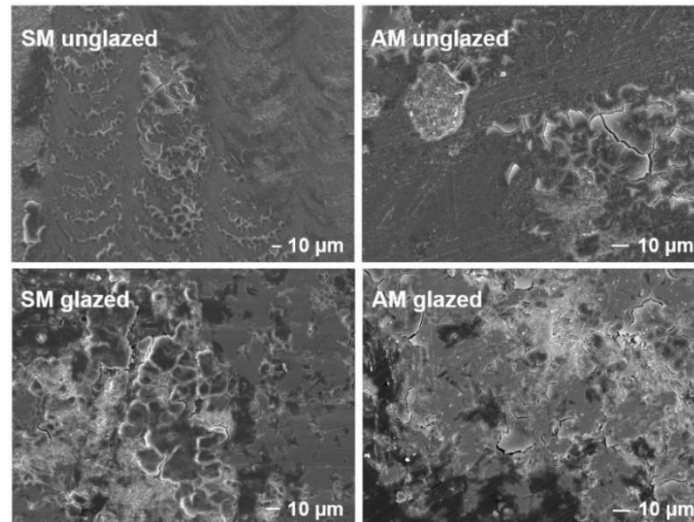


Figure 1. SEM images of unglazed/glazed SM and AM zirconia after wear testing.

Conclusions

Additive manufacturing seems to be a promising technique to produce zirconia dental pieces. The use of glaze induced a higher cusps' wear. The wear was higher for the cusps against SM samples (both unglazed and glazed).

References

- [1] Pollington S and Noort R Van, An update of ceramics in dentistry, J Clin Dent (2011).
- [2] Denry I and Kelly JR, Emerging Ceramic-based Materials for Dentistry, J Dent Res, 93 (2014) 1235-42.
- [3] R. Galante, C.G. Figueiredo-pina, A. Paula, Additive manufacturing of ceramics for dental applications: A review, Dent Mater, 35 (2019) 825-846.

Alginate-based hydrogels loaded with ibuprofen for articular cartilage substitution

Carolina Marto Costa ^{a,*}, Madalena Oom ^b, Célio Figueiredo-Pina ^c, Ana Paula Serro ^{a,b}

^a Centro de Química Estrutural (CQE), Institute of Molecular Sciences, Departamento de Engenharia Química, Instituto Superior Técnico, Universidade de Lisboa, Portugal

^b Centro de Investigação Interdisciplinar Egas Moniz (CiEM), Instituto Universitário Egas Moniz, Portugal

^c CDP2T and Department of Mechanical Engineering, Instituto Politécnico de Setúbal, Portugal

* carolina.marto.costa@tecnico.ulisboa.pt

Synopsis

This study aimed to develop hydrogels based on sodium alginate (SA) which are considered promising candidates due to their biocompatibility, hydrophilicity, and possibility of being tailored to mimic the natural cartilage tissue function. A methacrylic modification of the hydroxyl groups of SA's backbone enabled covalent bonding by UV exposure with further ionic bonding of the carboxyl groups with a 1M CaCl₂ aqueous solution. The obtained results show that double crosslinked methacrylic-alginate-based hydrogels present adequate properties for load-bearing cartilage substitution and can be used as drug delivery platforms for the vehiculation of an anti-inflammatory (ibuprofen) in the post-surgical period.

Introduction

The quality of life of millions of people is compromised by the pain and impaired mobility of synovial joints that outcomes from damaged or degenerated articular cartilage. Wear and deterioration of cartilage often progress towards degenerative pathologies, like osteoarthritis. The limited healing potential of articular cartilage impairs its normal load-carrying capacity. Currently used clinical methods provide temporary relief, but they do not restore long-term joint function [1],[2]. Hydrogels have been studied as potential substitutes for articular cartilage. Good candidates seek to work synergistically with native cartilage to withstand the harsh environment of diarthrodial joints. The artificial bearing replacement must, on the one hand, support the loads exerted by the skeletal system, which can reach about 2-4x the body weight when walking [2]. On the other hand, the engineered material's surface must be carefully adjusted to induce low friction against native cartilage with minimal wear [1], [3].

Hydrogels were prepared with sodium alginate, methacrylic anhydride and a photoinitiator and submitted to a double crosslinking procedure, first by exposure to UV radiation followed by immersion in CaCl₂ solution (SAM hydrogels). GO hydrogels were obtained by adding 0.3 %(w/v) graphene oxide (GO) to the prepared mixture, following a similar procedure.

Results and Discussion

Results demonstrated that GO significantly affected several properties of the SAM hydrogels:

- Lead to a lower equilibrium water content (decreased from 87.1 ± 2.6% to 81.1 ± 2.7%);
- Increased the Young's modulus and the ultimate tensile strength by 128% and 137%, respectively;
- Enhanced the hydrophilic character (water contact angle decreased from 33° ± 6° to ~0).

The tribological properties of SA and GO hydrogels were investigated under different load, measured in pin-on-disc equipment using pins of porcine knee cartilage as countersurface in either PBS or human synovial fluid lubricating media (Fig. 1). In general, the average friction coefficient slightly decreased for SA hydrogels by increasing the load from 0.32 MPa to 0.47 MPa. It also showed a dependence on lubricant's nature.

Lower friction coefficients were obtained in synovial fluid compared to PBS, due to the liquid's viscosity (10x superior for the former), and the presence of biomolecules that enhance lubrication. Evaluation of the material's degradation in PBS showed that GO hydrogels were severely affected after 3 days, losing about 90% of their mass, in contrast with SA which only lost 4%. Therefore, SA hydrogels were chosen to be loaded with the anti-inflammatory. A sustained drug-release profile was observed during 72 h,

revealing the material's ability to serve as a platform for the local delivery of ibuprofen in the post-operative period. Samples revealed to be non-irritating and non-cytotoxic.

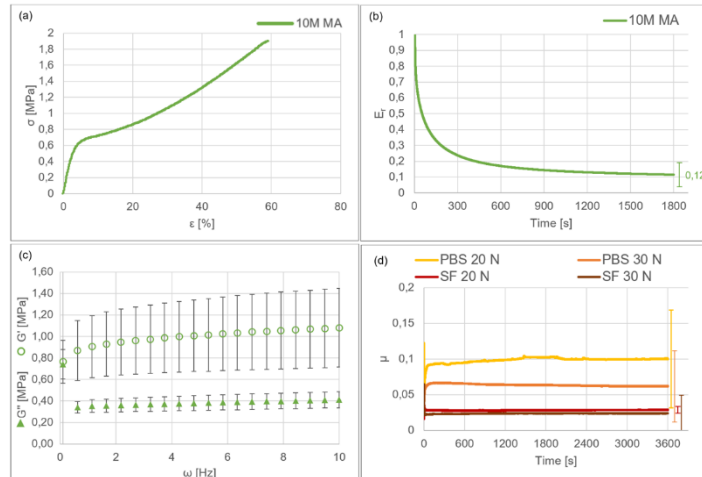


Figure 1. Mechanical characterisation of 10M MA hydrogels: (a) stress-strain curve, (b) normalised relaxation modulus as a function of time, (c) storage modulus (G') and loss modulus (G'') as a function of frequency (ω), and (d) friction coefficient over 3600 s under PBS or SF (synovial fluid).

Conclusions

A dual step crosslink proved to be a suitable approach to produce SA hydrogels for load-bearing cartilage substitution with tailored mechanical properties. The tribological behavior of the resulting materials mimics the cartilage-on-cartilage contact.

SA-modified hydrogels revealed the material's potential to serve as a drug-delivery platform for the local delivery of this anti-inflammatory in the post-operative period. Studies with human chondrocyte cells showed cell viability for non-loaded materials and minimal toxicity for the drug-loaded-ones. No signs of irritability were found for both hydrogels.

References

- [1] C. A. Baumann, B. B. Hinckel, C. C. Bozynski, and J. Farr, "Articular cartilage: Structure and restoration," *Jt. Preserv. Knee A Clin. Caseb.*, pp. 3–24, 2019.
- [2] T. Althoff, R. Sosič, J. L. Hicks, A. C. King, S. L. Delp, and J. Leskovec, "Large-scale physical activity data reveal worldwide activity inequality," *Nature*, vol. 547, no. 7663, pp. 336–339, 2017.
- [3] P. E. Milner et al., "A low friction, biphasic and boundary lubricating hydrogel for cartilage replacement," *Acta Biomater.*, vol. 65, pp. 102–111, 2018.

Tribomechanical behavior of gamma-irradiated Nomex[®] reinforced poly(vinyl alcohol)-based hydrogel for articular cartilage replacement

Francisco Santos^a, Andreia Sofia Oliveira^{a,c}, Célio Figueiredo-Pina^{b,c}, Ana Paula Serro^{a,d,*}

^a Centro de Química Estrutural (CQE), Institute of Molecular Sciences, Departamento de Engenharia Química, Instituto Superior Técnico, Universidade de Lisboa, Portugal;

^b CDP2T, Escola Superior de Tecnologia de Setúbal, Instituto Politécnico de Setúbal, Setúbal, Portugal;

^c CeFEMA, Instituto Superior Técnico, Universidade de Lisboa, Lisbon, Portugal;

^d Centro de Investigação Interdisciplinar Egas Moniz (CiEM), Instituto Universitário Egas Moniz, Portugal

* anapaula.serro@tecnico.ulisboa.pt

Synopsis

Polyvinyl alcohol (PVA) hydrogels were produced by cast drying, with different amounts of Nomex[®] (poly(m-phenylene isophthalamide) nanofibers (0, 1, 1.5 and 2 wt.%) and were gamma-irradiated (25 kGy). Samples morphology/topography was observed by scanning electron microscopy (SEM). The mechanical behaviour of the irradiated materials was assessed through compression tests. The friction coefficient (CoF) against 316L stainless steel balls (\varnothing 6 mm) was measured in linear reciprocating movement (at a frequency of 1 Hz), under the lubrication of phosphate buffered saline (PBS) solution, using applied loads in the range of 5-50 N for a duration of 20 minutes. The swelling capacity of the hydrogels in water and the water contact angle were also determined.

Introduction

Joint pathologies such as osteoarthritis and rheumatoid arthritis affect millions around the world, and their impact is expected to continue to increase with ageing populations and rising obesity [1]. These conditions, among others, lead to the deterioration of articular cartilage, which provides an almost frictionless surface and load-bearing capacity within joints. The use of biomaterials to replace the native tissue can avoid the full replacement of joints when cartilage damages are still limited. Hydrogels have raised great interest for this purpose, owing to their biocompatibility and physical properties that approach those of natural cartilage. Among these, PVA hydrogels have been quite explored, since they are biocompatible, present good swelling properties and have tunable mechanical properties [2]. However, it has been found that PVA hydrogels do not possess enough mechanical resistance to substitute cartilage. Therefore, different strategies, including the addition of reinforcement materials, have been proposed to improve the hydrogels' properties [3]. In this work, it was attempted, for the first time, to reinforce PVA hydrogels with Nomex[®], a fibre known for its high mechanical toughness, flexibility, and resilience [4]. The hydrogels were further gamma-irradiated to replicate a possible sterilization procedure.

Results and Discussion

The addition of 2% Nomex[®] impaired the materials' polymerization. SEM analysis of the remaining hydrogels showed that all presented a smooth surface and have a compact structure. The increase in the Nomex[®] nanofibers content led to an increase of the compressive strength of the hydrogels, approaching the behaviour of human cartilage (Fig. 1).

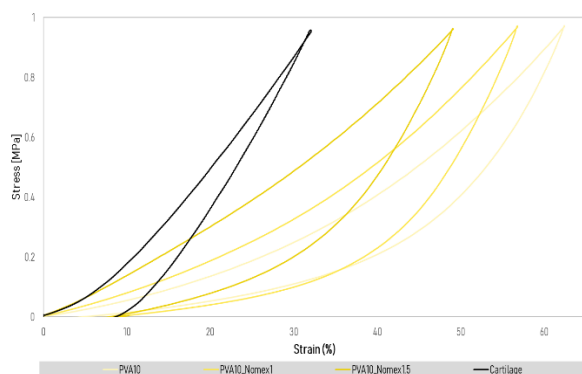


Figure 1. Compressive stress-strain curves of PVA hydrogels and of porcine cartilage.

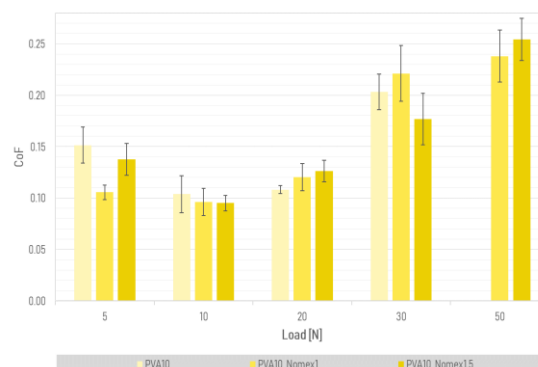


Figure 2. CoF of PVA hydrogels tested against stainless steel in lubricated conditions at different loads.

Concerning the tribological behavior, as the normal load increased, the values of CoF raised (Fig 2). This is due to the higher deformation of the hydrogels, that increases the contact area with the counterbody and promotes the adhesion between the surfaces. Due to its lower mechanical resistance, non-reinforced PVA did not withstand the higher applied load (50 N), degrading during the tribological tests. The reinforcement addition did not affect significantly the CoF observed at each load. Comparison with human cartilage tested in the same conditions (SS ball, lubricant PBS, load 10 N) showed that CoF values are almost double for the natural tissue (CoF = 0.19) [2].

The addition of 1% of Nomex® to PVA did not affect the swelling capacity of the PVA hydrogel (\approx 300%), which was quite similar to that observed for human cartilage [1]. However, 1.5% led to a slight decrease of the amount of water absorbed (around 20%), which may be due to the increase in hydrogel's stiffness.

The materials revealed to be highly hydrophilic. The reinforcement almost had no influence on the measured water contact angles (46-48°).

Conclusions

The reinforcement of PVA hydrogels with 1.5% meta-aramid nanofibers obtained from Nomex® followed by sterilization with gamma-radiation allowed to obtain homogeneous hydrogels with a mechanical behavior at compression significantly superior to PVA and friction coefficient lower than that observed for natural cartilage tested in the same conditions.

References

- [1] M. Cross et al., "The global burden of hip and knee osteoarthritis: estimates from the Global Burden of Disease 2010 study," *Ann. Rheum. Dis.*, vol. 73, no. 7, pp. 1323–1330, Jul. 2014
- [2] A. S. Oliveira, O. Seidi, N. Ribeiro, et. al., "Tribomechanical Comparison between PVA Hydrogels Obtained Using Different Processing Conditions and Human Cartilage," *Mater.* 2019, Vol. 12, Page 3413, vol. 12, no. 20, p. 3413, Oct. 2019
- [3] A. S. Oliveira et al., "Tough and Low Friction Polyvinyl Alcohol Hydrogels Loaded with Anti-inflammatories for Cartilage Replacement," *Lubr.* 2020, Vol. 8, Page 36, vol. 8, no. 3, p. 36, Mar. 2020.
- [4] DuPont Technical guide for Nomex® fiber, 2019.

Acknowledgements: To Fundação para a Ciência e a Tecnologia (FCT) by funding through the research project PTDC/CTM-CTM/29593/2017 and the unit projects UID/QUI/00100/2019 (CQE), and UID/CTM/04540/2020 (CeFEMA).

Tool condition monitoring of self-lubricating coatings to improve the lifetime of cutting tools

J. Perdigoto ^{a,*}, B. Martins ^a, J.P. Dias ^a, A. Cavaleiro ^{a,b}

^a LED&MAT- IPN, Instituto Pedro Nunes, Coimbra, Portugal

^b SEG-CEMMPRE, Departamento de Engenharia Mecânica- Universidade de Coimbra, Portugal

* jperdigoto@ipn.pt

Synopsis

The present abstract reports the use of self-lubricant films combining properties of high oxidation resistance coatings with lubricious elements, such as V addition to multilayered TiSiN/TiSiVN and monolayered TiSiVN, to reduce the rapid wear of cutting tools during dry machining through vacuum magnetron sputtering technologies.

To improve the lifetime of cutting tools, tool condition monitoring (TCM) of the wear level of the tools ensures the continuous evaluation in real time of the cutting edge until the detection of the optical layer, in this case TiN, which is deposited underneath the self-lubricant coating.

Introduction

The constant need to optimize processes, associated with productivity within the industrial environment, encourages the search for solutions that promote alternatives capable of competing in the global market. In this case, the manufacturing industry is fundamentally based on chip-start cutting technology, in which a large part of the production cost attributed to cutting tools is due to poor tool management and lack of knowledge of wear level. Increasing the lifetime of cutting tools involves optimizing the respective management system used in the manufacturing industry, based on chip-start cutting technology.

Given the cost of producing such tools, in order to improve their lifetime, the solution lies in the sustainability of processes, as well as tool condition monitoring (TCM) of the wear level on the tools, reducing their environmental impact through early disposal. The rapid wear of tools during dry machining presents an opportunity for the adoption of adaptative coatings, through vacuum magnetron sputtering technologies.

Self-lubricant coatings should combine a set of properties not easily found in nature in a simple material, such as high toughness, low friction, good wear-resistance and thermal stability at high temperature [1]. The TiSiN matrix, in these coatings, acts as an anti-diffusion barrier for the lubricant soft phase element, such as Ag or V, preventing their rapid wear onto the surface of the coating [2].

Results and Discussion

Monolayer TiAlN, TiSiN and TiSiVN and also multilayered TiSiN/TiSiVN coatings, with different V concentrations, were deposited by d.c. reactive magnetron sputtering, working in unbalanced mode, composed by two pairs of magnetrons facing each other.

These coatings present wear and oxidation resistance properties and also low friction at high temperatures, without liquid lubricants during the cutting process. These coatings were evaluated for their performance in dry machining tests on CK45 steel in a laboratory environment using an automated computer control- CNC machine. In Figure 1, a comparison is presented between cutting tools coated with TiSiN/TiSiVN before and after the machining tests, where the latter show adhesive wear on the cutting edge.



Figure 1. Cutting tool edge coated with TiSiN/TiSiVN during dry machining of CK45. Tool condition monitoring of the cutting edge to evaluate the performance of the tool.

Alongside these tests, the wear level of such coatings was monitored continuously and in real-time, based on optical characteristics and resistivity changes in the developed thin films. As shown in Figure 2, thanks to the EDS elemental distribution map, it is possible to distinguish between the top layer (self-lubricant or anti-wear coating) and the optical layer (TiN) both deposited in the carbide end mill.

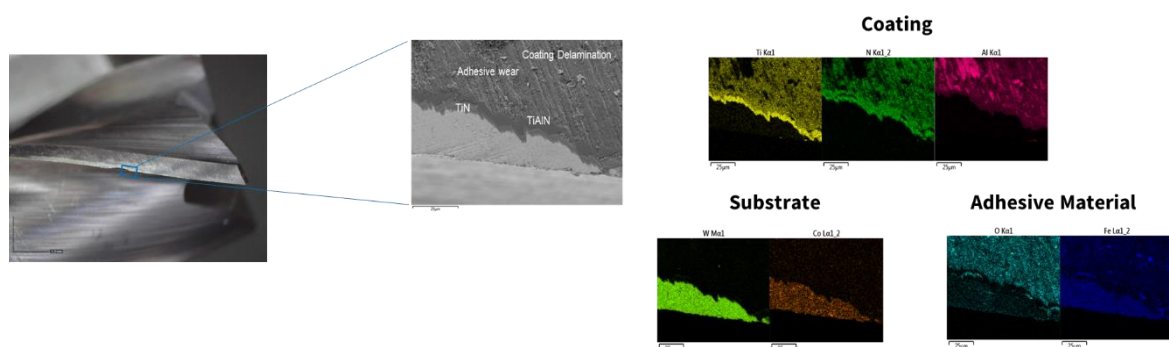


Figure 2. EDS elemental distribution maps of coated carbide end mill after 15 passes on a CK45 machined workpiece.

Conclusions

In this work, the effect of V alloying in the monolayered TiSiVN and in the multilayered TiSiN/TiSiVN coatings on the structure, mechanical properties, oxidation resistance and machinability are studied. According to the results, the addition of solid lubricant elements contributed to the wear reduction on cutting tools, proven by the tests carried out, thus increasing the lifetime of tools.

References

- [1] D. Cavaleiro, D. Figueredo, C.W. Moura, A. Cavaleiro, S. Carvalho and F. Fernandes, Machining performance of TiSiN (Ag) coated tools during dry turning of TiAl6V4 aerospace alloy, *Ceramics International*, 47 (2021) 11799-11806.
- [2] F. Fernandes, A. Loureiro, T. Polcar and A. Cavaleiro, The effect of increasing V content on the structure, mechanical properties and oxidation resistance of Ti-Si-V-N films deposited by DC reactive magnetron sputtering, *Applied Surface Science*, 289 (2014) 114-123.

Optimized surface engineering solutions for glass mould industry

J. Costa ^{a,*}, J.P. Dias ^b, A. Cavaleiro ^{a,b}

^aLED&Mat-IPN, Instituto Pedro Nunes, Coimbra, Portugal

^bSEG-CEMMPRE, Departamento de Engenharia Mecânica - Universidade de Coimbra, Portugal

* jcosta@ipn.pt

Synopse

Self-lubricant coatings offer an opportunity to increase tools lives under severe conditions [1]. Thus, this study was focused on the development of surface engineering solutions based on sputtering technology – PVD, by depositing thin films on mold surfaces for glass industry, which could improve wear resistance under aggressive conditions and increase durability relative to the state-of-the-art solutions. Within the frame of this work, transition metals were added to Titanium Nitride-based hard coatings during the deposition by DC magnetron sputtering. Two different structures configurations: monolayer and multilayer, were produced and optimized in order to achieve the best compromise between thermal, mechanical and tribological properties. Wear results showed that the coatings with multilayer structure are a very promising solution in order to overcome the fast degradation of molding parts, during the production process of bottles.

Introduction

One of the main problems in the glass industry is the fast wear of the surface of molding tools used in the glass manufacturing process which, in direct contact with the melted glass, are subjected to severe conditions of abrasion, corrosion and thermo-fatigue at high temperatures. The wear in these components (plungers, molds, neck rings, etc.) has led, in the last years, to efforts in order to overcome this problem. Therefore, the main goal of this study was to develop surface engineering solutions based on sputtering technology – PVD, in order to increase mold lifetime when exposed to abrasive and corrosive environments at high temperature.

Results and Discussion

Substrates of the same material used in molds manufacture for glass industry were coated with Ti-X-(Y)-N hard coatings (X and Y - transition metals) by PVD magnetron sputtering in two different structures configurations: monolayer and multilayer (Figure 1).

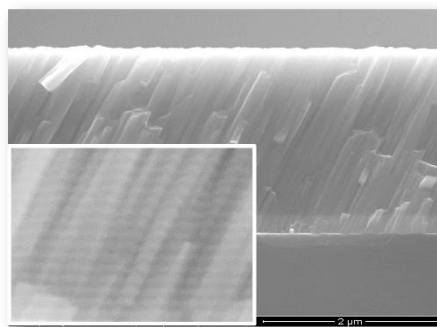


Figure 1. Scanning electron microscopy (SEM) image of the multilayer coating in cross section.

The tribological behavior of the coatings were evaluated at room temperature (RT) and 600°C, on a pin on disk tribometer equipment. Uncoated samples were also tested for comparative wear analysis purposes only. Figure 2 shows 3D profiles of the wear tracks after pin-on-disk tests against Al₂O₃ balls and Figure 3 shows the comparison of their specific wear rates.

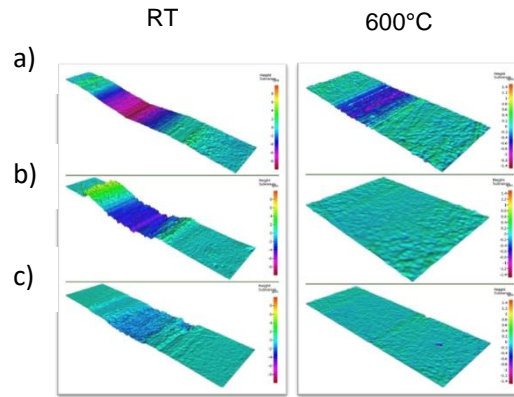


Figure 2. 3D profiles of the wear tracks after pin on disk tests at RT and 600°C. Type of sample: a) uncoated; b) monolayer coating and c) multilayer coating.

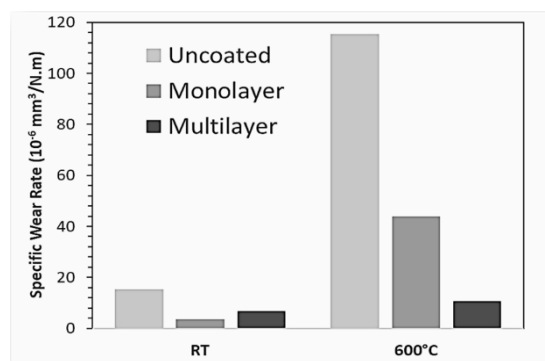


Figure 3. Specific wear rates of the coatings and uncoated sample tested against Al₂O₃ balls.

Conclusions

Tribological tests showed that the coatings with multilayer structure have ten times less specific wear rate than uncoated samples and four times less than monolayer coatings. This could be a good indicator of the coating's performance as a protective solution for molding parts during the production process of bottles, and therefore, achieving two main goals: reduce the cost of production and increase the energy efficiency due to carbon footprint reduction.

Acknowledgments

This research is sponsored by FEDER funds under the program COMPETE – Programa Operacional Factores de Competitividade, through the project Project ShellMould – POCI-01-0247-FEDER 039913.

References

- [1] Diogo Cavaleiro et al., Machining performance of TiSiN (Ag) coated tools during dry turning of TiAl₆V₄ aerospace alloy Coatings Deposited by Sputtering, *Ceramics International*, 47 (2021)11799.

ATTENDEES

Abreu, Cristiano (University of Minho, Portugal)
Angel Garrido, Miguel (University of Rey Juan Carlos, Madrid, Spain)
Antunes, Mónica (Instituto Superior Técnico, Lisbon, Portugal)
Bayón, Raquel (Fundación TEKNIKER, Spain)
Bianchi, Eduardo (São Paulo State University – Unesp, Brazil)
Biezma Moraleda, María Victoria (University of Cantabria, Spain)
Branco, Ana Catarina (Instituto Superior Técnico, Lisbon, Portugal)
Carneiro, Carla (Instituto Politécnico de Setúbal, Setúbal, Portugal)
Cascalheira, João (MTBrandão, Portugal)
Cavaleiro, Albano (University of Coimbra, Coimbra, Portugal)
Chico, Belén (CENIM-CSIC, Spain)
Colaço, Rogério (Instituto Superior Técnico, Lisbon, Portugal)
Costa, Carolina (Instituto Superior Técnico, Lisbon, Portugal)
Costa, João (Instituto Pedro Nunes, Coimbra, Portugal)
Da Cruz Lança, Marta (MRA | Grupo Álava, Portugal)
Del Sol Illana, Irene (University of Cádiz, Spain)
Dearnley, Peter (University of Southampton, UK)
Diniz, Bernardo (Instituto Superior Técnico, Lisbon, Portugal)
Escudero, María (CENIM-CSIC, Spain)
Favaro, Grégory (RTEC Instruments, Switzerland)
Fernández, Fátima Mariño (University of Santiago de Compostela, Spain)
Figueiredo-Pina, Célio (Instituto Politécnico de Setúbal, Setúbal, Portugal)
García, Alberto (Anton Paar, Spain)
García-Alonso, Cristina (CENIM-CSIC, Spain)
García Guimarey, María Jesus (University of Santiago de Compostela, Spain)
García-Ramírez, Ulises (University of Guadalajara, México)
Gomes, José (University of Minho, Portugal)
González, Rubén (University of Oviedo, Spain)
Guedes, Mafalda (Instituto Politécnico de Setúbal, Setúbal, Portugal)
Hutchings, Ian (Institute for Manufacturing, Cambridge, United Kingdom)
Iguarta, Amaya (Fundación TEKNIKER, Spain)
Khan, Sharjeel Ahmed (University of Coimbra, Coimbra, Portugal)
Linhardt, Paul (Institute for Chemical Technologies and Analytics, Austria)
Liñeira del Río, José Manuel (University of Santiago de Compostela, Spain)
Lopes, José Claudio (São Paulo State University – Unesp, Brazil)
Lopes, Lais (Falex Tribology, Belgium)

Lopez-Uruñuela, Fernando (Fundación TEKNIKER, Spain)
Fernández, Josefa (University of Santiago de Compostela, Spain)
Martinez, Paco (Scientec Ibérica, Spain)
Mathew, Mathew (University of Illinois Chicago, Chicago, USA)
Mingo, Pedro (Scientec Ibérica, Spain)
Múñez, Claudio (University of Rey Juan Carlos, Madrid, Spain)
Perdigoto, José (Instituto Pedro Nunes, Coimbra, Portugal)
Planells Torres, Mariano (Fundación Eurecat, Spain)
Ramalho, Amilcar (University of Coimbra, Coimbra, Portugal)
Ramírez-Arreola, Daniel (University of Guadalajara, México)
Rico, Álvaro (University of Rey Juan Carlos, Madrid, Spain)
Rodrigues, Ivan (Instituto Superior Técnico, Lisbon, Portugal)
Rodríguez Pérez, Jesús (University of Rey Juan Carlos, Madrid, Spain)
Salguero Pirés, José Eduardo (MRA | Grupo Álava, Portugal)
Sanchez, Luiz (São Paulo State University – Unesp, Brazil)
Sánchez-López, Juan Carlos (ICMSE, Spain)
Sánchez-López, Luna (CENIM-CSIC, Spain)
Santos, Francisco (Instituto Superior Técnico, Lisbon, Portugal)
Seabra, Jorge (University of Porto, Porto, Portugal)
Serro, Ana Paula (Instituto Superior Técnico, Lisbon, Portugal)
Silva, Diana (Instituto Superior Técnico, Lisbon, Portugal)
Soares, Daniel (Bruker, Germany)
Sousa, Filipe (MTBrandão, Portugal)
Staudinger, Paul (Anton Paar, Spain)
Tira-Picos, Noémia (Laborspirit, Portugal)
Tormos, Bernardo (Universitat Politècnica de València, Spain)
Vazquez Martinez, Juan Manuel (University of Cádiz, Spain)
Veeregowda, Deepak (Ducom Instruments, Netherlands)
Viesca, José (University of Oviedo, Spain)
Vilhena, Luís (University of Coimbra, Coimbra, Portugal)
Vuchkov, Todor (Instituto Pedro Nunes, Coimbra, Portugal)
Wimmer, Markus (Rush University Medical Center, Chicago, USA)

SPONSORS

